# Is the speed of light in vacuum really constant?

Julien Bolmont

## ▶ To cite this version:

Julien Bolmont. Is the speed of light in vacuum really constant?. Astrophysics [astro-ph]. UPMC, 2016. tel-01388037

# Is the speed of light in vacuum really constant?

Julien Bolmont

Laboratoire de Physique Nucléaire et de Hautes Energies

Université Pierre et Marie Curie, CNRS/IN2P3

Mémoire présenté en vue de l'obtention de l'

## Habilitation à diriger des Recherches
## de l'Université Pierre et Marie Curie

Spécialité : physique

Soutenue à Paris, le 9 mars 2016, devant le jury composé de

| | |
|---|---|
| Giovanni Amelino-Camelia | – Rapporteur |
| Aurélien Barrau | – Rapporteur |
| Paschal Coyle | – Rapporteur |
| Alessandro De Angelis | – Examinateur |
| Peter Wolf | – Examinateur, Président du jury |

*À Elsa et Corentin*

# Contents

# Introduction

**Personal path**

At the time I write these lines, I have been working on Lorentz Invariance Violation (LIV), more particularly on experimental search for modified photon dispersion relations in vacuum, for more than ten years. And in a sense, I started working on that topic because of a tragic accident.

My PhD was supposed to be entirely dedicated to the *Alpha Magnetic Spectrometer AMS-02*, more precisely to its capability to detect photons. At the time I began, *AMS-02* was supposed to be installed on the *International Space Station* at the beginning of 2005. In that case, I would have had a few months to analyze the first data taken in orbit.

But everything changed on Feb. 1, 2003. On that day, space shuttle *Columbia* disintegrated over Texas and Louisiana as it reentered Earth's atmosphere, killing all seven crew members. As a result, the whole US space program was delayed by two years and *AMS-02* was grounded. It was necessary to change the focus of my PhD so that I could analyze "real" data in addition to "simulated data". At that time, Quantum Gravity phenomenology exploration with astrophysical sources was not a new, but still a largely unexplored topic. Only a handful of physicists, mainly in Europe, were spending some time on analyzing data from satellites to put some constraints on modified photon dispersion relations in vacuum. Even if the amount of data available for this type of investigation was limited at the time, I thought it was very exciting to be able to explore the fundamental nature of spacetime through astrophysics.

So, under the supervision of Agnieszka Jacholkowska, I started in 2003 to analyze the data taken by the satellite *HETE-2*, looking for Quantum Gravity-induced energy-dependant time lags in Gamma-ray Bursts light curves. Since then, I never really stopped working on that topic, even if I decided to broaden my views on astroparticle physics going into neutrino astronomy during the post-doctoral fellowship I made between 2005 and 2008. After this parenthesis, I went back to LIV studies joining the H.E.S.S. collaboration, first as a postdoc (2008–2010) and then as a staff member of *Université Pierre et Marie Curie* at LPNHE (*Laboratoire de Physique Nucléaire et des Hautes Energies*). I had first the opportunity to study the gigantic flare of the blazar PKS 2155-304 that ocured in 2006. Later, I was involved in the analysis of four bright bursts detected by the *Fermi* satellite. I have been invited twice in conferences to show my results on these two analyses. Then, I went back to H.E.S.S., focusing on pulsars with my first student, Mathieu Chretien, who defended his PhD on October the 2$^{\text{nd}}$ 2015. Since the end of 2015, I am back to Active Galactic Nuclei, with my second PhD student, Cédric Pérennes, with the aim of better understanding intrinsic effects and to learn how to deal with them in LIV studies. I also worked to evaluate the performances of the future high energy gamma-ray observatory CTA (*Cherenkov Telescope Array*) as far as LIV searches are concerned. Between 2010 and 2015, I supervised four Master's students internships on LIV searches.

I would like to stress here that searching for LIV is only one part of my activities. Since 2010, I have been spending most of my time teaching. In addition, my second main topic of interest after LIV searches is instrumentation. Since I started my PhD in 2002, I have been involved on

the hardware side for *AMS-02*, IceCube, H.E.S.S. and CTA. I chose not to cover this part of my activities in the present memoir.

**Scientific revolution**

According to Thomas Kuhn (1922–1996), normal scientific progress is a "development-by-accumulation" of accepted facts and theories [105]. From time to time, such "normal science" can be interrupted by periods of revolutionary science, where a prevailing paradigm [1] has to be replaced by a new one.

As we shall see later, the fate of Lorentz Invariance has known an increasing interest in the last decade because LIV appears as a striking outcome of some approaches aiming at elaborating a quantum theory of gravitation (Quantum Gravity, or QG for short). Such a theory is still under construction but it is believed that it will be the next scientific revolution... if theorists succeed in finalizing it someday! This revolution will have profound consequences: both Standard Model (SM) of particle physics and General Relativity (GR) will be abandoned in the same way Newtonian gravitation was cast aside when Einstein came up with his theory of GR in 1915. As both SM and GR are at the heart of modern physics, the consequences will be profound.

In the previous paragraph, I wrote that when I started working on LIV, I thought it was very exciting to be able to explore the fundamental nature of spacetime through astrophysics. More than ten years later, I am still excited working in that field: how not to be excited to be involved (even very humbly) in the process that will (maybe one day) allow a new scientific revolution?

**Menu**

Through all this monograph, I will focus on Lorentz Invariance Violation searches with astrophysical sources. More precisely, I will focus on tests of modified dispersion relations (MDR) for photons in vacuum with transient high energy gamma-ray sources. The question I want to address is the following: is the velocity of photons in vacuum always equal to $c$, whatever their energy?

As a teacher, I of course tried to write this text in a pedagogical way. By doing so, I could not just write a synthesis of my work, disconnecting it from a broader context. I chose to carefully explain some notions that are generally considered as obvious in the LIV literature and which are sometimes difficult to find clearly explained. So I start with a chapter concerning Lorentz Invariance (Chapter 1). In this chapter, I explain what is meant by invariance, what are Lorentz transformations and how they can be derived from the nature of spacetime itself. I can then introduce Lorentz Invariance (LI). As key element of Special Relativity (SR), LI has been tested for a long time, well before scientists started to work on QG. At the end of the chapter, I briefly discuss the tests of LI that are not related to QG phenomenology, focusing on two optical experiments.

After discussing the broad context, I will come to the core of this monograph concerning LIV tests with variable or transient astrophysical gamma-ray sources (Chapter 2). These tests have known a growing interest in the past 15 years in the context of QG phenomenology. As an experimentalist, I will not go too far in the theory side. I will simply give some examples of models of QG which predict MDR, and which can be tested with astrophysical photons. Testing MDR is done by looking for energy-dependent time-lags. By searching for such lags, it is necessary to understand whether some time-lags are introduced by the emission mechanisms at play at the source. We will see that this question is still mainly unexplored. Then, I will quickly review most of the results available in the literature. At this occasion, I will have the opportunity to discuss

---

[1]A paradigm is the whole of techniques, patents and values shared by the members of the scientific community. See *e.g.* [10].

some of the main results I published myself. To end the chapter, I will discuss the other effects that a quantum spacetime could induce on photon propagation.

I will conclude this memoir (Chapter 3) discussing the future of LIV searches. I will give the key points that, in my opinion, will be essential on the road to a possible detection of LIV effects, especially with a new generation of instruments such as CTA.

**Thanks**

I express my gratitude to Giovanni Amelino-Camelia, Aurélien Barrau, Paschal Coyle, Alessandro De Angelis and Peter Wolf who kindly accepted to participate in the jury. Special thanks to Giovanni, Aurélien and Paschal for their careful reading of the draft.

Before I start, I also would like to take this opportunity to thank the people who allowed me to make a living as a physicist and a teacher and to work on astroparticle physics: Bernard Tamain, who allowed me to enter the world of research for my first internship in Caen (2000); Corinne Charbonnel, who allowed me to enter the domain of astrophysics as an intern in Toulouse (2001); Agnieszka Jacholkowska, who supervised my PhD, who allowed me to discover LIV and QG (2002-2005) – we have been working together for 13+ years as I write these lines! –; Stefan Schlenstedt and Christian Spiering who allowed me to open my horizon and work on something else than LIV for a while (2005-2008); and Pascal Vincent who allowed me to come back to LIV as a postdoc and finally as a *Maître de Conférences*.

I also want to thank a lot Jean-Philippe Lenain, Jean-Paul Tavernet, Agnieszka for their useful comments on the draft, as well as Laurent Le Guillou, Nicolas Regnault, Arache Djanati-Ataï, Hélène Sol for insightful discussions.

Finally, thanks to Elsa and Corentin for their love and support during the writing of this monograph. I do not know how I could spend more time thinking about photons than thinking about them !

# Chapter 1

# Context: Lorentz Invariance
# and its violation

> ❝ *Space by itself, and time by itself, are doomed to fade away into mere shadows, and only a kind of union of the two will preserve an independent reality.* ❞
>
> – H. Minkowski, *Space and Time* (1908)

Lorentz Invariance (LI) is a key ingredient of modern physics. It is indeed a cornerstone of our present description of both microscopic and macroscopic worlds. In this chapter, I will first explain as simply as possible what we mean by "invariance" and "invariance violation". After that, I will explain what is Lorentz Invariance, Lorentz Invariance Violation (LIV). Then, I will briefly describe the classical tests of LI, "classical" in the sense they have been developed in the framework of Special Relativity and not in connexion with Quantum Gravity (QG), which I will discuss in the next chapter.

## 1.1 Symmetry, symmetry breaking and some other definitions

In this section, for illustrative purposes, I will take a pre-relativistic, post-Maxwellian point of view as a physicist could have done at the end of the 19$^{\text{th}}$ century. Therefore, I will assume that the Galilean relativity principle holds and that photons obey Maxwell equations as well as Galilean velocities composition law.

### 1.1.1 Observer transformations, particle transformations, invariance and symmetry

Let me consider a reference frame $E$, in which I define a base $\{\vec{e_i}\}$, with $i \in \{1, 2, 3\}$. This base provides a specific coordinate system I can use to describe any process I want. In the reference frame $E$, let me consider that an operator controls a light source that emits photons with velocity $\vec{V} \equiv \vec{V}_{L/E}$ (Fig. 1.1).
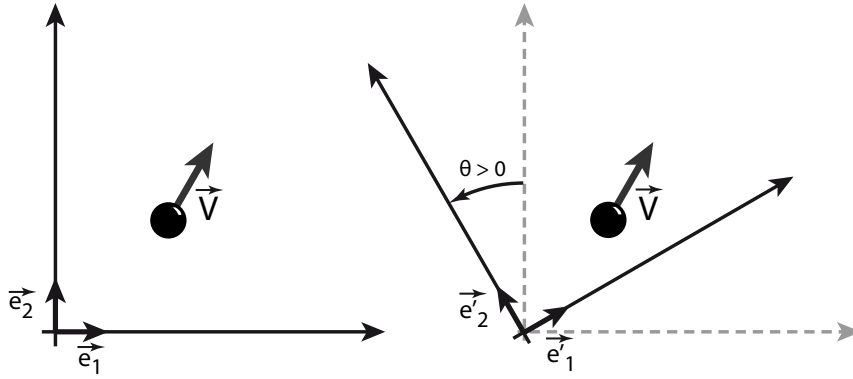
**Figure 1.1:** A photon with velocity $\vec{V}$ is travelling through vacuum. Two different reference frames are drawn, the one on the right being obtained by a rotation of the one on the left. As the choice of the reference frame is done by the observer, this transformation is called *observer transformation*.
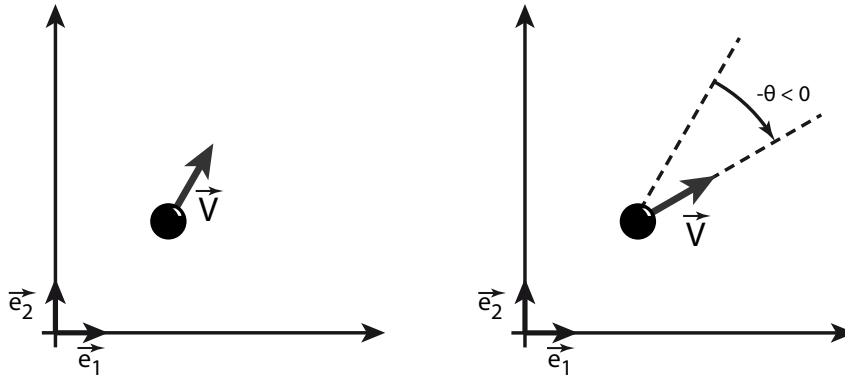


**Figure 1.2:** A photon with velocity $\vec{V}$ is travelling through vacuum. The picture on the right is obtained from the one on the left by rotating the particle by an angle $-\theta$, with $\theta$ defined as shown in Fig. 1.1. Since the particle is rotated (and not the reference frame), this transformation is called a *particle transformation*.

For now, I assume that the photons propagate through vacuum and that no interaction of any kind can affect their propagation.

As an observer, I can chose the reference frame I want to describe what I see, as long as this frame is inertial. In a pre-relativistic context, this principle applies only for laws of mechanics. This is what is called the *Galilean relativity principle*. This principle says that laws of mechanics are the same in all inertial frames: in other word, there is no *preferred* frame of reference, a frame of reference in which the laws of mechanics would be fulfiled while they would not be true in some other frame.

Since I can choose whatever frame of reference I want, I can decide to use the reference frame corresponding to the base $\{\vec{e_i}\}$ or another reference frame with base $\{\vec{e_i'}\}$ obtained from $\{\vec{e_i}\}$ by a rotation: $\vec{e_i'} = R^j{}_i \vec{e_j}$ (rotation matrix $R$). Such a transformation is called an *observer transformation*. $\vec{V}$ can be expressed in either of these two bases: $\vec{V} = v^i \vec{e_i} = v'^i \vec{e_i'}$. Since $\vec{e_i'} = R^j{}_i \vec{e_j}$, we have $\vec{V} = v^i \vec{e_i} = v'^i R^j{}_i \vec{e_j}$ and so we obtain the relation between the coordinates of $\vec{V}$ in the two bases: $R^j{}_i v'^i = v^j$, or $v'^i = (R^{-1})^i{}_j v^j$ (rotation matrix $R^{-1}$).

Instead of rotating the reference frame, I can also imagine that the operator changes the orientation of his light source and throws the photons in a different direction (Fig. 1.2). This is called a *particle transformation*. From the simple calculation above, I can infer that rotating
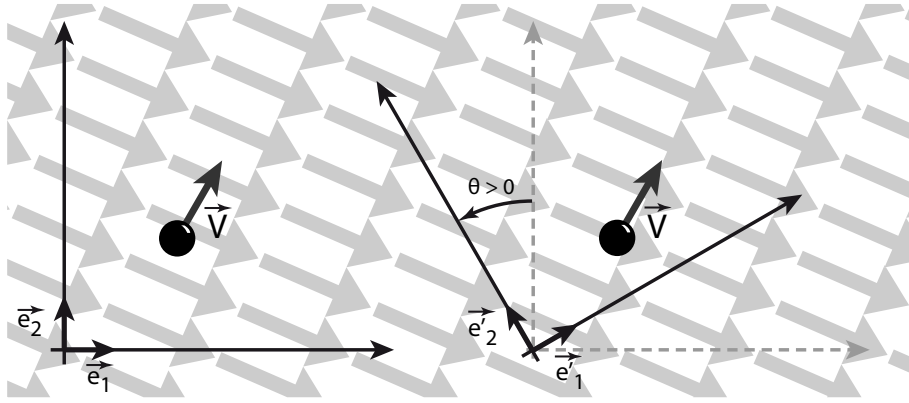
**Figure 1.3:** A photon with velocity $\vec{V}$ as measured by an observer is travelling through aether. Aether drifts with speed $\vec{V}_{A/E}$ (grey arrows) as seen from the observer frame of reference. Two different observer reference frames are drawn. The system remains invariant under observer transformations: in particular, the scalar product $\vec{V} \cdot \vec{V}_{A/E}$ does not change.

the reference frame counterclockwise by an angle $\theta$ is equivalent to rotating the direction of the photon by an angle $-\theta$. In other words, in vacuum, *observer transformation* and *particle transformation* are inversely related [1].

Obviously enough, a given quantity is said to be *invariant* under a given transformation if it stays unchanged when this transformation is applied to it. From what we have seen, we can state that the invariance under observer transformations is not related to any physics. The choice of the reference frame is the only thing we need to define what will be invariant or not under observer transformations. On the contrary, invariance under particle transformations correspond to a *physical symmetry* of the system. Under this invariance condition, the two situations represented in Fig. 1.2 are totally equivalent.

### 1.1.2 Invariance violation and symmetry breaking

Now, let me consider a different situation. This time, I assume the photon is not in vacuum anymore but in a medium called *aether*. In the pre-relativistic era, aether is the medium light needs to propagate, as the sound needs air to propagate [2]. In that sense, there is an intimate connexion between photons and aether and the presence of aether should affect in some way the propagation of the photons. Aether is assumed to be homogeneous so that the light has the same speed in the frame of reference of the aether, whatever its direction of propagation. Let me also assume the experiment is done in an inertial frame moving with respect to the aether so that for the observer, the aether appears to move with speed $\vec{V}_{A/E}$. That is the *aether wind*.

Fig. 1.3 shows what happens for observer transformations. The system remains invariant as can be illustrated by the fact the scalar product $\vec{V} \cdot \vec{V}_{A/E}$ remains unchanged.

The situation is very different in the case of a particle transformation (Fig. 1.4). It can be seen in particular that the scalar product $\vec{V} \cdot \vec{V}_{A/E}$ is not the same before and after the particle transformation. The *particle invariance* (here the rotation invariance) is *violated*. And since every invariance corresponds to a symmetry, the rotational symmetry is said to be *broken*. In other words, the system is physically distinguishable of its transformed version, and the existence of the aether wind could be deduced from an experiment.

Let me consider such an experiment and assume the laboratory travels with a constant speed

---

[1] Observer transformations and particle transformations are sometimes referred to as *passive* and *active* respectively.
[2] Interested readers can find a detailed discussion on aether theories in [168].
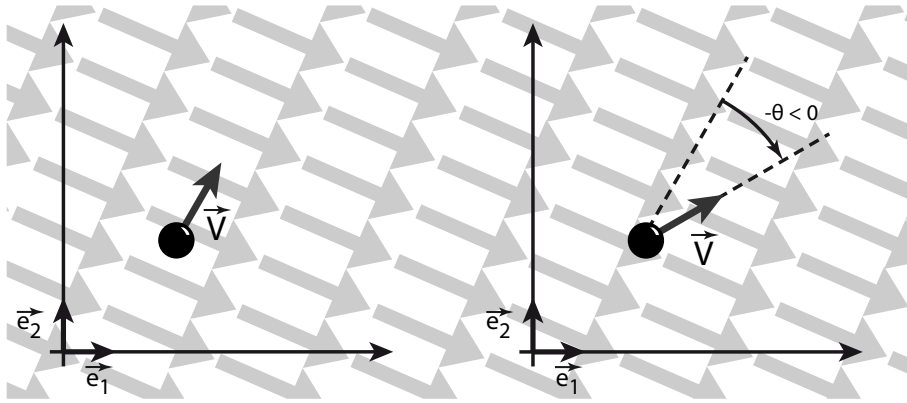
**Figure 1.4:** A photon with velocity $\vec{V}$ as measured by an observer is travelling through aether. Aether drifts with speed $\vec{V}_{A/E}$ (grey arrows) as seen from the observer frame of reference. The system is clearly not invariant under particle transformations: the scalar product $\vec{V} \cdot \vec{V}_{A/E}$ is not invariant.
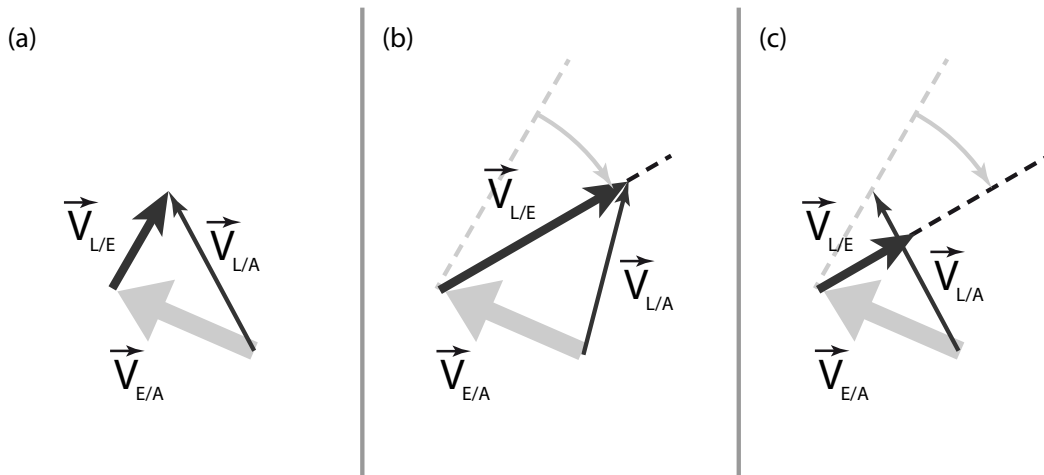


**Figure 1.5:** A particle transformation and its effect on the Galilean speed composition law. See the text for the full description.

$\vec{V}_{E/A}$ in the frame of reference of the aether ($\vec{V}_{E/A} = -\vec{V}_{A/E}$). An observer measures the speed of light to be $\vec{V}_{L/E}$ in the reference frame of his laboratory, and the speed of light in the frame of the aether [3] is $\vec{V}_{L/A}$. *A priori*, the norms of $\vec{V}_{L/A}$ and $\vec{V}_{L/E}$ are not equal: $V_{L/A} \neq V_{L/E}$.

Then, using the Galilean speed composition law, we have $\vec{V}_{L/A} = \vec{V}_{L/E} + \vec{V}_{E/A}$ (Fig. 1.5 (a)). The situation is similar to the one illustrated by Fig. 1.4: rotational invariance is violated and when the operator rotates the experiment in a different direction (Fig. 1.5 (b)), he can measure an increase of the value of $V_{L/E}$. On the contrary, if the operator does not see any change of the value of $V_{L/E}$ (Fig. 1.5 (c)), the only possibility is that $V_{E/A} = 0$ and this imposes that $\vec{V}_{L/E} = \vec{V}_{L/A}$. In that case, the operator can conclude that the rotational invariance is not violated and that either he is at rest in the frame of reference of the aether, either aether does not exist.

Finally, consider again Fig. 1.5 (a and b) and assume this time that rotationnal invariance *is* violated. The observer who measures $\vec{V}_{L/E}$ will be able to deduce the invariance violation from his experiment. However, another observer at rest in the reference frame of the aether will see

---

[3]Aether was proposed as the absolute and unique frame of reference in which Maxwell's equations hold. So, the value of $V_{L/A}$ can be obtained from Maxwell equations: $V_{L/A} = 1/\sqrt{\epsilon_0 \mu_0}$ where $\epsilon_0$ and $\mu_0$ are respectively the vacuum permittivity and permeability.

that $\vec{V}_{L/E} = \vec{V}_{L/A}$ whatever the direction of the light beam and for him the invariance will not be violated. As a result, the relativity principle fails and as a consequence, there exists a *preferred frame of reference*. This preferred frame is often chosen in such a way that physics is isotropic so in our example, the preferred frame is the one of the aether, where the speed of light is isotropic.

Now we are ready to introduce Lorentz Invariance.

## 1.2  Lorentz Invariance and Lorentz Invariance Violation

Considering what we have seen in the previous section, *Lorentz Invariance* (LI) can easily be defined: a quantity is Lorentz invariant if it is not modified by Lorentz transformations. So, in order to understand what it really means, it is necessary to spend some time on Lorentz transformations. However, I am pretty sure the reader is familiar already with Lorentz transformations, so I will emphasize a bit more on how Lorentz transformations are derived. As my main topic of interest is Lorentz invariance, it is interesting to notice that Lorentz transformations are themselves obtained from invariance principles.

The content of this section is inspired from readings of several text books about special relativity. In particular, I follow the approach and definitions of [74].

### 1.2.1  Minkowski spacetime

**Historical note**

The two postulates formulated by Albert Einstein (1879–1955) when he introduced Special Theory of Relativity in 1905 [53] were the following:

- The *Principle of Relativity* – "Not only in mechanics, but also in electrodynamics, no properties of the phenomena correspond to the concept of absolute rest, but rather that for all coordinate systems for which the mechanical equations hold, the equivalent electrodynamical and optical equations hold also...";

- The *Principle of Invariant Light Speed* – "Light in empty space always propagates with a velocity which is independent of the state of motion of the emitting body."

The first postulate is an extension of Galilean relativity principle to electromagnetism. Rephrased in a modern way, this principle states that the laws of physics are the same in all inertial reference frames. All these inertial frames are physically equivalent or, as already mentionned in §1.1.1, there is no preferred frame of reference.

As far as the second postulate is concerned, it was soon understood after Einstein's paper was published that such an hypothesis is not necessary to derive Lorentz transformations. It was first noticed by Vladimir S. Ignatowski (1875–1942) [85, 86, 87, 88] and after him, several authors were able to derive Lorentz transformations without using the invariance of light speed. References [109] and [111] provide two recent examples of such derivations. In addition to the relativity principle, and causality [4], the hypotheses used are about fundamental nature of spacetime: homogeneity and isotropy.

This notion of *spacetime* is due to Hermann Minkowski (1864–1909). Minkowski realized that special relativity could be understood much better considering a single entity grouping space and time together [128]. The structure of *Minkowski spacetime* is all what is needed to derive Lorentz transformations and the two Einstein postulates appear as consequences of this structure.

---

[4]The causality principle states that the time difference between two events always has the same sign (the order of the events is the same), regardless of the choice of the reference frame in which this time difference is measured.

**Minkowski spacetime**

Minkowski spacetime has the following ingredients:

- a real affine space $\mathscr{E}$ of dimension four, with an associated vector space $E$. $\mathscr{E}$ is called *spacetime*. Each element of $E$ is called a four-vector (or simply vector). A vector $\vec{\mathbf{x}}$ can be decomposed over a basis $\{\vec{\mathbf{e}_\alpha}\}$ of $E$: $\vec{\mathbf{x}} = x^\alpha \vec{\mathbf{e}_\alpha}$ (greek indices go from 0 to 3) using Einstein summation convention. As an example, the vector position has the components

$$x^\alpha = (Ct, x, y, z) \tag{1.1}$$

using cartesian spatial coordinates. It is very important to understand here that at the moment, $C$ is only a coefficient allowing to convert a time to a distance. It could be indifferently noted $v$, $k$, etc.;

- a nondegenerate, symmetric bilinear form with a signature [5] $(-, +, +, +)$, called *metric tensor* and noted $\mathbf{g}$. The coefficients of $\mathbf{g}$, noted $g_{\alpha\beta}$, are the scalar products of basis vectors:

$$g_{\alpha\beta} = \mathbf{g}(\vec{\mathbf{e}_\alpha}, \vec{\mathbf{e}_\beta}), \tag{1.2}$$

and the scalar product of two vectors is given by

$$\forall (\vec{\mathbf{v}}, \vec{\mathbf{w}}) \in E \times E, \ \vec{\mathbf{v}} \cdot \vec{\mathbf{w}} = \mathbf{g}(\vec{\mathbf{v}}, \vec{\mathbf{w}}) = g_{\alpha\beta} v^\alpha w^\beta. \tag{1.3}$$

Due to the signature $(-, +, +, +)$, the scalar product of two vectors can be positive, negative, or null. Obviously, this is also true for the scalar product of a vector with itself. A vector $\vec{\mathbf{v}}$ is said to be *space-like* if and only if $\mathbf{g}(\vec{\mathbf{v}}, \vec{\mathbf{v}}) > 0$, *time-like* if and only if $\mathbf{g}(\vec{\mathbf{v}}, \vec{\mathbf{v}}) < 0$ and *light-like* if and only if $\vec{\mathbf{v}} \neq 0$ and $\mathbf{g}(\vec{\mathbf{v}}, \vec{\mathbf{v}}) = 0$. The norm of a vector is then given by

$$\forall \vec{\mathbf{v}} \in E, \ \left\| \vec{\mathbf{v}} \right\|_{\mathbf{g}} = \sqrt{|\mathbf{g}(\vec{\mathbf{v}}, \vec{\mathbf{v}})|}. \tag{1.4}$$

In the particular case of a flat spacetime, the basis $\{\vec{\mathbf{e}_\alpha}\}$ is orthonormal and the matrix of $\mathbf{g}$ is called the Minkowski matrix, noted $\eta$:

$$g_{\alpha\beta} = \eta_{\alpha\beta} = \begin{pmatrix} -1 & 0 & 0 & 0 \\ 0 & 1 & 0 & 0 \\ 0 & 0 & 1 & 0 \\ 0 & 0 & 0 & 1 \end{pmatrix}. \tag{1.5}$$

Then,

$$\vec{\mathbf{v}} \cdot \vec{\mathbf{w}} = \eta_{\alpha\beta} v^\alpha w^\beta = -v^0 w^0 + v^1 w^1 + v^2 w^2 + v^3 w^3, \tag{1.6}$$

and the squared norm of a vector $\vec{\mathbf{v}}$ is given by

$$\vec{\mathbf{v}} \cdot \vec{\mathbf{v}} = \vec{\mathbf{v}}^2 = \eta_{\alpha\beta} v^\alpha v^\beta = -(v^0)^2 + (v^1)^2 + (v^2)^2 + (v^3)^2; \tag{1.7}$$

- if $\vec{\mathbf{v}}$ is a light-like vector, then $-(v^0)^2 + (v^1)^2 + (v^2)^2 + (v^3)^2 = 0$, which is the equation of a hypercone. $\vec{\mathbf{v}}$ is the direction vector of the world line of any massless particle, in particular a photon. That is why the hypercone is simply called the *light cone*. It is divided in two unbounded nappes, one towards the future and one towards the past. Deciding which nappe is towards the future is chosing the *arrow of time*. An orientation can be chosen for spacetime: this is equivalent to chosing an oriented reference basis. The orientation is given by the determinant of the metric $\mathbf{g}$.

---

[5] $(+, -, -, -)$ can be used as well. Which signature is better is a matter of taste.
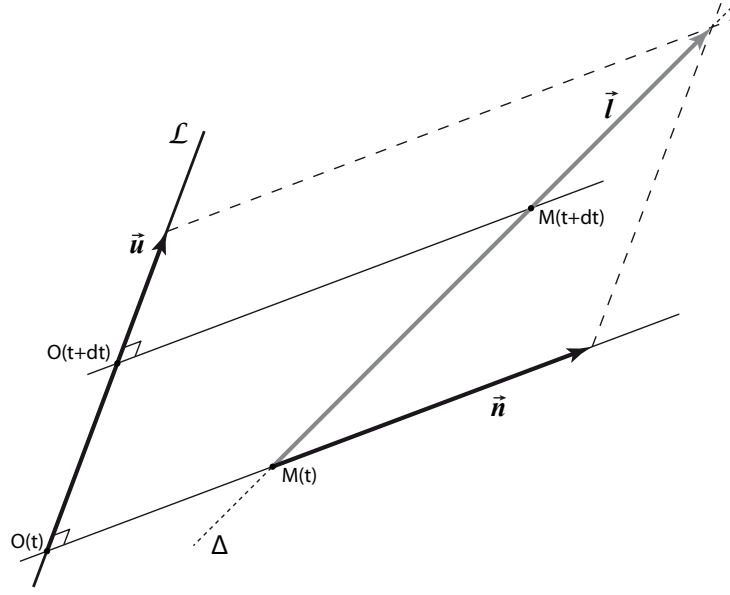
**Figure 1.6:** A photon moving along a geodesic $\Delta$ while an inertial observer moves along a world line $\mathscr{L}$ at speed $\vec{\mathbf{u}}$. This figure is inspired from Fig. 4.6 of [74].

The structure of Minkowski spacetime is all what is needed to describe almost every aspect of special relativity. Proper time, the Lorentz factor, four-speed, four-acceleration, etc. can be defined from it. We can also retrieve important results such as length contraction, time dilation, relativistic speed composition law, etc.

I will not go into all this, but as an example, and since I will need this definition in the next section, proper time $d\tau$ is defined that way:

$$\begin{cases} C\, d\tau = \|\vec{\mathbf{x}}\|_{\mathbf{g}} = \sqrt{-\mathbf{g}(d\vec{\mathbf{x}}, d\vec{\mathbf{x}})} \text{ when } d\vec{\mathbf{x}} \text{ is directed towards the future} \\ C\, d\tau = -\|\vec{\mathbf{x}}\|_{\mathbf{g}} = -\sqrt{-\mathbf{g}(d\vec{\mathbf{x}}, d\vec{\mathbf{x}})} \text{ when } d\vec{\mathbf{x}} \text{ is directed towards the past,} \end{cases} \tag{1.8}$$

so for an orthonormal basis,

$$C\, d\tau = \pm\sqrt{(dx^0)^2 - (dx^1)^2 - (dx^2)^2 - (dx^3)^2}, \tag{1.9}$$

where the sign $\pm$ corresponds to the two cases of Eq. 1.8.

### 1.2.2 The invariance of the speed of light as a consequence of the structure of Minkowski spacetime

Since my main topic of interest is to test if the speed of the photons is really constant, I think it is interesting at least to demonstrate the invariance of the speed of light directly from the structure of Minkowski spacetime, *i.e.* even before introducing Lorentz transformations.

So, let me now consider the situation depicted by Fig. 1.6. An inertial observer $\mathcal{O}$ follows a world line $\mathscr{L}$. When his proper time changes by an amount $dt \equiv d\tau$, his position changes by an amount $d\vec{\mathbf{x}}$, this vector being necessarily directed towards the future. Then, his four-speed is defined by

$$\vec{\mathbf{u}} = \frac{1}{C}\frac{d\vec{\mathbf{x}}}{dt}. \tag{1.10}$$

From Eq. 1.9, it comes easily that $\vec{\mathbf{u}}^2 = -1$.

Between times $t$ and $t + dt$, the observer moves from $O(t)$ to $O(t + dt)$ so that $d\vec{\mathbf{x}} = \overrightarrow{O(t)O(t + dt)}$. As a result, his four-speed can be written as

$$\vec{\mathbf{u}} = \frac{1}{C} \frac{\overrightarrow{O(t)O(t + dt)}}{dt}, \tag{1.11}$$

which gives the relation

$$\begin{aligned} \overrightarrow{O(t)O(t + dt)} &= C\vec{\mathbf{u}}\, dt, \text{ or} \\ \overrightarrow{O(t + dt)O(t)} &= -C\vec{\mathbf{u}}\, dt. \end{aligned} \tag{1.12}$$

I consider now a photon propagating in the vicinity of ☺. Between times $t$ and $t + dt$ (again, as measured by ☺), the photon moves along a light-like geodesic $\Delta$ from $M(t)$ to $M(t + dt)$. Vectors $\overrightarrow{O(t)M(t)}$ and $\overrightarrow{O(t + dt)M(t + dt)}$ are necessarily orthogonal to vectors $\overrightarrow{O(t)O(t + dt)}$ and $\vec{\mathbf{u}}$. In particular, we will need the following relation later:

$$\vec{\mathbf{u}} \cdot \overrightarrow{O(t + dt)M(t + dt)} = 0. \tag{1.13}$$

Now we would like to have a unit vector that could be used to describe the trajectory of the photon. Unfortunately, as the norm of a light-like vector is null, we cannot normalize it, so there is no unit vector tangent to $\Delta$. The only thing we can do is to define at point $M(t)$ a light-like vector $\vec{\mathbf{l}}$ such that

$$\vec{\mathbf{l}} \cdot \vec{\mathbf{u}} = -1, \tag{1.14}$$

and use it to define a unit vector. $\vec{\mathbf{l}}$ is unique and we can define another vector $\vec{\mathbf{n}}$ such that

$$\vec{\mathbf{l}} = \vec{\mathbf{u}} + \vec{\mathbf{n}}. \tag{1.15}$$

So it comes that

$$\underbrace{\vec{\mathbf{l}} \cdot \vec{\mathbf{u}}}_{-1} = \underbrace{\vec{\mathbf{u}} \cdot \vec{\mathbf{u}}}_{-1} + \vec{\mathbf{n}} \cdot \vec{\mathbf{u}} \implies \vec{\mathbf{n}} \cdot \vec{\mathbf{u}} = 0. \tag{1.16}$$

Then, $\vec{\mathbf{n}}$ and $\vec{\mathbf{u}}$ are orthogonal. In addition, since $\vec{\mathbf{l}}$ is a light-like vector,

$$\vec{\mathbf{l}}^2 = \underbrace{\vec{\mathbf{u}}^2}_{-1} + 2\underbrace{\vec{\mathbf{n}} \cdot \vec{\mathbf{u}}}_{0} + \vec{\mathbf{n}}^2 = 0 \implies \vec{\mathbf{n}}^2 = 1, \tag{1.17}$$

so $\vec{\mathbf{n}}$ is a unit vector. $\vec{\mathbf{n}}$ defines the direction of propagation of the photon as seen by observer ☺.

I can now calculate the speed of the photon as seen by ☺ at time $t$:

$$\vec{\mathbf{V}}(t) = \frac{d\overrightarrow{OM}}{dt}. \tag{1.18}$$

For this, I need to express $d\overrightarrow{OM}$:

$$\begin{aligned} d\overrightarrow{OM} &= \overrightarrow{O(t + dt)M(t + dt)} - \overrightarrow{O(t)M(t)} \\ &= \overrightarrow{O(t + dt)O(t)} + \overrightarrow{O(t)M(t)} + \overrightarrow{M(t)M(t + dt)} - \overrightarrow{O(t)M(t)} \\ &= \overrightarrow{O(t + dt)O(t)} + \overrightarrow{M(t)M(t + dt)}. \end{aligned} \tag{1.19}$$

$\overrightarrow{O(t + dt)O(t)}$ is given by Eq. 1.12, but I still need to express the vector $\overrightarrow{M(t)M(t + dt)}$. For this, I can use Eq. 1.13. Indeed,

$$\vec{\mathbf{u}} \cdot \overrightarrow{O(t + dt)M(t + dt)} = \vec{\mathbf{u}} \cdot \left[ \overrightarrow{O(t + dt)O(t)} + \overrightarrow{O(t)M(t)} + \overrightarrow{M(t)M(t + dt)} \right] = 0.$$

Using Eq. 1.12 and since $\vec{\mathbf{u}}$ and $\overrightarrow{O(t)M(t)}$ are orthogonal, we obtain

$$\vec{\mathbf{u}} \cdot \overrightarrow{M(t)M(t+dt)} = -C\,dt. \tag{1.20}$$

It is clear however that vectors $\overrightarrow{M(t)M(t+dt)}$ and $\vec{\mathbf{l}}$ are colinear so we can write

$$\overrightarrow{M(t)M(t+dt)} = k\,\vec{\mathbf{l}}$$

where $k$ is a constant. Since we have the relation 1.14, we obtain simply that $k = C\,dt$.

So, Eq. 1.19 gives

$$d\overrightarrow{OM} = -C\,\vec{\mathbf{u}}\,dt + C\,\vec{\mathbf{l}}\,dt, \tag{1.21}$$

and since $\vec{\mathbf{l}} = \vec{\mathbf{u}} + \vec{\mathbf{n}}$, we have

$$\vec{\mathbf{V}}(t) = \frac{d\overrightarrow{OM}}{dt} = C\,(\vec{\mathbf{l}} - \vec{\mathbf{u}}) = C\,\vec{\mathbf{n}}. \tag{1.22}$$

Since $\vec{\mathbf{n}}$ is a unitary vector, we obtain finally

$$\left\|\vec{\mathbf{V}}\right\|_{\mathbf{g}} = C. \tag{1.23}$$

Then, we have verified that the speed of a photon is constant and always measured to be $C$, for any observer, and whatever his state of motion. Note that I have considered here that the observer is inertial. The result above can be generalized to any accelerating or rotating observer but in that case, the observer has to measure the speed of the photon at his own location ($\overrightarrow{OM} = 0$).

I did not elaborate on the meaning of constant $C$ so far. This parameter was first introduced in Eq. 1.1 as a conversion factor from a time to a distance. From Eqs. 1.8 and 1.9, $C$ appears as a link between proper time and the metric:

$$C^2 d\tau^2 = -g_{\alpha\beta}x^\alpha x^\beta \equiv ds^2. \tag{1.24}$$

It can then be considered as a fundamental constant of spacetime. Now, I have come to a point where it appears that $C$ is the speed of massless particles, but it is only the experiment that allows to identify this constant to the velocity of electromagnetic waves in vacuum: $C \equiv c$. The possible meanings of $c$ are nicely discussed in reference [57].

### 1.2.3 Lorentz transformation

The aim of this section is to give the modern definition of Lorentz transformations and to show that Lorentz transformation includes rotations and boosts. If the reader consider all this as obvious, then he can go directly to Section 1.2.4. In my opinion however, the fact that Lorentz transformation includes rotations and boosts is too often taken for granted in physics text books.

**Definition**

Using the notations defined above, we call Lorentz transformation any linear map

$$\Lambda: \begin{array}{ccc} E & \longrightarrow & E \\ \vec{\mathbf{v}} & \longmapsto & \Lambda(\vec{\mathbf{v}}) \end{array} \tag{1.25}$$

such that

$$\forall(\vec{\mathbf{v}}, \vec{\mathbf{w}}) \in E \times E,\ \Lambda\left(\mathbf{g}(\vec{\mathbf{v}}, \vec{\mathbf{w}})\right) = \mathbf{g}\left(\Lambda(\vec{\mathbf{v}}), \Lambda(\vec{\mathbf{w}})\right) = \mathbf{g}(\vec{\mathbf{v}}, \vec{\mathbf{w}}) \tag{1.26}$$

In other words, $\Lambda$ leaves the scalar product induced by $\mathbf{g}$ invariant.  Being defined from the metric, the norm (Eq. 1.4, page 16) is also invariant:

$$\forall \vec{v} \in E, \ \|\Lambda(\vec{v})\|_{\mathbf{g}} = \|\vec{v}\|_{\mathbf{g}}. \tag{1.27}$$

Using index notation, a Lorentz transform $\vec{w} = \Lambda(\vec{v})$ is noted

$$w^{\alpha} = \Lambda^{\alpha}{}_{\beta} v^{\beta}, \tag{1.28}$$

while the invariance of the scalar product translates into

$$\Lambda^{\mu}{}_{\alpha} \Lambda^{\nu}{}_{\beta} g^{\alpha\beta} = g^{\mu\nu}. \tag{1.29}$$

The set of all Lorentz transformations associated with a composition law forms a group [6], the *Lorentz group*, noted $O(3,1)$, $O$ because it is an orthogonal group, and $(3,1)$ because the signature $(-,+,+,+)$ has three '+' and one '-'.

The problem is now to interpret the above definition and give the physical meaning of Lorentz transformations. For this, it is common to classify them according to the value of $\det \Lambda$ (which is equal to $\pm 1$) and the sign of the coefficient $\Lambda^{0}{}_{0}$ (which can only take values $\geqslant 1$, or $\leqslant -1$) when $\Lambda$ is expressed in an orthonormal basis. From all the possible combinations for the choice of these parameters, the most important is the one for which $\det \Lambda = +1$ and $\Lambda^{0}{}_{0} \geqslant 1$ because it relates the local frames of two observers. These transformations are called *restricted* Lorentz transformations [7]. They form a group noted $SO_{o}(3,1)$.

It is possible to show that from any Lorentz transformation of $O(3,1)$, one can switch to a restricted Lorentz transformation using one of the two operators noted $\mathbf{P}$ and $\mathbf{T}$ or a combination $\mathbf{I} \equiv \mathbf{P} \circ \mathbf{T} = \mathbf{T} \circ \mathbf{P}$. $\mathbf{P}$ is the parity transformation, the simultaneous flip in the sign of all three spatial coordinates, and $\mathbf{T}$ is the time-reversal transformation[8]:

$$\begin{aligned}
I^{\alpha}{}_{\beta} &= \text{diag}(-1,-1,-1,-1), \\
P^{\alpha}{}_{\beta} &= \text{diag}(1,-1,-1,-1), \\
T^{\alpha}{}_{\beta} &= \text{diag}(-1,1,1,1).
\end{aligned} \tag{1.30}$$

So the only thing we need to do is to study restricted Lorentz transformations.

**Restricted Lorentz transformations**

As we have seen, restricted Lorentz transformations fulfill the conditions $\det \Lambda = +1$ and $\Lambda^{0}{}_{0} \geqslant 1$. What we need to do now is to express the coefficients of the matrix $\Lambda$ in a well-chosen orthonormal basis in order to reveal the physical meaning of the transformation.

Let me note this orthonormal basis $(\vec{e_0}, \vec{e_1}, \vec{e_2}, \vec{e_3})$. It is not straightforward to define such a basis from scratch, but another basis $(\vec{l}, \vec{k}, \vec{e_2}, \vec{e_3})$ where $\vec{l}$ and $\vec{k}$ are light-like can be used

---

[6]If the composition law is noted $\circ$, it means that:

- if $\Lambda_1$ and $\Lambda_2$ are Lorentz transformations, $\Lambda_1 \circ \Lambda_2$ is a Lorentz transformation too;

- if $\Lambda_1$, $\Lambda_2$ and $\Lambda_3$ are Lorentz Transformations, then $(\Lambda_1 \circ \Lambda_2) \circ \Lambda_3 = \Lambda_1 \circ (\Lambda_2 \circ \Lambda_3)$;

- the identity is a Lorentz transformation;

- every Lorentz transformation $\Lambda$ has an inverse $\Lambda^{-1}$.

[7]Transformations for which $\det \Lambda = +1$ are called *proper* transformations. They form a group noted $SO(3,1)$. The transformations for which $\Lambda^{0}{}_{0} \geqslant 1$ are called *orthochronous*, they transform a time-like vector oriented towards the future into a time-like vector oriented towards the future. Again, these transformations form a group, noted $O_{o}(3,1)$.

[8]$\mathbf{I}$, $\mathbf{P}$ and $\mathbf{T}$ are Lorentz transformations. It is obvious since $\mathbf{I} = \mathbf{I}^{-1}$, $\mathbf{P} = \mathbf{P}^{-1}$ and $\mathbf{T} = \mathbf{T}^{-1}$ so Eq. 1.29 is verified for each one of these transformations.
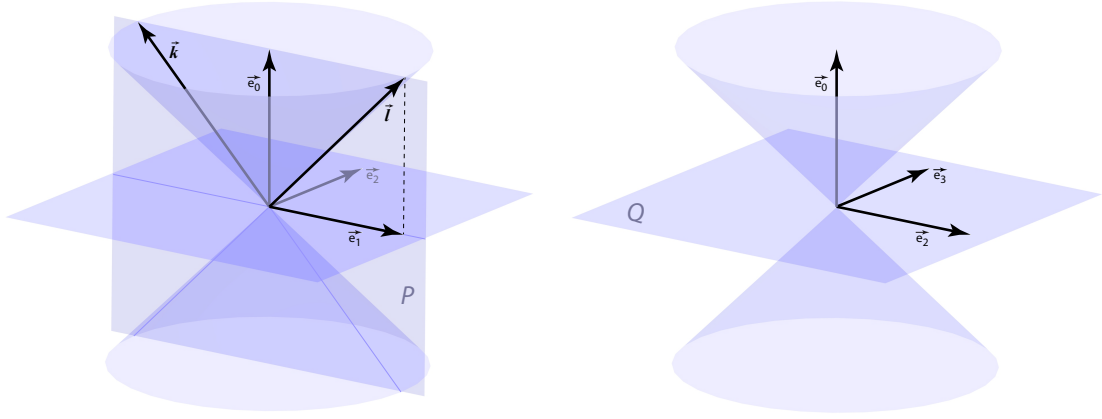
**Figure 1.7:** Left: basis vectors $\vec{e_0}$ and $\vec{e_1}$ are defined from two light-like vectors $\vec{l}$ and $\vec{k}$. Dimension along vector $\vec{e_3}$ has been suppressed. Right: dimension along vector $\vec{e_1}$ has been suppressed.

as an intermediate. A way of defining the latter basis is to start from the fact that a restricted Lorentz transformation admits at least one invariant light-like direction [9].

If we note such a direction $\Delta$, it means that $\Lambda(\Delta) = \Delta$. Equivalently, there exists a light-light vector $\vec{l}$ such that $\Lambda(\vec{l}) = \lambda \vec{l}$ where[10] $\lambda > 0$. Then, $\vec{l}$ appears to be an eigen vector of $\Lambda$ and $\lambda$ an eigen value. Since $\lambda > 0$, we can define a real parameter $\psi = \ln \lambda$ such that

$$\Lambda(\vec{l}) = e^{\psi} \vec{l}. \tag{1.31}$$

Then we can consider a second light-like vector $\vec{k}$ oriented towards the future, such that $\vec{k}$ and $\vec{l}$ are not colinear. From these two vectors, $\vec{e_0}$ and $\vec{e_1}$ are constructed such that $\vec{e_0} = (\vec{l} + \vec{k})/2$ and $\vec{e_1} = (\vec{l} - \vec{k})/2$. *A priori,* $\vec{k}$ can be chosen arbitrarily as long as it is not colinear to $\vec{l}$ but in order that $\vec{e_0}$ and $\vec{e_1}$ are orthogonal, $\vec{k}$ and $\vec{l}$ have to verify the condition

$$\vec{k} \cdot \vec{l} = -2. \tag{1.32}$$

This imposes that $\vec{k}$ is in plane $P$ as represented on Fig. 1.7 (left). Another consequence is that basis $(\vec{l}, \vec{k}, \vec{e_2}, \vec{e_3})$ cannot be orthonormal.

The fact that $\vec{l}$ is invariant does not mean that $\vec{k}$ is. $\vec{k}$ will always be light-like, but in general, we can write

$$\Lambda(\vec{k}) = \underbrace{a \vec{l} + b \vec{k}}_{\in P} + \underbrace{\vec{m}}_{\in Q}, \tag{1.33}$$

where the plane $Q$ is orthogonal to plane $P$ (Fig. 1.7, right). Using (*i*) relation $\Lambda(\vec{k}) \cdot \Lambda(\vec{l}) = -2$, (*ii*) the fact $\vec{l}$ and $\vec{k}$ are light-like vectors, and (*iii*) that $\vec{m}$ is orthogonal to both $\vec{l}$ and $\vec{k}$, it comes that $b = e^{-\psi}$ and

$$\vec{m} \cdot \vec{m} = 4a \, e^{-\psi}. \tag{1.34}$$

Since $\vec{m}$ is in plane $Q$, $\vec{m}$ is space-like, so $a \geqslant 0$. From $\vec{m}$, we define a unit vector $\vec{e_2} = e^{\psi}/(4\alpha)\vec{m}$ where $\alpha = \sqrt{a}e^{\psi/2}/2 \geqslant 0$ [11]. By construction, $\vec{e_2}$ is orthogonal to both $\vec{l}$ and $\vec{k}$. We can then write

$$\Lambda(\vec{k}) = e^{-\psi} \left( 4\alpha^2 \vec{l} + \vec{k} + 4\alpha \vec{e_2} \right). \tag{1.35}$$

---

[9] Again, I will not demonstrate that. This is done in [74].

[10] $\Lambda$ is an isomorphism so $\lambda \neq 0$, and it is also orthochronous, so $\lambda > 0$.

[11] Parameter $a$ could be used instead of $\alpha$, but $\alpha$ allows to simplify notations.

From this equation, it can be seen that when $\alpha = 0$, $\overrightarrow{\mathbf{k}}$ is invariant. In that case, $\overrightarrow{\mathbf{e_2}}$ can be chosen arbitrarily in plane $Q$ and as $\overrightarrow{\mathbf{l}}$ is invariant too, there are two distinct invariant light-like directions.

To complete the basis we are looking for, we need a fourth vector $\overrightarrow{\mathbf{e_3}}$ and we need to express $\Lambda(\overrightarrow{\mathbf{e_2}})$ and $\Lambda(\overrightarrow{\mathbf{e_3}})$. For this, we can still use vectors $\overrightarrow{\mathbf{l}}$ and $\overrightarrow{\mathbf{k}}$ to decompose $\Lambda(\overrightarrow{\mathbf{e_2}})$:

$$\Lambda(\overrightarrow{\mathbf{e_2}}) = u\,\overrightarrow{\mathbf{l}} + v\,\overrightarrow{\mathbf{k}} + x\,\overrightarrow{\mathbf{e_2}} + y\,\overrightarrow{\mathbf{e_3}}. \tag{1.36}$$

From Eqs. 1.31, 1.32, and using the fact that $\overrightarrow{\mathbf{l}}\cdot\overrightarrow{\mathbf{e_2}} = 0$, it comes that $v = 0$. Since $\overrightarrow{\mathbf{e_2}}$ is normalized, $\overrightarrow{\mathbf{e_2}}\cdot\overrightarrow{\mathbf{e_2}} = 1$, which leads to $x^2 + y^2 = 1$. Then, we can introduce a parameter $\varphi \in [0, 2\pi[$ so that $x = \cos\varphi$ and $y = \sin\varphi$. Finally, from Eq. 1.33, and since $\overrightarrow{\mathbf{k}}\cdot\overrightarrow{\mathbf{e_2}} = 0$, we get that $u = 2\alpha\cos\varphi$. So,

$$\Lambda(\overrightarrow{\mathbf{e_2}}) = (2\alpha\,\cos\varphi)\,\overrightarrow{\mathbf{l}} + \cos\varphi\,\overrightarrow{\mathbf{e_2}} + \sin\varphi\,\overrightarrow{\mathbf{e_3}}. \tag{1.37}$$

$\Lambda(\overrightarrow{\mathbf{e_3}})$ is obtained with exactly the same method. From Eq. 1.31 and 1.33, and using the expressions of $\overrightarrow{\mathbf{e_0}}$ and $\overrightarrow{\mathbf{e_1}}$ as a function of $\overrightarrow{\mathbf{l}}$ and $\overrightarrow{\mathbf{k}}$, we can at last deduce the general form of a restricted Lorentz transformation in the orthonormal basis $\{\overrightarrow{\mathbf{e_\mu}}\}$:

$$\Lambda^\alpha{}_\beta = \begin{pmatrix} \cosh\psi + 2\alpha^2 e^{-\psi} & \sinh\psi - 2\alpha^2 e^{-\psi} & 2\alpha\cos\varphi & -2\alpha\sin\varphi \\ \sinh\psi + 2\alpha^2 e^{-\psi} & \cosh\psi - 2\alpha^2 e^{-\psi} & 2\alpha\cos\varphi & -2\alpha\sin\varphi \\ 2\alpha e^{-\psi} & -2\alpha e^{-\psi} & \cos\varphi & -\sin\varphi \\ 0 & 0 & \sin\varphi & \cos\varphi \end{pmatrix}, \tag{1.38}$$

where $\psi \in \mathbb{R}$, $\alpha \in \mathbb{R}^+$ and $\varphi \in [0, 2\pi[$.

**Pure boosts and pure rotations**

Two cases are of particular interest [12]:

- $\psi = 0$ and $\alpha = 0$. The matrix $\Lambda^\alpha{}_\beta$ is reduced to

$$\Lambda^\alpha{}_\beta = R^\alpha{}_\beta = \begin{pmatrix} 1 & 0 & 0 & 0 \\ 0 & 1 & 0 & 0 \\ 0 & 0 & \cos\varphi & -\sin\varphi \\ 0 & 0 & \sin\varphi & \cos\varphi \end{pmatrix}. \tag{1.39}$$

  The time component is left unchanged and the spatial coefficients correspond to a rotation matrix of angle $\varphi$. This transformation is called a *pure rotation*. The rotation leaves the time-like plane $P$ invariant.

- $\varphi = 0$ and $\alpha = 0$. The matrix of Eq. 1.38 becomes

$$\Lambda^\alpha{}_\beta = B^\alpha{}_\beta = \begin{pmatrix} \cosh\psi & \sinh\psi & 0 & 0 \\ \sinh\psi & \cosh\psi & 0 & 0 \\ 0 & 0 & 1 & 0 \\ 0 & 0 & 0 & 1 \end{pmatrix}, \tag{1.40}$$

  which is called a *pure boost* of rapidity $\psi$. This transformation leaves the space-like plane $Q$ invariant. In that sense, it can be considered as a *spacetime rotation*. The rapidity $\psi$ meets

---

[12]For completeness, the case where $\psi = 0$ and $\varphi = 0$ corresponds to what are called *null* or *light-like rotations*. These rotations leave the light-like plane containing vectors $\overrightarrow{\mathbf{l}}$ and $\overrightarrow{\mathbf{e_3}}$ invariant.

the requirement [13] $\cosh\psi \geqslant 1$. It is related to speed $v$ by the relation $\tanh\psi = v/c = \beta$ and the quantity $\cosh\psi$ is the Lorentz factor $\cosh\psi = \gamma = 1/\sqrt{1 - v^2/c^2}$. In the case where $\Lambda^0{}_0 = 1 = \cosh\psi$, $v = 0$. Additionally, due to the properties of hyperbolic tangent, $|v| < c$, so $c$ appears as a limit for velocities, only reached by massless particles, as we have seen already.

Finally, it is possible to demonstrate that every restricted Lorentz transformation has a unique decomposition as a composition of a pure rotation and a pure boost:

$$\Lambda = \mathbf{B} \circ \mathbf{R}. \tag{1.41}$$

From the general form given by Eq. 1.38, this decomposition appears clearly in the case $\alpha = 0$. This case corresponds to a transformation that leaves two distinct light-like directions invariant. These transformations are sometimes called *four-screws* [74].

### 1.2.4 Lorentz Invariance and Lorentz Invariance Violation

Some of the readers may have found the three previous sections lengthy, but I think it was necessary to spend some time describing carefully Lorentz Transformations. Indeed, they are often taught to students considering only boosts [14] and ignoring rotations: it is probably tempting to go straight to what is really new and fun.

**Lorentz Invariance**

From what we have seen above, we finally obtain the following definition of *Lorentz invariance*:

> Lorentz Invariance corresponds to invariance by rotations and boosts.

In §1.1, using a rotation as an example of a basic transformation, I actually illustrated one aspect of Lorentz invariance and Lorentz invariance violation. Lorentz invariance guarantees that the photons emitted by a light source will all have the same velocity, regardless the direction they have (rotation invariance) and no matter if the light source and the observer are moving or not (boost invariance). In addition, all inertial observers will agree on these results (relativity principle).

We already encountered a quantity which is obviously Lorentz invariant: the metric tensor $g^{\alpha\beta}$. Indeed, we have seen (Eq. 1.29) that:

$$\Lambda^\mu{}_\alpha \Lambda^\nu{}_\beta g^{\alpha\beta} = g^{\mu\nu}.$$

We have seen also that all ingredients of Special Relativity can be deduced from the structure of Minkowski spacetime and the principle of invariance of the metric. Lorentz symmetry is therefore the defining property of Special Relativity. Special Relativity is in turn a building block of both Quantum Field Theory (QFT) and General Relativity (GR). Through GR, it is also a crucial ingredient of modern cosmology. Actually, it is very often considered as the building block of modern physics as a whole.

**Lorentz invariance and dispersion relations**

Let me consider now the four-vector energy-momentum components $p^\mu = (E/c, \vec{p}) = (m\gamma c, m\gamma \vec{v})$. For a massless particle, $m = 0$ and it comes immediately that this vector is light-like. So, in a flat spacetime,

$$\eta_{\mu\nu} p^\mu p^\nu = -(E/c)^2 + p^2 = 0, \tag{1.42}$$

---

[13] Remember that $\Lambda^0{}_0 \geqslant 1$ since $\Lambda$ is orthochronous.
[14] I used to do that too, shame on me!

where I have noted $p^2 \equiv \vec{p} \cdot \vec{p}$. We then obtain the dispersion relation [15]

$$E^2 = p^2 c^2. \tag{1.43}$$

Finally, if we remember that the group velocity is given by $v_g = \partial E / \partial p$, it appears obviously what we already knew: the speed of a massless particle is such that

$$v_g = \frac{\partial E}{\partial p} = c. \tag{1.44}$$

For a particle of mass $m \neq 0$, the dispersion relation becomes

$$\eta_{\mu\nu} p^\mu p^\nu = -(E/c)^2 + p^2 = -m^2 \gamma^2 c^2 + m^2 \gamma^2 v^2, \tag{1.45}$$

which gives

$$E^2 = p^2 c^2 + m^2 c^4. \tag{1.46}$$

In that case, the group velocity depends on the energy of the particle:

$$v_g = \frac{p c^2}{E}. \tag{1.47}$$

**Lorentz Invariance Violation**

In §1.1.2, I illustrated a case where rotation invariance is violated. As rotation is part of Lorentz transformations, I actually gave an example of Lorentz Invariance Violation (LIV). This violation appears as a change of the measured velocity of photons when the operator change the direction of the light beam. This can be generalized to boost invariance. Boost invariance violation would manifest itself if two operators, one of them moving in the reference frame of the other, would not measure the same speed of light. As the two observers would not agree on their results, they would immediatly conclude that the relativity principle fails: their reference frames are not equivalent.

As we have already seen, this last point translates into the fact there is a preferred frame of reference. As a result, in all theories where LI can be violated, the chosen frame of reference has to be specified explicitly. Two frames are commonly chosen: the rest frame of the Cosmic Microwave Background (CMB) and the Sun-centered frame.

The use of the rest frame of the CMB as the preferred frame is nicely justified by the observation of the dipole anisotropy component of the CMB. This component is due to the Doppler shift of CMB photons due to the movement of the solar system in the Galaxy and to the movement of the Galaxy itself in the rest frame defined by the last scattering surface of the CMB. The latest results from the *Planck* satellite are illustrated in Fig. 1.8 [145]. Such a map illustrates the fact the barycentre of the Solar System is moving in the direction of $+\vec{\beta}_\parallel$ as compared to the CMB rest frame. Its speed in the CMB rest frame as measured by *Planck* is 384 km.s$^{-1}$ ± 78 km.s$^{-1}$ (stat.) ± 115 km.s$^{-1}$ (syst.). A part of this speed is due to the movement of the Sun around the Galactic center (~230 km.s$^{-1}$). For an experiment located on Earth, the motion of the Earth around the Sun and the rotation of the Earth around its axis have to be taken into acount too. As a result, the velocity of a laboratory located on Earth with respect to the CMB rest frame shows daily and yearly modulations (Fig. 1.9). Considering the fact that the Sun takes roughly 240 million years to orbit around the Galaxy, a duration considerably longer than the duration of any experiment, it is reasonable to assume its movement is rectilinear with respect to the CMB rest frame. Then,

---

[15]When considering photons as quanta of electromanetic waves, this relation can of course be obtained from Maxwell equations and take the form $\omega^2 = k^2 c^2$.
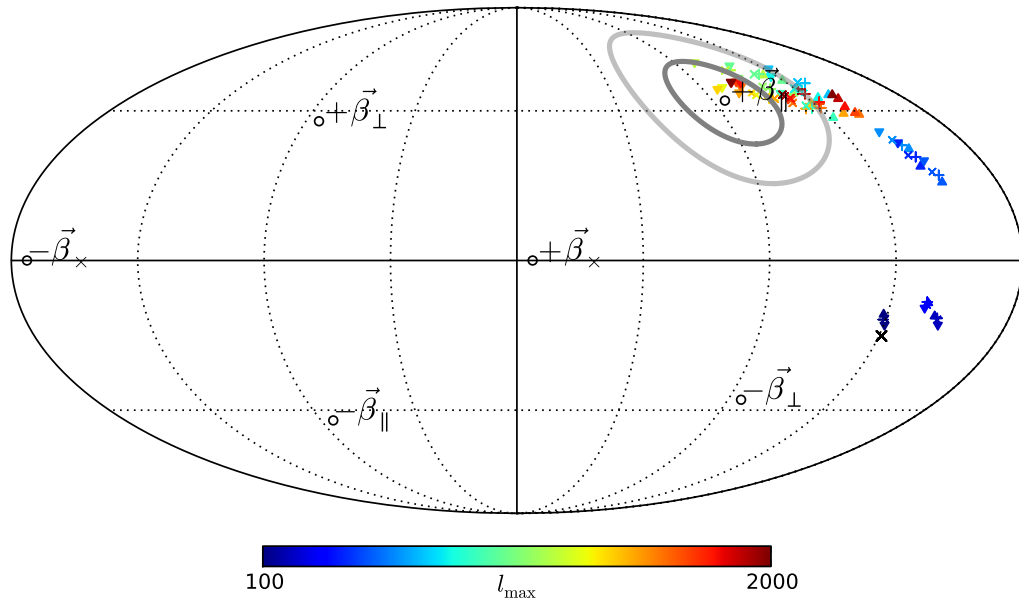
**Figure 1.8:** CMB dipole direction as measured by Planck in galactic coordinates. The direction $\vec{\beta}$ is given by its components $\vec{\beta}_{\perp}$ and $\vec{\beta}_{\parallel}$. Uncertainty on dipole direction are given by 14° and 26° radius circles. For more details on the data points, see [145].
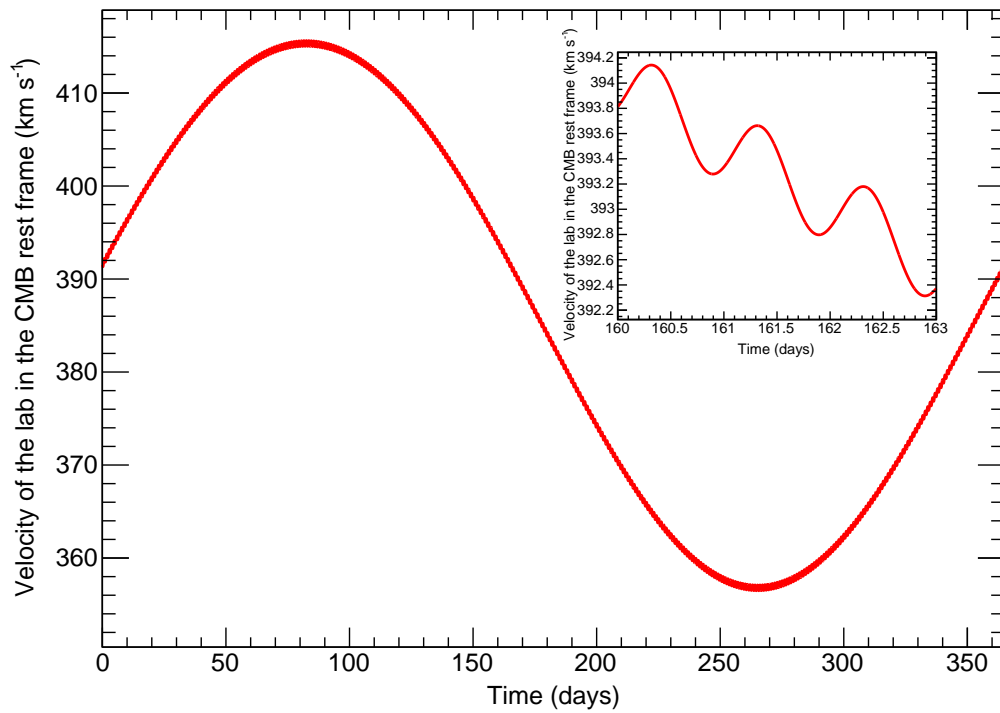


**Figure 1.9:** Velocity of a laboratory located on Earth (in Paris) with respect to the CMB rest frame as a function of time. The inset shows a zoom of the curve emphasizing the daily modulation of the velocity.

the Sun-centered reference frame can be considered to be inertial. That is why it is used for LIV studies in some frameworks (see §1.3).

As a consequence of LIV, SR falls apart. And if SR falls apart, then QFT and GR do the same. Furthermore, I have tried to show in the previsous sections that Lorentz Invariance is intimately connected to the fundamental nature of spacetime. Therefore, as stated by S. Liberati [111], it is our "*compelling duty*" to test LI as far as we can.

LIV could manifest itself in a number of ways in addition to the example I gave earlier (§1.1.1). I shall discuss some of its consequences in the context of astroparticle physics in Chapter 2. As a first glimpse, let me give another example. A *modified dispersion relation* (MDR) for photons propagating *in vacuum* would result in LIV. In that case, we could have $E^2 \neq p^2 c^2$ for massless particles, whatever the way this inequality is obtained. For example, in the context of QG phenomenology, we will encounter a MDR [16] of the form

$$E^2 = p^2 c^2 + f(E, E_{QG}),  \tag{1.48}$$

where $f$ is a function of the photon energy and of $E_{QG}$, the energy scale of hypothetical QG effects.

Comparing this dispersion relation with the one of a massive particle (Eq. 1.46), we can notice that QG effects result in the fact the photon acquire an *effective mass* $m_\gamma^2 = f(E, E_{QG})/c^4$. So QG effects, in addition to introduce a dependance of the speed of the photons with their energy, can also modify the dynamics of particle interactions which involve photons, such as the pair production mechanism $\gamma_{VHE} + \gamma_{CMB} \rightarrow e^+ + e^-$. I will discuss this a little further in the next chapter.

### Violation and deformation

Back in the 60s, it was proposed that there could be a second observer-independant length scale, in addition to the observer-independant velocity scale $c$ [139]. This initial proposal was justified observing that the values accepted at that time for the strong interaction distance, the diameter of a proton and the classical radius of the electron were all of the order $\sim 10^{-13}$ cm.

This kind of idea re-emerged recently due to both the fundamental importance of the Planck scale in the context of Quantum Gravity and the appearance of MDR in some QG approaches [17]. The basic idea is that the Planck length (or at least a Planckian length scale) should have the same meaning and the same value for all inertial observers, *i.e.* QG effects should arise at the same scale for all of them. This led G. Amelino-Camelia to propose the so-called *Doubly-Special Relativity* (DSR) (see [18] for the original paper and [16] for a recent progress report). This scenario naturally introduce a MDR of the form given by Eq. 1.48, but all inertial observers agree on this relation: there is no preferred frame of reference. Because of this key feature, Lorentz Invariance is said to be *deformed* rather than *violated*.

### Local Lorentz Invariance

Special relativity is a theory of flat spacetime *i.e.* a spacetime with no gravity. However, while conducting experiments, we cannot get rid of spacetime inhomogeneities brought by gravity, unless we consider a region of spacetime small enough and freely falling so that it can be considered as gravity-free according to the equivalence principle. In that case, inhomogeneities can be ignored and spacetime can be considered as flat. That is what the adjective *local* means.

Local Lorentz Invariance (LLI) means that "the outcome of any local non-gravitational experiment is independent of the velocity of the freely-falling reference frame in which it is performed."

---

[16]The fact the dispersion relation can be modified for photons in vacuum implies necessarily that Maxwell equations have to be modified as well.

[17]The connexion between Planck scale and QG will be discussed in the next chapter.

[169]. LLI is a part of Einstein Equivalence Principle (EEP), which is itself a building block of all metric theories of gravitation, including GR.

### Lorentz covariance

The expression "*Lorentz covariance*" is sometimes used when refering to invariance of *equations* instead of simple quantities such as the norm or the scalar product of vectors. An equation $A^{\mu\nu} = B^{\mu\nu}$ satisfied in a given frame is Lorentz covariant if it holds in any other frame:

$$(A^{\mu\nu})' = \Lambda^\mu{}_\alpha \Lambda^\nu{}_\beta A^{\alpha\beta} = \Lambda^\mu{}_\alpha \Lambda^\nu{}_\beta B^{\alpha\beta} = (B^{\mu\nu})' \,.$$

### Lorentz and CPT symmetries

I have already introduced **P** and **T** operators in §1.2.3: **P** is the parity transformation, the simultaneous flip in the sign of all three spatial coordinates, and **T** is the time-reversal transformation. In "*CPT*", **C** corresponds to the charge conjugation operation, the transformation that allows to flip the sign of all charges (not only the electrical charge but also *e.g.* the color charge of quarks, etc.) in the theory. Combining the discrete [18] symmetries **C**, **P** and **T**, one gets the CPT symmetry. Until now, CPT has always been found to be an exact symmetry, whereas **C**, **P** and **T** as well as the pairs **CP**, **CT**, **PT** have all been found to be violated in some conditions. Very accurate tests of CPT symmetry can be achieved using neutral mesons (see *e.g.* [100, 133]).

Charge conjugation is not related to the Lorentz group of spacetime symmetries in any obvious way. However, it is possible to understand that they are linked together considering that for a given theory, (*i*) **C** is an internal symmetry of the theory itself and (*ii*) Lorentz symmetry is bounded to the structure of spacetime and any theory has to be settled in a given spacetime.

As a result, CPT symmetry is tightly connected to Lorentz symmetry since "*every relativistic quantum field theory has a symmetry that simultaneously reverses charge (**C**), reverses the orientation of space (or parity, **P**), and reverses the direction of time (**T**).*" (quoted from [75], another similar formulation can be found in [155]). This is the so-called *CPT theorem*. Now of course, since every *relativistic* Quantum Field Theory (QFT) has Lorentz symmetry, the theorem can be reduced to "*Lorentz symmetry implies CPT symmetry*".

It is then no surprise if CPT symmetry violation and Lorentz violation are considered together in theoretical frameworks such as the Standard Model Extension (SME, see §1.2.4).

### Section Summary

In this section, I have tried to introduce as carefully as possible several important notions: Minkowski spacetime, Lorentz Transformations, Lorentz Invariance and Lorentz Invariance Violation. In the process, I have shown that Lorentz Transformations and therefore also Lorentz Invariance are emanations of the fundamental structure of spacetime. Therefore it is not really surprising if different approaches of Quantum Gravity, where spacetime is supposed to become a quantum medium, have questioned the fate of Lorentz Invariance.

Before introducing tests of Lorentz Invariance with photons from astrophysical sources in the context of Quantum Gravity phenomenology in the next chapter, I will discuss two test theories used for LI tests, and I will comment on some "classical" optical tests of Lorentz Invariance, designed and conducted out of Quantum Gravity phenomenology.

---

[18]A symmetry can be discrete or continuous. **C** is a discrete symmetry since, *e.g.* considering the electrical charge, positrons and electrons have a charge $\pm e$. Lorentz symmetry is continuous since, *e.g.* considering rotations, the angle of the rotation can take any value between 0 and $2\pi$.

## 1.3  Test theories for Lorentz Invariance

When a theory needs to be tested, it cannot be considered as true. Therefore another framework has to be used. This framework usually has a broader scope and is designed so that it includes free parameters which allow to recover the theory to be tested when they are equal to specific values, *e.g.* zero. I will now briefly discuss two test theories of interest in the context of LI tests. The first one, the Robertson-Mansouri-Sexl (RMS) framework is *purely kinematical*: it is all about the relations between different observers. The second one, the Standard Model Extension (SME) is a *dynamical* test theory: it is based on a generalization of the equations of motion. As its name can suggest, the scope of SME is very broad: it is an extension of the Standard Model of particle physics including gravity and all possible terms for Lorentz and CPT violation. A third test theory will be introduced when I will discuss modified photon dispersion relations in the context of QG (Chapter 2). The reader should be aware that other frameworks exist: *e.g.* the $c^2$ framework [169], the $TH\epsilon\mu$ framework [112], etc. I will not discuss them here.

### 1.3.1  The Robertson-Mansouri-Sexl framework

In his paper of 1949 [147], H. P. Robertson purposely replaced Einstein twin postulates by some other hypotheses:

- There exist a reference frame $\mathcal{R}$ in which light is propagated rectilinearly and isotropically with a constant speed $c$. $\mathcal{R}$ is the preferred frame, usually considered to be the rest frame of the CMB;

- There exist another frame $\mathcal{R}'$ which is moving with a constant velocity $\vec{v}$ with respect to $\mathcal{R}$;

- Space is euclidian, and cartesian coordinates are used.

Then he proceeds to determine the coefficients of the matrix he notes $a$ allowing to change from the coordinates of an event in $\mathcal{R}$, $x^\mu = (t, x, y, z)$, to its coordinates in $\mathcal{R}'$, $x'^\mu = (t', x', y', z')$:

$$x'^\mu = a^\mu_\nu x^\nu. \tag{1.49}$$

Using appropriate choices for clock synchronization, spatial axes and noticing the only important vector to describe the kinematics of the system is $\vec{v} = v\vec{e_x}$, most of the sixteen coefficients $a^\mu_\nu$ vanish and only three free parameters remain [19], which *a priori* depend on $v$:

$$a^\mu_\nu = \begin{pmatrix} a^0_0 & va^1_1/c^2 & 0 & 0 \\ va^0_0 & a^1_1 & 0 & 0 \\ 0 & 0 & a^2_2 & 0 \\ 0 & 0 & 0 & a^2_2 \end{pmatrix}. \tag{1.50}$$

SR is recovered when $a^0_0 = a^1_1 = \gamma$ and $a^2_2 = 1$.

Reza Mansouri and Roman U. Sexl introduced a very similar framework in 1977 [118, 119, 120]. Even if they discussed the issue of clock synchronization in much more depth than Robertson and used different notations, the similarities between the two approaches justify the fact they are usually considered together under the name *Robertson-Mansouri-Sexl* (RMS) framework.

As all papers discussing experiments in the RMS framework use Mansouri and Sexl notations, I will close this section by describing very quickly their formalism.

---

[19]Note that only boosts are considered here.

Mansouri and Sexl transformation laws are given by [20]

$$
\begin{cases}
t' = & a(v)t + \epsilon(v)x' \\
x' = & b(v)(x - vt) \\
y' = & d(v)y \\
z' = & d(v)z.
\end{cases}
\tag{1.51}
$$

The new parameter $\epsilon(v)$ is entirely determined by chosing a synchronization procedure, whereas $a(v)$, $b(v)$ and $d(v)$ are the free parameters of the model.

Considering the Galilean transformations should be obtained in the limit of small speeds [21], $a$, $b$, and $d$ are expanded to leading order in $v^2/c^2$:

$$
\begin{aligned}
a(v) &\sim & 1 + \alpha \, v^2/c^2 \\
b(v) &\sim & 1 + \beta \, v^2/c^2 \\
d(v) &\sim & 1 + \delta \, v^2/c^2,
\end{aligned}
\tag{1.52}
$$

where $\alpha$, $\beta$ and $\delta$ are the new parameters to be determined. The fact that $a$, $b$, and $d$ are even functions can be viewed as a consequence of isotropy in the preferred frame of reference. From Eqs. 1.51 and 1.52, we can notice that $\alpha$, $\beta$ and $\delta$ are related respectively to time, length in the direction of motion, and length perpendicular to the direction of motion.

The parameters $\alpha$, $\beta$ and $\delta$ are used by Mansouri & Sexl to express the speed of light $c'$ in $\mathscr{R}'$ as a function of the angle $\theta$ between the direction of light propagation and the direction of $\vec{v}$ (magnitude $v$), the velocity of the reference frame $\mathscr{R}'$ in the preferred frame $\mathscr{R}$:

$$
\frac{c'(\theta, v)}{c} \sim 1 + \underbrace{(\alpha - \beta + 1)}_{A} \frac{v^2}{c^2} + \underbrace{(\beta - \delta - 1/2)}_{B} \frac{v^2}{c^2} \sin^2 \theta.
\tag{1.53}
$$

Experimental searches for LIV in the RMS framework usually provide limits on the terms $A \equiv \alpha - \beta + 1$, $B \equiv \beta - \delta - 1/2$ and $C \equiv \alpha + 1/2$. Special Relativity is recovered for $\alpha = -1/2$, $\beta = 1/2$ and $\delta = 0$. In that case, lengths are contracted ($\beta = 1/2$) in the direction of motion ($\delta = 0$), time is dilated ($\alpha = -1/2$), $c'(\theta, v)/c \sim 1$ and Lorentz Invariance holds.

**Some remarks on RMS framework**  RMS framework is not used in the context of QG phenomenology where a framework like the one I will introduce in Chapter 2 is generally preferred. However, because it is very simple, it is still widely used in addition to SME for optical experiments. RMS framework is fully contained into the SME.

### 1.3.2   Standard Model Extension

In this section, natural units are used: $c = \hbar = 1$.

The Standard Model Extension (SME), developed by V. A. Kostelecký and his collaborators is a *dynamical* framework based on Lagrangian formalism including the Standard Model (SM), General Relativity (GR) and all possible terms accounting for CPT and LI violation [22] (CPTV+LIV) [101, 48, 49]:

$$
\mathscr{L}_{SME} = \mathscr{L}_{SM} + \mathscr{L}_{GR} + \mathscr{L}_{CPTV+LIV}
\tag{1.54}
$$

In such a framework, both SM and GR are considered as low energy effective field theories (EFTs) of a *full* theory beyond the Sandard Model (*e.g.* Quantum Gravity): SM and GR are

---

[20]Note the parameter $x'$ in the expression of $t'$. This is not a typo.

[21]Galilean transformations are obtained for $a(v) = b(v) = d(v) = 1$. Time is universal, so there is no need for a synchronization procedure. Hence, $\epsilon(v) = 0$.

[22]The violation involves only particle transformations. The symmetry under observer transformations is preserved.

low-energy limits of the underlying theory of QG and additional terms (here for LIV, which is not observed at low energies) are assumed to be suppressed by some energy scale $M$:

$$\mathscr{L}_{LIV} = \sum_{n}^{\infty} c_n \frac{E^n}{M^n}, \tag{1.55}$$

where coefficients $c_n$ have to be constrained by experiments. In pratice, the series expansion is limited to some finite value for $n$ considering that high order terms are usually negligible and impossible to constrain experimentally. For more details on EFTs, readers are kindly invited to have a look at reference [97].

Let me now give an explicit example, focusing on the photon sector of the full SME [103] which is of particular interest for astrophysical tests of modified photon dispersion relations [102]. The Lagrangian is given by

$$\mathscr{L} = -\frac{1}{4} F_{\mu\nu} F^{\mu\nu} + \frac{1}{2} \epsilon^{\kappa\lambda\mu\nu} A_\lambda (\hat{k}_{AF})_\kappa F_{\mu\nu} - \frac{1}{4} F_{\kappa\lambda} (\hat{k}_F)^{\kappa\lambda\mu\nu} F_{\mu\nu}, \tag{1.56}$$

where $A_\mu$ is the four-potential and $F_{\mu\nu} = \partial_\mu A_\nu - \partial_\nu A_\mu$ the field strength. Series expansions appear in the definition of the two parameters $(\hat{k}_{AF})_\kappa$ and $(\hat{k}_F)^{\kappa\lambda\mu\nu}$:

$$(\hat{k}_{AF})_\kappa = \sum_{d \text{ is odd}} \left( k_{AF}^{(d)} \right)_\kappa^{\alpha_1...\alpha_{(d-3)}} \partial_{\alpha_1}...\partial_{\alpha_{(d-3)}} \tag{1.57}$$

$$(\hat{k}_F)^{\kappa\lambda\mu\nu} = \sum_{d \text{ is even}} \left( k_F^{(d)} \right)^{\kappa\lambda\mu\nu\alpha_1...\alpha_{(d-4)}} \partial_{\alpha_1}...\partial_{\alpha_{(d-4)}} \tag{1.58}$$

In the previous expressions, $d > 4$ is the dimension of the tensor operator controlling the amount of LIV. Since we are going to mention *linear* and *quadratic* LIV effects in the next chapter, it is worth to mention now that linear (resp. quadratic) effects correspond to $d = 5$ (resp. $d = 6$) operators.

$(\hat{k}_{AF})_\kappa$ and $(\hat{k}_F)^{\kappa\lambda\mu\nu}$ terms involve CPT-odd and CPT-even violations respectively [23]. In the case there is no LIV, $(\hat{k}_{AF})_\kappa = (\hat{k}_F)^{\kappa\lambda\mu\nu} = 0$ and the Lagrangian is reduced to its "standard" well-known expression:

$$\mathscr{L} = -\frac{1}{4} F_{\mu\nu} F^{\mu\nu}. \tag{1.59}$$

As it is possible to derive *classical* Maxwell equations from the electromagnetic Lagrangian of Eq. 1.59, it is possible to obtain a modified version of Maxwell equations including LIV starting from Eq. 1.56. I will not go into the details on this and I will go directly to what is really interesting for the rest of this memoir: dispersion relation.

In SME, the dispersion relation is obtained when considering a special model of vacuum, where electromagnetic fields are approximated by plane waves. The dispersion relation is given by

$$\left(p^\mu p_\mu - (\hat{c}_F)^{\mu\nu} p_\mu p_\nu\right)^2 - 2(\hat{\chi}_w)^{\alpha\beta\gamma\delta} \times (\hat{\chi}_w)_{\alpha\mu\gamma\nu} p_\beta p_\delta p^\mu p^\nu - 4(p^\mu (\hat{k}_{AF})_\mu)^2 \simeq 0, \tag{1.60}$$

where $(\hat{\chi}_w)_{\alpha\mu\gamma\nu}$ and $(\hat{c}_F)^{\mu\nu}$ are new coefficients obtained from $\hat{k}_{AF}$ and $\hat{k}_F$ in a rather complex way I will not detail. It is enough to remember that $(\hat{\chi}_w)_{\alpha\mu\gamma\nu}$ is related to *birefringence*, a property of vacuum which result in the fact that the speed of photons can depend on their polarization. $(\hat{c}_F)^{\mu\nu}$ term is related to nonbirefringent effects, namely the dependance of the speed of the photons with their energy. Note that the standard dispersion relation $p^\mu p_\mu = 0$ (Eq. 1.42) is recovered when all SME coefficients are set to zero.

---

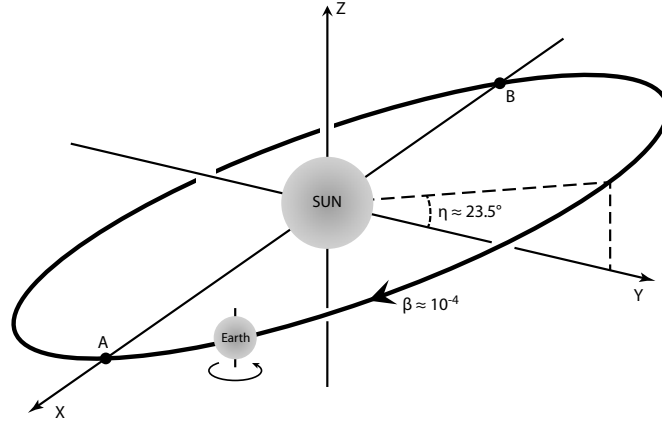[23]CPT-odd(-even) because the number of indices is odd (even).

**Figure 1.10:** The Sun-centered equatorial frame as used in SME. The origin of the frame is the center of the Sun and the time T = 0 is taken at the Vernal Equinox of year 2000. The X axis cross Earth's orbit in A (Vernal Equinox) and B (Autumnal Equinox). Axis Z is parallel to the Earth's rotation axis at T = 0 and directed North. The Y axis completes a right-handed system.

**Table 1.1:** Summary of the SME coefficients in the photon sector and the possible ranges of the indices $d$ and $j$. The last column gives the total number of coefficients.

| Coeff. | $d$ | $j$ | Number of coefficients |
|---|---|---|---|
| $c_{(I)jm}^{(d)}$ | even, $\geqslant 4$ | $0, 1, ..., d-2$ | $(d-1)^2$ |
| $k_{(E)jm}^{(d)}$ | even, $\geqslant 4$ | $2, 3, ..., d-2$ | $(d-1)^2 - 4$ |
| $k_{(B)jm}^{(d)}$ | even, $\geqslant 4$ | $2, 3, ..., d-2$ | $(d-1)^2 - 4$ |
| $k_{(V)jm}^{(d)}$ | odd, $\geqslant 3$ | $0, 1, ..., d-2$ | $(d-1)^2$ |

Eq. 1.60 has two solutions at leading order:

$$k(\omega) \approx \left[ 1 + \varsigma^0 \pm \sqrt{(\varsigma^1)^2 + (\varsigma^2)^2 + (\varsigma^3)^2} \right] \omega \tag{1.61}$$

where $k$ is the wave number and $\omega$ the frequency (remember that we use natural units: $c = 1$). Considering that propagation in vacuum is studied using photons from astrophysical sources, it is natural to introduce decompositions using spin-weighted spherical harmonics in the expressions of $\varsigma$ parameters:

$$\begin{aligned}
\varsigma^0 &= \sum_{djm} \omega^{d-4} \, {}_0Y_{jm}(\hat{\mathbf{n}}) c_{(I)jm}^{(d)}, \\
\varsigma^1 \pm i\varsigma^2 &= \sum_{djm} \omega^{d-4} \, {}_{\pm 2}Y_{jm}(\hat{\mathbf{n}}) \left( k_{(E)jm}^{(d)} \mp i k_{(B)jm}^{(d)} \right), \\
\varsigma^3 &= \sum_{djm} \omega^{d-4} \, {}_0Y_{jm}(\hat{\mathbf{n}}) k_{(V)jm}^{(d)},
\end{aligned} \tag{1.62}$$

where $\hat{\mathbf{n}}$ is a unit vector pointing to the astrophysical source under study, where $j$ varies in a range depending on $d$ (See Table 1.1) and where $m$ satisfies the condition $-j \leqslant m \leqslant j$. The new coefficients $c_{(I)jm}^{(d)}$, $k_{(E)jm}^{(d)}$, $k_{(B)jm}^{(d)}$ and $k_{(V)jm}^{(d)}$ can of course be expressed as functions of "initial" parameters $(\hat{k}_{AF})_\kappa$ and $(\hat{k}_F)^{\kappa\lambda\mu\nu}$. $\hat{\mathbf{n}}$ is expressed in the Sun-centered equatorial frame

[29] (Fig. 1.10), considered as inertial [24]. Its coordinates are directly related to the equatorial coordinates of the source (see Section V of reference [103]): $\hat{\mathbf{n}}(90^o - \delta, \alpha)$ where $\delta$ is the declination and $\alpha$ the right ascension. Remember that if LI is violated, then rotation invariance is violated, therefore the speed of the photons on their way to Earth is allowed to vary with the coordinates of the source, *i.e.* with the direction of photon propagation. On the contrary, if rotation invariance is assumed (isotropic case), then $j = m = 0$.

In the context of LIV studies with astrophysical sources, only the cases where $d = 5$ or $d = 6$ are considered. Higher order terms are out of reach for present experiments. If we forget about birefringence for a while, the dispersion relation is simply given by

$$k(\omega) \approx \left[1 + \varsigma^0\right] \tag{1.63}$$

where $\varsigma^0$ will account for either linear or quadratic effects in energy for $d = 5$ or $d = 6$ respectively. The velocity defect $\delta v$ for a photon of energy $E$ is then given by

$$\delta v \simeq -\varsigma^0 = -\sum_{djm} E^{d-4} {}_0Y_{jm}(\hat{\mathbf{n}})c^{(d)}_{(I)jm} \tag{1.64}$$

taking into account anisotropies. For the isotropic case,

$$\delta v \simeq -\frac{1}{\sqrt{4\pi}} \sum_d E^{d-4} \, c^{(d)}_{(I)00}, \tag{1.65}$$

where the fact that ${}_0Y_{00} = Y_{00} = 1/\sqrt{4\pi}$ has been taken into account. Note that the speed of photons can increase or decrease with increasing energies, depending on the sign of the coefficients $c^{(d)}_{(I)jm}$ and $c^{(d)}_{(I)00}$.

The terms in the summations on $d$ are usually considered separately. Going back to the general case where birefringence is allowed, the coefficients that are constrained by experiments (finally!) appear in Eq. 1.62:

$$\sum_{jm} {}_0Y_{jm}(\hat{\mathbf{n}})c^{(d=5,6)}_{(I)jm} \tag{1.66}$$

for non-birefringent CPT-even operators,

$$\sum_{jm} {}_{\pm 2}Y_{jm}(\hat{\mathbf{n}}) \left( k^{(d=5,6)}_{(E)jm} \mp ik^{(d=5,6)}_{(B)jm} \right) \tag{1.67}$$

for CPT-even operators leading to birefringence, and

$$\sum_{jm} {}_0Y_{jm}(\hat{\mathbf{n}})k^{(d=5,6)}_{(V)jm} \tag{1.68}$$

for CPT-odd birefringence. An up-to-date list of all constraints on SME parameters obtained by all possible kinds of experiments can be found on the arXiv [104].

**Some remarks on SME**   By construction, SME is firmly rooted in a hard ground (the standard model of particle physics) and its scope is very wide. It is indeed a very powerful tool. However, as the reader may have noticed, it is rather difficult to introduce SME in a simple way and as a result, it is rather difficult to fully understand it. In my opinion, the fact that its scope is wide can also be a drawback. In addition, on the contrary to what is sometimes claimed, SME is *not* really helpful when comparing different kinds of experiments, since each kind of experiment

---

[24]As we have seen earlier, the Sun can be considered to have a rectilinear motion and a constant velocity in the CMB reference frame.

will constrain different SME parameters. For example, astrophysical tests of modified dispersion relations constrain parameters listed in Table 1.1 while Michelson-Morley experiments constrain other parameters, $\tilde{\kappa}_{e^-}$ and $\tilde{\kappa}_{o^+}$, related to the isotropy of the speed of light. That is probably why people working on astrophysical tests of LI have been quite reluctant to use the SME framework for a long time, and why they would never use it *alone*, but in addition to a simpler test theory as the one I will introduce in Chapter 2.

## 1.4  Classical optical tests of Lorentz Invariance

Historically, LI was first tested using optical experiments. The first one was of course due to Michelson, first alone in 1881 [126] and then in collaboration with Morley in 1887 [127]. Since then, this experiment has been redone numerous times bringing significant technical improvements allowing better and better sensitivities. These "*classical* optical experiments" have been designed and conducted with no connexion with Quantum Gravity phenomenology [25].

### 1.4.1  Two kinds of experiments

The Michelson-Morley (noted MM in the following) experiment is a test of the isotropy of the speed of light, *i.e.* a test of the invariance of $c$ through rotations (as a particle transformation). The other pioneering experiment by Kennedy & Thorndike [99] (KT), which is a test of boost invariance, was also improved continuously up to now. In the following sections, I will focus on these two kinds of experiments, which are, still today, two major ways to test LI. Because of their historical importance I will for each one of them present the original experiment in addition to the modern setups.

As we have seen, in the RMS framework, the speed of light $c'$ in the reference frame of the experiment is given by

$$\frac{c'\left(\theta(t), v(t)\right)}{c} \sim 1 + (\alpha - \beta + 1)\,\frac{v(t)^2}{c^2} + (\beta - \delta - 1/2)\,\frac{v(t)^2}{c^2}\sin^2\theta(t). \tag{1.69}$$

where $c$ is the speed of light in the preferred frame, $v(t) = \|\vec{v}(t)\|$ is the speed of the experiment as measured from the preferred frame and $\theta(t)$ is the angle between the direction of light propagation and $\vec{v}(t)$. Remember that $\alpha$, $\beta$ and $\delta$ are related respectively to time, length in the direction of motion, and length perpendicular to the direction of motion.

The MM and KT experiments are done on Earth, which is spinning around its axis and orbiting around the Sun. As we have seen earlier, the Sun has approximately a rectilinear motion as respect to the CMB rest frame, considered as the preferred frame, but the rotation of the Earth around the Sun and around its own axis results in the fact that the speed of the experiment $v$ as measured in the preferred frame shows yearly and daily modulations. The search for a possible modulation is therefore a key element of the analysis of experimental data.

As a summary,

- MM experiments compare the speed of light in two different directions, corresponding to two different values of $\sin^2\theta(t)$ for a given time. In the RMS framework, they allow to constrain parameter $B = (\beta - \delta - 1/2)$. Since $B$ is multiplied in Eq. 1.69 by a factor $v(t)^2/c^2$, a modulation is expected in the results due to the movement of the apparatus in the preferred frame;

- KT experiments test a combined modulation of the speed of light and of the rate of a clock due to their movement in the preferred frame. They allow to constrain parameter $A = (\alpha - \beta + 1)$.

---

[25] It is worth mentioning however that QG phenomenology recently revived the interest in these *classical* experiments.
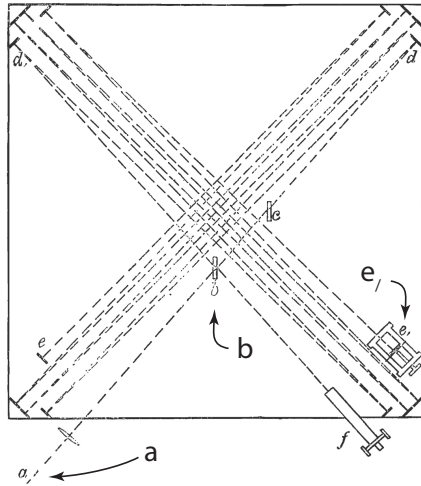
**(a)** The Michelson & Morley apparatus as seen from the top. Figure taken from [127]. Measurements are made using white light emitted in $a$ and split in $b$. The mirror $e_{/}$ (bottom right) can be adjusted to tune the apparatus. Fringes are observed using the telescope $f$. The whole apparatus is allowed to rotate around a vertical axis.
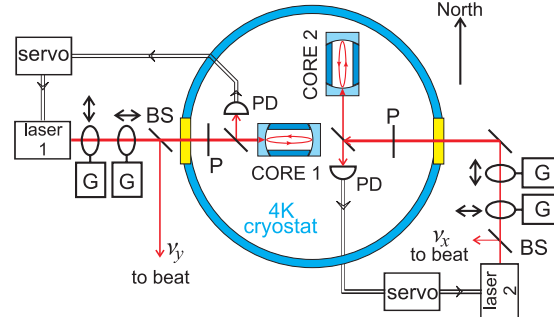
**(b)** Setup used by Müller *et al.* [131]. The two arms of the MM interferometer are replaced by two cryogenic optical resonators (CORE 1 and 2). The cavities are used to stabilize the frequencies of the two laser beams. The beams coming out in "$\nu_y$ to beat" and "$\nu_x$ to beat" are sent to a frequency mixer which is used to measure the beat frequency $\nu_x - \nu_y$. The apparatus cannot be rotated so only the rotation of the Earth is used.

**Figure 1.11:** The original Michelson & Morley experiment, and a modern version of it. 116 years separate these two setups.

MM and KT experiments constrain only combinations of parameters $\alpha$, $\beta$ and $\delta$. In order to find the values of the three parameters, a third experiment is needed, the one first performed by Ives & Stilwell in the late 30s. This beautiful experiment allows to measure directly parameter $\alpha$ by comparing the rates of moving clocks, *i.e.* the frequencies of atomic electron transitions of moving atoms. I will not discuss it further. The interested reader may refer to the original papers [91, 92] and have a look at the results of one of the latest versions of the Ives-Stilwell experiment, described in [33], which allow to obtain the limit $|\alpha| \leqslant 2.0 \times 10^{-8}$.

Before discussing in more details MM and KT experiments, let me mention that LI can be tested with other particles than photons, and with a great deal of different experiments. These tests are beyond the scope of this monograph. A detailed review on "modern" searches for LIV is available [123], although it is ten years old already.

### 1.4.2   From Michelson & Morley to Hermann *et al.*

The Michelson & Morley interferometer is shown on Fig. 1.11a. The light, produced by an oil lamp, is split into two beams. The two arms of the interferometer have the same length. Each beam is reflected 15 times before crossing the beam splitter again, where they interfere. This corresponds to a total length of the arms of ~11 m. The interference fringes are observed (by eye) using a telescope precise enough so that a displacement of 1/100 of a fringe could be detected. This sensitivity made necessary to protect the device against strong temperature variations, vibrations, etc. The entire interferometer was revolved at the slow speed of one turn every 6 minutes and several readings were done for each turn. The measurements were repeated at the same times (so that $\overrightarrow{v}(t)$ and $v(t)^2/c^2$ is kept constant from one measurement to the other), twice per day for three days (a duration small enough to neglect the rotation of the Earth around the Sun).

The expected result was a displacement of 0.4 fringe amplitude, modulated with the rotation of the interferometer. The result of Michelson & Morley was a displacement $\lesssim 0.01$ fringe. So, they concluded that "*[...] if there be any relative motion between the earth and the luminiferous ether, it must be small [...]*". As expressed in the RMS framework, this result leads to $|B| \approx 10^{-3}$. Another parameter is commonly used to express the results of MM experiments: the relative variation of the speed of light for different propagation directions, noted $\Delta_\theta c / c_0$, where $c_0$ is the speed of light in the preferred frame of reference. The MM experiment leads to $\Delta_\theta c / c_0 \approx 10^{-9}$.

The null result of the MM experiment was soon explained using the Fitzgerald-Lorentz contraction hypothesis, a contraction of length in the direction parallel to the direction of motion [68, 113]. However, Lorentz understood [114] that if the proper lengths of the two arms of the interferometer are the same ($L'_1 = L'_2$), then the lengths as seen from a moving frame ($L_1$, $L_2$) just need to verify the relation

$$\frac{L_2}{L_1} = \frac{L'_2 / \varphi}{L'_1 / \gamma \varphi} = \gamma$$

to explain MM null result, where $\varphi$ can be any function of the velocity.

Fig. 1.11b shows a modern version of the MM experiment, used by Müller *et al.* in 2003 to test isotropy of the speed of light [131]. Two cryogenic optical resonators (noted CORE 1 and CORE 2 on the figure) are used to compare the speed of light in two perpendicular directions. On the contrary to MM experiment, the device cannot be rotated so only the rotation of the Earth is used to search for a modulation of the speed of light.

An optical resonator, also called "cavity", is an optical device made of two facing mirrors separated by a transparent material with index of refraction $n$, in which standing light waves are formed for certain resonance frequencies. These frequencies are given by

$$\nu_{\text{cav}} = \frac{k \, c}{2 \, n \, L}$$

where $L$ is the optical path length between the mirrors and $k = 1, 2, 3...$ the mode number.

From this formula, it can be noticed that the frequency of each mode depends on the ratio $c/nL$. For a constant $L$, any variation of the speed of light in the cavity $c/n$ will lead to a shift of its resonance frequencies. Cavities are usually made of extremely stable materials such as sapphire so that variations of $L$ and $n$ due to any possible cause are negligible compared to the change in $c$ due to LI. That is why cryogenic optical cavities are sometimes considered as *length standards*.

Optical resonators have also some drawbacks. Cavities have to be cooled down to ~4 K using liquid Helium, and the temperature has to be controlled precisely since the frequency of cavities, heated by the laser beam, can vary by ~10 Hz/$\mu$W.

In modern MM experiments, cryogenic optical cavities are used to stabilize the wavelength of two lasers using the *Pound-Drever-Hall* (PDH) technique [27, 51] so that a variation of the speed of light in a cavity results in a variation of the frequency of the corresponding laser [26]. The accuracy of the frequency tuning is extreme: the spectral line at 1064 nm obtained with a Nd:YAG laser, corresponding to a frequency of ~280 THz can have a width of 50 kHz to 100 kHz only. The frequencies of the two cavities ($\nu_x$ and $\nu_y$ on the figure) are compared using a frequency mixer that allows to compute the difference $\nu_x - \nu_y$ (beat frequency). A non zero value of this difference, together with daily and yearly modulations would indicate a LIV effect. As each beam of light is reflected ~$10^5$ times in each cavity, and since the cavities are 3 cm long, the light travels ~3 km in each resonator. This fact, together with the extreme accuracy achievable for frequency tuning, explains why resonators are used in MM-type experiments since the 50s in place of old-style optical interferometer experiments.

---

[26]The PDH technique uses a feedback loop architecture. A photodiode (PD on Fig. 1.11b) measures the frequency of the laser beam, a servomechanism (servo) computes a correction that is sent back to the laser for frequency adjustment.
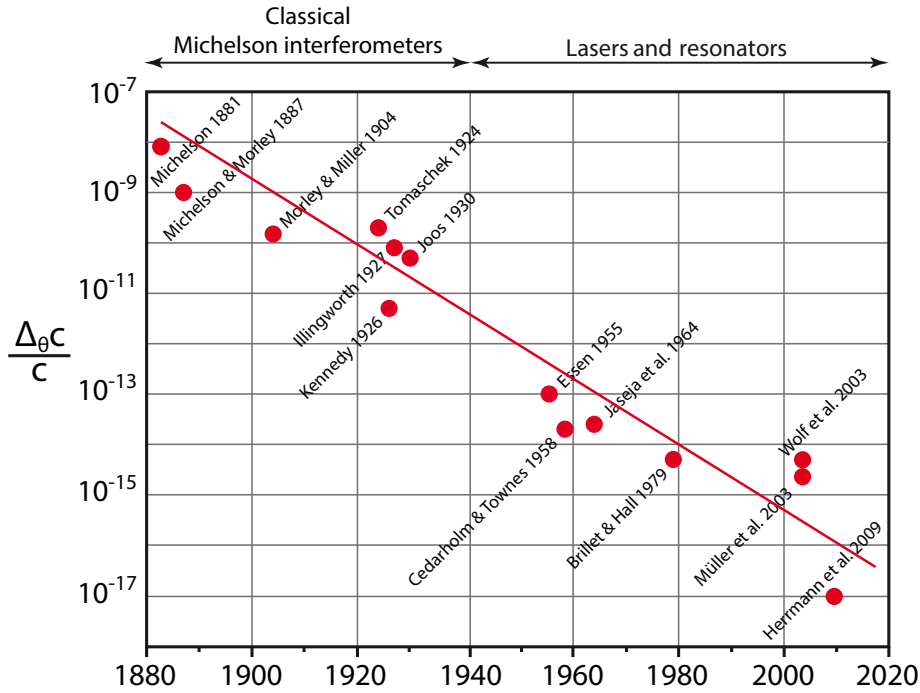
**Figure 1.12:** A selection of measured values of $\Delta_\theta c/c$ from various MM-like optical experiments. Figure from [78], updated to include Hermann *et al.* 2009 data point. Note that the points correspond to measurements, and not to upper limits. List of references: Michelson 1881 [126], Michelson & Morley 1887 [127], Morley & Miller 1904 [130], Tomaschek 1924 [159], Illingworth 1927 [89], Joos 1930 [95], Kennedy 1926 [98], Essen 1955 [64], Cederholm & Townes 1958 [40], Jaseja *et al.* 1964 [94], Brillet & Hall 1979 [35], Wolf *et al.* 2003 [170], Müller *et al.* 2003 [131], Hermann *et al.* 2009 [79].

Müller *et al.*, using 3461 hours of data taking, obtained a value of $B = (-2.2 \pm 1.5) \times 10^{-9}$, which corresponds to $\Delta_\theta c/c_0 \approx (2.6 \pm 1.7) \times 10^{-15}$. The latest result of a MM experiment was obtained by Hermann *et al.* [79] using two cryogenic optical resonators mounted on a rotating table. It is of course a real challenge to design such an experiment where the whole apparatus, including a very stable cryostat, has to rotate. As an example, the position of the rotation axis has to be carefully controlled to minimize systematics: Hermann *et al.* manage to reduce the tilt variations to $< 1$ $\mu$rad using active stabilization. These technical difficulties lead to different sources of systematics that need to be carefully understood and studied. Cumulating data over more than a year and ~130000 rotations of the device, Hermann *et al.* obtained the most stringent results to date: $B = (4 \pm 8) \times 10^{-12}$, corresponding to $\Delta_\theta c/c_0 \approx 10^{-17}$. These last two results as well as many older ones are presented in Fig. 1.12 (next page).

### 1.4.3   From Kennedy & Thorndike to Tobar *et al.*

The goal of the Kennedy-Thorndike (KT) experiment [99] was to test whether the frequency of light depend on the velocity of the Earth in the preferred frame: "*The principle on which this experiment is based is the simple proposition that if a beam of homogeneous light is split [...] into two beams which after traversing paths of different lengths are brought together again, then the relative phases of the superposed beams will depend upon the velocity of the apparatus unless the frequency of the light depends upon the velocity in the way required by relativity.*". Therefore KT experiment is a test of time dilation.

The two assumptions used by Kennedy & Thorndike are: (*i*) the existence of a preferred frame where the speed of light is isotropic, and (*ii*) the fact that, following MM experiment,

lengths are contracted in the direction of motion by a factor $\gamma = (1 - v^2/c^2)^{-1/2}$. Starting from these hypotheses, Kennedy & Thorndike used a MM-like interferometer, but with unequal arms and calculated the fringe shift to be (Eq. 4 in [99]):

$$n = \frac{\Delta L}{\lambda} \gamma,$$

where $\Delta L$ is the difference between the lengths of the interferometer arms and $\lambda$ the wavelength of the light source. A variation of speed, due to a change of the orientation of $\vec{v}$ or of its modulus $v$ would lead to a fringe shift, because of factor $\gamma$, unless $\lambda$ is modified by a factor $\gamma$ as well.

From the previous equation, it can be seen that in addition to using interferometer arms of unequal lengths so that $\Delta L \neq 0$, the use of monochromatic light is essential. In contrast to MM experiment where polychromatic (yellowish) light was used, the use by Kennedy & Thorndike of an emission line of mercury allows to detect a change in the frequency of light due to the movement of the apparatus in the preferred frame. As the mercury radiation frequency only depends on electronic energy levels, it is considered as a *standard of time*.

The original KT experiment is shown in Fig. 1.13a. A prism allows to select the spectral line of mercury at wavelength 546.1 nm. The lamp was carefully designed to minimize the average speed of mercury vapor molecules that would result in a Doppler shift of the spectral lines. Its temperature is also controlled precisely. The interferometer is placed in a vacuum chamber, which is itself surrounded by a water tank. These two improvements as compared to MM experiment allows to reduce temperature variations (to less than 0.001°C) and other environmental changes to minimize modifications of light paths. The difference of the arms lengths is 318 mm. Finally, the interference patterns (rings) are not observed directly but are photographed using plates. Each plate can be used to record several images taken at different times. This facilitates the comparison of the different images, which is done following a rigorous procedure allowing the measurement of tiny variations of rings radii of $\sim 10^{-4}$ fringe. The device cannot be rotated but the expected LIV effect due to daily Earth rotation is a variation of rings radii by a few thousandths fringe.

After several months of data taking, Kennedy & Thorndike did not measure any significant effect. They concluded that "*[...] the frequency of a spectral line varies in the way predicted by relativity*". That is, time is dilated and length is contracted by the same factor. In the RMS framework, the original KT experiment allows to put the constraint [27] $A \lesssim 2 \times 10^{-2}$.

After the original KT experiment performed in 1932, it is necessary to wait 1990 to find a second attempt to perform the same kind of measurement. The experiment designed by Hils & Hall [80] is of course quite different from the original one. They start from the statement that "*The KT experiment can be viewed as a differential comparison between a standard of time defined by a mercury lamp and a standard of length in the form of an unequal-arm Michelson interferometer.*" and use the best standards available at this time. The length standard is given by an optical resonator while the time standard is obtained from an atomic clock. This kind of setup has been used continuously up to now to constrain RMS framework parameter $A$. Hils & Hall obtain an upper limit on $A < 6.6 \times 10^{-5}$.

As an example, I describe the experiment performed by Braxmaier *et al.* in 2002 [34] (Fig. 1.13b). The left part of the figure (labelled "*Length Standard: CORE*") is similar to the setup discussed in the section concerning MM tests: a cryogenic optical resonator (CORE) is used to stabilize the frequency of a Nd:YAG laser. Any variation of the speed of light in the cavity translates into a variation of the frequency. The goal of the right part (labelled "*Time Standard: Iodine transition*") is to translate a possible LIV-induced fluctuation of the rate of an atomic clock,

---

[27]Due to the similarities of MM and KT experiments, it is fairly easy to realize that KT experiments can also be used to constrain parameter $B$. This is done for example in [170]. Some other authors (see *e.g.* [34]) neglect $B$ to give constraints on $A$ only.

**(a)** The Kennedy & Thorndike apparatus as seen from the top. Figure taken from [99]. A mercury line at $\lambda = 546.1$ nm is selected using the prism $P$ and slits. The interferometer itself is placed into a vacuum chamber $V$. The temperature is kept constant to within less than 0.001°C thanks to a tank of water $B$. The interference pattern is photographed using a plate $H$.

**(b)** A modern version of the KT experiment, performed by Braxmaier *et al.* [34]. On the left, a cryogenic optical resonator (CORE) is used as a length standard (as explained in the paragraph concerning MM experiments) to stabilize the frequency of a first laser. On the right, an atomic clock is used as a time standard and stabilize the frequency of a second laser. The frequency outputs of the cavity and the atomic clock are compared to each other in order to detect a correlated variation of length and time standards.
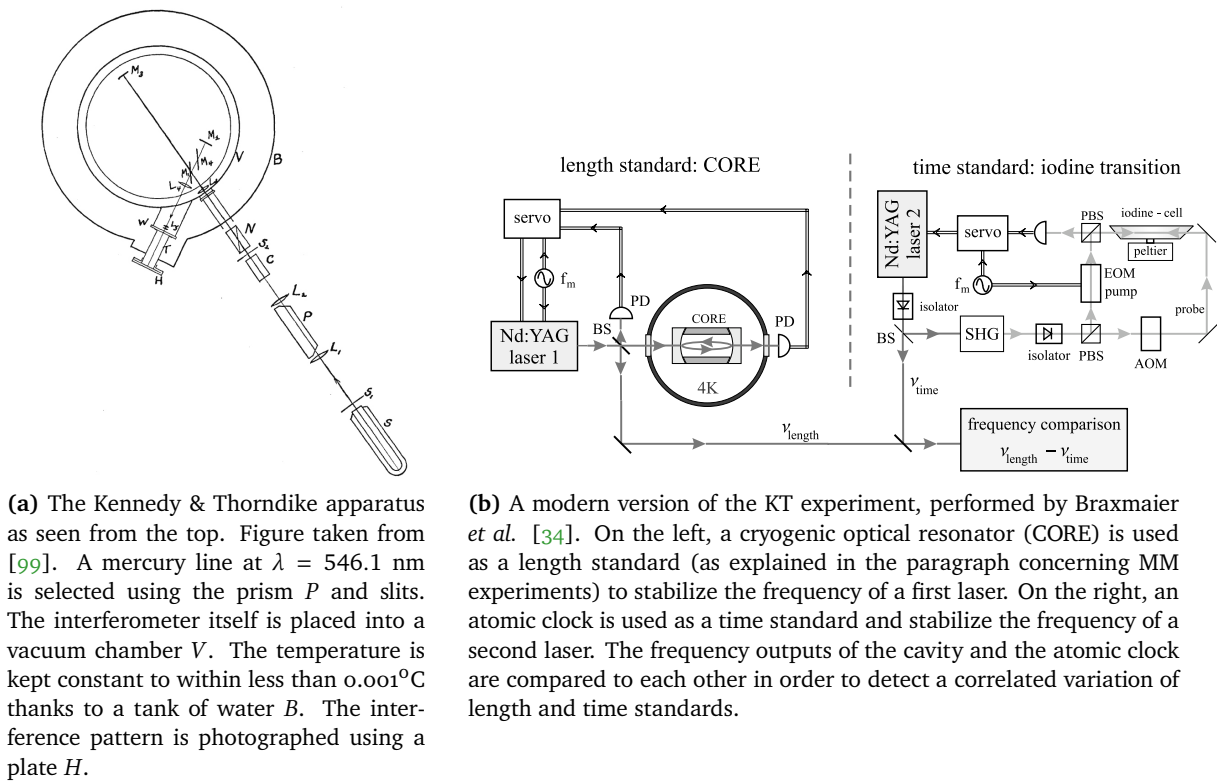
**Figure 1.13:** The original Kennedy & Thorndike experiment, and a modern version of it. 70 years separate these two setups.

that is the frequency of a transition of molecular iodine, into a variation of the frequency of a second laser. This is done through a technique called "Modulation Transfer Spectroscopy" (MTS, see the first chapter of [82] and references therein). By comparing the frequencies of the two lasers through the beat frequency, it is possible to look for possible daily and yearly modulations that would indicate a violation of LI.

Cumulating 190 days of data taking, Braxmaier *et al.* obtain the result $A = (1.9 \pm 2.1) \times 10^{-5}$. This result, as well as several others, is shown on Fig. 1.14. The most recent result to date was obtained by M. E. Tobar and collaborators in 2010 [158].

**Section summary**

When a theory has to be tested, it has to be considered as wrong. Another theory (a *test theory*) has to be constructed instead to introduce free parameters, which will be constrained by experiments. To test Special Relativity, and therefore Lorentz Invariance (LI), several test theories have been introduced, including the two I have discussed: the Robertson-Mansouri-Sexl (RMS) framework, and the Standar Model Extension (SME). The RMS framework is purely kinematical and is widely used for all terrestrial optical experiments. The SME is a dynamical framework, which can be used to test Lorentz Invariance in numerous contexts. It is used in particular in Quantum Gravity phenomenology. Since my interest lies in tests of modified dispersion of photons from astrophysical sources (see the next chapter), I focused my description of the SME on this particular espect.

After discussing test theories, I briefly mentioned two classes of experiments that are used today to test LI with photons: Michelson-Morley experiments are used to probe rotational invariance, while Kennedy-Thorndike experiments test boost invariance.

Because my interest lies in tests of LI with photons, I focused on this particular aspect. The
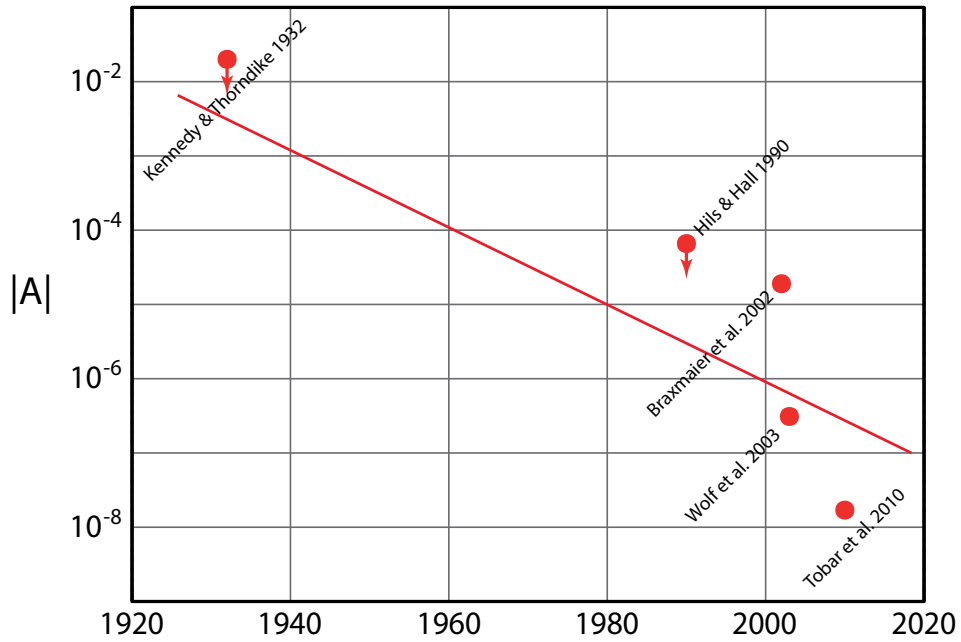
**Figure 1.14:** A selection of measured values of RMS parameter |*A*| from various KT optical experiments. Note that except for Kennedy & Thorndike 1932 and Hils & Hall 1990, the points correspond to measurements, and not to upper limits. List of references: Kennedy & Thorndike 1932 [99], Hils & Hall 1990 [80], Braxmaier *et al.* 2002 [34], Wolf *et al.* 2003 [170], Tobar *et al.* 2010 [158].

reader should be aware that LI can be tested with other particles such as electrons, protons, neutrinos, etc. For more on this, see [104] and [123].

Now, let see what astrophysical photons can tell us about Lorentz Invariance.

# Chapter 2

# Searching for Quantum Gravity signatures with high-energy gamma-ray sources

> 66 *It is a task for the nearest future to identify the ties between quantum mechanics and the theory of gravitation* 99
>
> – M. P. Bronstein, *The Structure of Atom* (1930)

As discussed in the previous chapter, first tests of Lorentz Invariance (LI) were performed with the goal of testing Special Relativity (SR). At the end of the 90s, the situation changed: LI violation (LIV) appeared for the first time as an outcome of a model of String Theory, one of the most popular paths to a full theory of Quantum Gravity (QG). The prediction of this model is that the refraction index of vacuum depends linearly with energy, resulting in the fact the speed of photons in vacuum varies with energy as well. Soon after, G. Amelino-Camelia and collaborators proposed that since QG deals with fundamental (quantum) nature of spacetime, QG effects should have a higher amplitude if photons propagate on a long distance. At that time, LI tests with distant astrophysical sources appeared as a major (and quite unique) way to constrain QG models and hopefuly to reject some of them.

I will start this chapter (Section 2.1) by discussing some key points about QG. As an experimentalist, I could not pretend to give a full overview of all existing models or even fully understand them. I will focus on some QG models which lead to modified dispersion relations (MDR) for photons in vacuum.

Then, I will focus on tests of LIV with high energy photons produced by astrophysical sources. In particular, I will focus on tests of MDR with transient or variable sources: gamma-ray bursts (GRB), flaring active galactic nuclei (AGN) and pulsars (PSR). In Section 2.2, I will come to my main topic of interest: the search for energy dependant time lags. I will first explain what exactly we want to measure. The gamma-ray sources play the role of particle accelerators. I will comment on these accelerators. Then, I will give the current status of experimental searches for MDR with photons from astrophysical sources (Section 2.3). By doing this, I will have the

opportunity to comment on some of my publications. To conclude this chapter (Section 2.4), I will quickly review the other QG effects that could be detected with high energy gamma-rays.

## 2.1   LIV in Quantum Gravity models

### 2.1.1   The need for a quantum theory of gravity

The aim of QG is to describe *quantum properties of the gravitational interaction*. And since gravitation is understood in General Relativity as a curvature of spacetime, QG has to describe *quantum properties of spacetime*.

General Relativity, introduced by Einstein in 1915 [54], is a classical and not a quantum theory. On the other hand, the other three interactions (weak, strong, electromagnetic) are described in the framework of quantum mechanics through Quantum Field Theory (QFT), the field theory underlying the Standard Model (SM) of particle physics. Both GR and QFT/SM are tested to a remarkable precision. A review concerning experimental tests of GR is given in [169], while the success of SM was lately illustrated again by the discovery of a new particle that is most probably the Higgs boson [42], more than 50 years after its prediction.

Einstein himself commented (for the first time in 1916 and several times after that) on the possible connexion between quantum mechanics and GR. His argument was basically that an electron moving around an atom following quantum mechanics laws should produce gravitational waves in addition to electromagnetic radiation. He considered this fact as *"hardly true in nature"* [55], therefore concluding: *"It seems that a more complete quantum theory would also have to bring about a modification of the theory of gravitation"* [56].

At the very end of his book about GR, "Report on Relativity Theory of Gravitation" [52], Arthur S. Eddington (1882–1944) notes that *"the relativity theory is indifferent to hypotheses as to the nature of gravitation"*. He proceeds by noting that a length scale obtained from the speed of light, the constant of Newton gravitation and what he called the *"quantum"* should be of some importance to understand the deepest nature of gravitation: *"[...] it is evident that this length must be the key to some essential structure"*. The *"quantum"* Eddington is refering to is now called the Planck constant. The length he mentions is the Planck length.

**The Planck scale**

In the last paragraph of a paper published in 1899, thirty years before Eddington's book, Max Planck (1858–1947) introduced a new system of units based on four constants [1] he qualified as "universal": the Boltzmann constant $k_B$, the Planck constant $h$ (or $\hbar = h/2\pi$), the speed of light in vacuum $c$, and the Newton gravitational constant $G$ [144]. The current values of these constants are given in Table 2.1. Planck used the adjective *"universal"* because his system of units was based on universal phenomena such as gravitation and black body heat radiation, his main topic of interest at that time. Actually, Planck pointed out that from the four constants $c$, $G$, $\hbar$ and $k_B$, it is impossible to get a dimensionless quantity, and that, on the contrary, it is possible to obtain a length (the Planck length, noted $l_P$), a time (the Planck time $t_P$), a mass (the Planck

---

[1]Here I use the modern notations of these constants. In addition, Planck used $h$ and not $\hbar$.

**Table 2.1:** Current (late 2015) accepted values of some fundamental constants. All values from http://physics.nist.gov.

| Constant | Value | Uncertainty |
|---|---|---|
| Newtonian constant of gravitation ($G$) | $6.674\,08(31) \times 10^{-11}$ m³ kg⁻¹ s⁻² | $4.7 \times 10^{-5}$ |
| Speed of light in vacuum ($c$) | $299\,792\,458$ m s⁻¹ | exact |
| Planck constant over $2\pi$ ($\hbar$) | $6.582\,119\,514(40) \times 10^{-16}$ eV s | $6.1 \times 10^{-9}$ |
| Boltzmann constant ($k_B$) | $8.617\,3303(50) \times 10^{-5}$ eV K⁻¹ | $5.7 \times 10^{-7}$ |

mass, $m_P$) and a temperature (the Planck temperature $T_P$) through the following relations [2]:

$$l_P \;=\; \sqrt{\frac{\hbar\,G}{c^3}} = 1.616\,229(38) \times 10^{-35} \text{ m}, \tag{2.1}$$

$$t_P \;=\; \sqrt{\frac{\hbar\,G}{c^5}} = \frac{l_P}{c} = 5.391\,16(13) \times 10^{-44} \text{ s}, \tag{2.2}$$

$$m_P \;=\; \sqrt{\frac{\hbar\,c}{G}} = 2.176\,470(51) \times 10^{-8} \text{ kg}, \tag{2.3}$$

$$T_P \;=\; \sqrt{\frac{\hbar\,c^5}{G\,k_B^2}} = \frac{m_P\,c^2}{k_B} = 1.416\,808(33) \times 10^{32} \text{ K}. \tag{2.4}$$

From the Planck mass, it is possible to deduce the Planck energy $E_P$, which will be of particular interest in the rest of this chapter:

$$E_P = m_P\,c^2 = 1.220\,910(29) \times 10^{19} \text{ GeV}. \tag{2.5}$$

The role of the Planck mass as a limit of quantum relativistic theory was first pointed out by Matvei P. Bronstein [3] (1906–1938) [36]. In 1955, John A. Wheeler (1911–2008) proved that the Planck length is the quantum limit of GR [167]. Following these seminal contributions, the search for a quantum theory of gravity was on its way in late 50s [4].

Since then, more and more arguments were found to support the Planck scale, not only as the characteristic scale for QG but also as a minimum length scale. Thought experiments played an important role in that process. As an example, and following [9], I will focus on one in particular, consisting in shrinking a volume of matter and examine its fate from quantum mechanics and GR perspectives.

The thought experiment is illustrated by Fig. 2.1. We consider a three-dimensional volume of mass $M$ and size $\ell$. From the GR point of view, the volume can be shrunk until its size reach the Schwarzschild radius

$$\ell \approx \frac{G\,M}{c^2}. \tag{2.6}$$

At this point, the volume reaches a minimum size: it collapses and a black hole is created. From GR perspective, $M$ can be made as small as desired so there is no lower limit for $\ell$. Now, we assume that the volume with mass $M$ contains particles with (average) momentum $\bar{p}$. The energy contained in the volume is then $E^2 = M^2\,c^4 + \bar{p}^2\,c^2$. In addition, the uncertainty on $\bar{p}$ is limited

---

[2]Numerical values are from NIST web site http://physics.nist.gov.

[3]For more on Bronstein remarkable contributions in the early days of Quatum Gravity, see [72].

[4]I will not go further into the history of QG. Interested readers may refer to [149] for more details. Concerning in particular the early (1916–1940) developments of QG, have a look at [153].
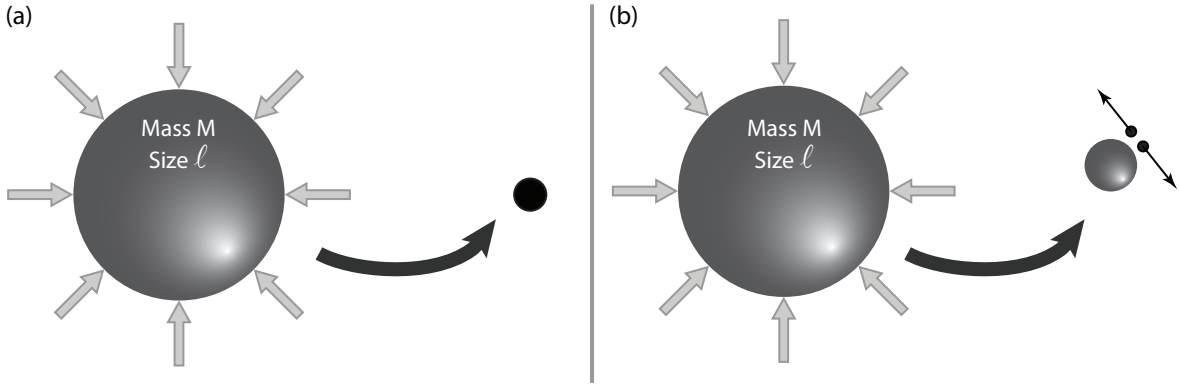
**Figure 2.1:** A volume of size $\ell$ and containg mass $M$ is shrunk. (a) Point of view of General Relativity. Once the size of the volume reaches the Schwarzschild radius, it collapses and a black hole is formed. (b) Point of view of quantum mechanics. The volume can shrink, but only up to the point the energy contained in the volume is high enough to create a particle anti-particle pair. At that point, localization is ruined and the volume cannot be shrunk anymore.

by Heisenberg principle to $\Delta \bar{p} \approx \hbar/\ell$. The uncertainty on $E$ is then simply given by

$$\Delta E \approx c\,\Delta \bar{p} \approx \frac{\hbar c}{\ell}.$$

From the previous expression, we notice that if the volume shrinks, $\Delta E$ increases. At some point, the energy contained in the volume will exceed $2\,M\,c^2$, and pairs of particle and anti-particle will be created in the vicinity of the volume, therefore ruining its localization and forbidding any further shrinkage. At this point,

$$\Delta E \approx M\,c^2 \approx \frac{\hbar c}{\ell},$$

which gives

$$\ell \approx \frac{\hbar}{M\,c}. \tag{2.7}$$

$\ell$ then reaches the Compton wavelength, the distance at which the concept of a single pointlike particle breaks down. From Eqs. 2.6 and 2.7, we can deduce that $\ell$ reaches a minimum

$$\ell_{min} \approx \frac{\hbar}{M\,c} \approx \frac{G\,M}{c^2}$$

for

$$M^2 \approx \frac{\hbar\,c}{G} = M_P^2 \tag{2.8}$$

while

$$\ell_{min} \approx \frac{\hbar}{M_P\,c} \approx \sqrt{\frac{\hbar\,G}{c^3}} = l_P. \tag{2.9}$$

Several other thought experiments are described at introductory level in [9]. A more detailed discussion on minimum length scale in the context of QG can be found in the review [83].

**Remark on the definition of the Planck scale**   The way the Planck scale is defined may seem questionable since its basic ingredients, in particular the constants $c$ and $G$ are only known in the low energy regime. We will see in the following that the group velocity of light in vacuum may depend on the energy of the photons. In addition, Newton's constant is known only down to a distance $\sim 1$ mm, corresponding to an energy of $\sim 10^{-3}$ eV [84]. So, it is important to keep in mind that the Planck scale only provides an *order of magnitude* for QG phenomena.

**The limits of General Relativity**

The theory of General Relativity [5] (GR) is a metric theory of gravitation where spacetime geometry is directly related to its energy-momentum content. There is no force anymore. Spacetime is curved by energy-momentum, in particular by mass, and particles follow geodesics of spacetime.

Within GR, gravitation is described by a set of ten equations, the Einstein field equations (EFE):

$$R_{\mu\nu} - \frac{1}{2} R\, g_{\mu\nu} + \Lambda\, g_{\mu\nu} = \frac{8\pi G}{c^4} T_{\mu\nu}, \tag{2.10}$$

where $R_{\mu\nu}$ is the Ricci curvature tensor, $R = R^\nu{}_\nu$ is the Ricci scalar, $g_{\mu\nu}$ is the metric tensor, $\Lambda$ the cosmological constant, $G$ the Newton's gravitational constant, and $T_{\mu\nu}$ the stress-energy tensor. As the Ricci tensor is itself obtained from the metric tensor, we can state that the left side of Eq. 2.10 is related to geometry of spacetime, while the right side of is related to matter and energy. Solving Einstein field equations consists in computing the coefficients of the metric $g_{\mu\nu}$ for a given mass distribution given by coefficients $T_{\mu\nu}$.

Since the first publication by Einstein in 1915, GR has proven to be extremely successful [6]. However, there are strong indications that it is incomplete. A striking illustration of this is the fact GR allows the existence of singularities, spacetime points where curvature becomes infinite. As an example, let me consider a particular solution of EFE, the Schwarzschild metric, obtained for a static and spherically symmetric spacetime, and neglecting the cosmological constant $\Lambda$:

$$ds^2 = \left(1 - \frac{r_s}{r}\right) c^2 dt^2 - \left(1 - \frac{r_s}{r}\right)^{-1} dr^2 - r^2 \left(\sin^2\theta\, d\varphi^2 + d\theta^2\right), \tag{2.11}$$

where $r_s$ is the Schwarzschild radius

$$r_s = \frac{2GM}{c^2}. \tag{2.12}$$

In Eq. 2.11, two singularities appear: one for $r = r_s$, and the other for $r = 0$.

The case $r = r_s$ is called a *coordinate singularity*: it can be avoided by chosing another system of coordinates. As an example, the use of Lemaître coordinates $(\tau, \rho)$ instead of Schwarzschild coordinates $(t, r)$ leads to the following expression:

$$ds^2 = d\tau^2 - \frac{2M}{r} d\rho^2 - r^2 \left(\sin^2\theta\, d\varphi^2 + d\theta^2\right), \tag{2.13}$$

with

$$r = \left[\frac{3}{2}(\rho - \tau)\right]^{2/3} r_s^{1/3}.$$

From Eq. 2.13, we can see that the singularity at the Schwarzschild radius has disappeared. However, the singularity at $r = 0$ ($\rho - \tau = 0$) still remains.

The singularity at $r = 0$ corresponds to a true physical singularity, a *gravitational singularity*. To see this, it is common to use a particular contraction of the Riemann tensor, sometimes called the Kretschmann [7] invariant, which measures the curvature. For the Schwarzschild metric, it is given by

$$K = R_{\alpha\beta\gamma\delta}\, R^{\alpha\beta\gamma\delta} = \frac{48G^2 M^2}{c^4 r^6}.$$

Then, the curvature becomes infinite when $r$ tends to zero.

This established, we are now ready to enounce the first reason why QG seems to be needed:

---

[5]Various textbooks were consulted to write this section. In particular, [22, 115, 160, 129, 142, 166].
[6]The recent discovery of gravitational waves [1] is yet another stricking evidence of GR validity.
[7]After Erich Justus Kretschmann (1887–1973), German physicist.

---
**1. Gravitational singularities**

General Relativity indicates the existence of spacetime singularities. A quantum theory of gravity should avoid singularities, *e.g.* by introducing a minimum length scale.

---

Another important feature of GR is that it provide the tools to describe the Universe as a whole. The ΛCDM model, presently considered as the standard model of cosmology, which contains a cosmological constant Λ (dark energy) and Cold Dark Matter (CDM) rely on the Friedman-Lemaître-Robertson-Walker (FLRW) metric. Dark energy is currently estimated to represent about 68% of the universe total energy density, while dark matter acounts for about 25%. While the accelerating expansion of the universe favors the existence of dark energy, its exact nature is still unknown and its extremely low density ($\sim 10^{-27}$ kg/m$^3$) will probably prevent its detection before long anywhere else than in cosmology [121]. As far as dark matter is concerned, even if there are solid evidences for its existence, it has not been detected so far and its exact nature remains mysterious [8] [24]. These facts suggest a second argument in support of QG, which is more a hope:

---
**2. Dark Energy/Dark Matter**

QG could help understanding the true nature of dark matter and dark energy.

---

The FLRW metric is a particular solution of EFE describing a homogeneous, isotropic expanding universe. The fact that the universe is not static imply that the metric will depend on time, through the scale factor $a(t)$. This parameter is a measurement of the expansion of the universe, achieved *e.g.* by a measurement of the distance between two galaxies. The expansion translates in the fact $\dot{a} \equiv da(t)/dt > 0$. That means $a$ should tend to zero in the past. This is in contradiction with quantum mechanics, where a particle cannot occupy a volume of size smaller than its Compton wavelength.

The FLRW metric is given by:

$$ds^2 = dt^2 - a^2(t) \left( \frac{d\sigma^2}{1 - k\sigma^2} + \sigma^2 \left( \sin^2 \theta \, d\varphi^2 + d\theta^2 \right) \right), \tag{2.14}$$

where $\sigma \equiv r/a(t)$ and $k$ is a parameter defining geometry: $k = +1$ for a 3-sphere, $k = 0$ for flat space and $k = -1$ for an hyperboloid. From the definition of $\sigma$, the primordial singularity appears clearly. This leads to the third reason in support of QG:

---
**3. Quantum Cosmology**

The ΛCDM model, through the use of FLRW metric, indicates the universe began from a singularity. This initial singularity results in the breakdown of classical physics. Quantum Gravity should be able to describe the origin of the universe, possibly as some sort of quantum state.

---

**Black holes evaporation**

In the classical picture, no radiation can escape a black hole. However, by quantizing matter fields on a classical, fixed gravitational background, Stephen Hawking has shown that radiation can escape a black hole [77]. This radiation (*Hawking radiation*) decreases the mass of the black

---

[8]Some authors have proposed modified theories of gravity (*e.g.* MOND [66]) which could explain the shape of rotation curves of galaxies without the need for CDM. However, all these theories have numerous problems. In particular, they cannot explain some observations of colliding clusters [47].

hole which will ultimately disappear. The corresponding temperature of a black hole of mass $M$ is given by the expression

$$T = \frac{\hbar c^3}{8\pi G k_B M}. \tag{2.15}$$

As $M$ decreases, $T$ increases, and so Hawking radiation becomes more and more intense, which in turn induce a decrease of the mass. As a result, the mass will decrease faster and faster. The temperature will finally diverge when $M$ tends to zero. However, since the Planck length can be considered as a minimum length, the size of the black hole will ultimately reach it. At that point, its mass will reach the Planck mass [9]. That limit is also the limit of validity of Hawking's calculation, therefore a theory of QG would be needed to understand further the fate of black holes:

---
**4. The fate of Black Holes**

Due to Hawking's radiation, Black Holes evaporate. Ultimately, their size approaches the Planck length and their mass approaches the Planck mass. Quantum Gravity is therefore needed to fully describe the fate of Black Holes.

---

**The limit of the Standard Model of particle physics**

As already mentionned above, the SM of particle physics has been extremely successful. Its biggest success is probably the prediction of the Higgs boson, discovered in 2012 [10]. Other successes include the predictions of the W and Z bosons, of the gluon, of the top and charm quarks, of the anomalous magnetic dipole moment of the electron.

However, SM suffers from some failures. Three of them are : (*i*) it predicts that neutrinos should be massless, while they oscillates indicating they have a non-zero mass; (*ii*) it cannot explain the hierarchy problem, namely why the weak nuclear force is $10^{32}$ times weaker than gravity; and, (*iii*) more importantly:

---
**5. SM does not include Gravitation**

SM is formulated using the Minkowski metric, *i.e.* for a flat spacetime, meaning that gravitation is altogether neglected. It is then not valid anymore for energies approaching the Planck scale.

---

**The roads to a single theory of Quantum Gravity**

In the previous paragraphs, I gave some of the arguments why a full theory of QG is needed. Interested readers will find more detailed discussions of this topic in the literature (see *e.g.* [90]).

The question is now: how could we get to a full theory of QG ? At present, there is no clear answer to that question, but a lot of different possible answers: it is fair to say that research on QG is still in a phase of proliferation. String theory, Loop Quantum Gravity, Asymptotic safety, Horova-Lifshitz gravity, Causal dynamical triangulations, Causal sets, Non-commutative geometry, etc. are all possible candidates for a full theory of QG.

However, some approaches have gathered a significant fraction of the community. In the next section, I will discuss two of these most popular approaches to QG, which have the particularity to predict a breakdown (or a deformation) of Lorentz symmetry: String Theory (ST) and Loop Quantum Gravity (LQG). The reader should keep in mind however that other approaches can lead to MDR, *e.g.* non-commutative geometry [21].

---

[9]Such a black hole is called a *Planckian Quantum Black Hole*, [38].

[10]Some properties of the new boson have still to be measured to fully ascertain its true nature, but it seems that it is indeed the Higgs boson.
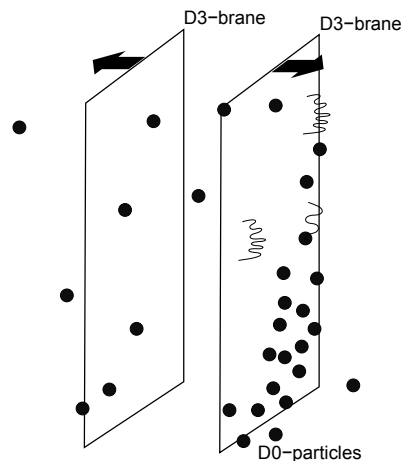
**Figure 2.2:** Model of a D-particle foam. Our universe, represented by a D3-brane, is slowly moving in the bulk. D0-particles crossing the D3-brane appear as flashing on and off, resulting in a foamy spacetime. This spacetime foam can have noticeable effects on photon propagation.

These predictions are of course arguable. It seems to me, as an experimentalist, that LIV never appears naturally in any of these models: more or less questionable assumptions need to be made that I am not really able to decide if they are really justified or not...

### 2.1.2   Two models which predict MDR for photons in vacuum

In this section, I will give two examples of models which predict a modified dispersion relation for photons. For brevity, I will stick to the two main roads followed to get to a full theory of QG: String Theory and Loop Quantum Gravity.

**Stringy spacetime foam**

In String Theory (ST), all particles are obtained through different vibration modes of a single object, a string. ST unifies all known interactions by considering they are due to the exchange of bosons. For gravity, this boson is the graviton, which ST predict to be massless, with a spin 2. As a result, ST allows to unify all interactions and is a natural candidate theory for Quantum Gravity.

One of the striking feature of ST is that it requires extra spatial dimensions to be mathematically consistent. These *extra dimensions* could be *compactified*: they could "close up" on themselves to form circles. These circles would be only observable at very high energies, while at lower energies they would be seen as points, resulting in the classical four-dimensional spacetime.

There are five string theories. They are named type I, type IIA, type IIB, SO(32) and $E_8 \times E_8$. Each type allows different types of strings (opened or closed), different versions of supersymmetry, different kinds of gauge symmerties. In 1995, E. Witten proposed that these five theories are the limiting cases of a single broader theory he named "M-theory", $M$ standing for "Magic", "Mysterious" or "Membrane".

As we are interested in the connexions between ST and Lorentz Invariance, it is important to note that ST is formulated in a flat (classical) background spacetime. As such, ST is not a theory of quantum spacetime but only a quantization of the gravitational interaction, and it naturally preserves Lorentz Invariance.

However, G. Amelino-Camelia, J. Ellis and collaborators proposed, at the end of the 90s, a particular version of ST where they found that vacuum has a non-trivial refractive index: the

refractive index of vacuum is not equal to one, but depends linearly on the energy of the photons [19, 59, 60]. I will now give some details about this particular model, following [124].

Interestingly, the model includes a cosmology. Our universe is a 8-dimensional D-brane (compactified to our three spatial dimensions so it is noted "D3-brane") in a 10-dimensional bulk (Fig. 2.2). In the past, our D3-brane collided with another one: this collision corresponds to the Big Bang. Since the collision, the two D3-branes have been slowly moving away from each other. Photons (open strings) are propagating in our universe, while the bulk is punctured by point-like, electrically neutral and massive D0-particles. The mass of D0-particles is related to the string mass scale $M_s$, which is in general different from the Planck scale, and which could be as low as a few TeV. D0-particles crossing the D3-brane appear as flashing on and off as seen from our universe, resulting in a *foamy* spacetime.

The question is now how this D-particle spacetime foam can affect the propagation of photons. In Fig. 2.3, a D-particle is represented crossing our universe D-brane while a photon of energy $p^0$ is propagating on it. The speed of the photon is $c$, the conventional speed of light in vacuum. When the photon reach the D-particle, because of energy conservation, an intermediate string state is produced (the thick string on the figure). This string will stretch and oscillates, with decreasing amplitude, re-emitting a wave at each oscillation. The re-emitting of the first wave, the one with the maximum energy, is delayed by

$$\Delta t \sim \alpha' p^0,$$
(2.16)

where $\alpha'$ is the string scale ($\alpha' \sim 10^{-34}$ m). This delay is the result of one interaction between the photon and the D-particle. If we imagine now that there is a foam of D-particles, with a density $n^*$ per string length, the total delay for a propagation on a distance $D$ is

$$\Delta t_{\text{total}} \sim \frac{p^0}{M_s} n^* D.$$
(2.17)

As we shall see later (Section 2.2.1), if the gamma-ray source is located at cosmological distance, the expansion of the universe has to be taken into account. This leads to the final expression of the delay between two photons emitted at the same time, with an energy difference $\Delta E$:

$$\Delta t_{\text{observed}} \sim \frac{\Delta E}{M_s} \int_0^z n^*(z') \frac{(1+z')^n}{H(z')} \, dz',$$
(2.18)

where $H(z)$ is the Hubble parameter.

The effect implied by Eq. 2.18 is deterministic. Note however that the foamy spacetime (D-particles randomly popping in and out of our universe) can also introduce a stochastic spread of the velocities of the photons of the same energy [60]. This phenomena is sometimes called spacetime *fuzziness*.

After this quick description, we can make two comments on this model.

- The effect can only be subluminal;

- The energy scale is not related to the Planck scale but to the string mass scale $M_s$. If considering a source nearby, or alternatively considering the distribution of D-particles in the bulk is homogeneous, the energy scale is $M_s/n^*$.

As we will see later in Section 2.3, the satellite *Fermi* [11], in particular with GRB 090510, has allowed to obtain a limit on the QG energy scale above the Planck scale for a linear effect with the energy. As a result, it was argued that a linear model like the one I just discussed should be
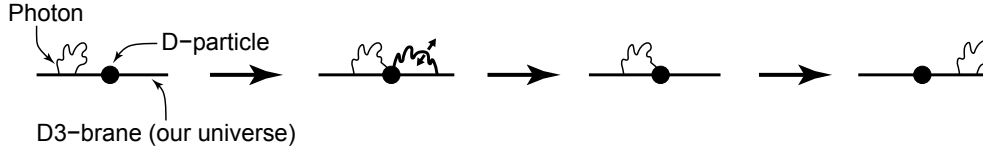
---

[11] http://fermi.gsfc.nasa.gov/

**Figure 2.3:** Capture and re-emission process of a photon by a D-particle. The thick string corresponds to an intermediate state, which can stretch to a maximal length of order $\alpha'p^0$, where $p^0$ is the energy of the incident photon and $\alpha'$ is the string scale.

ruled out. However, it is not really the case since $M_s$ do not have *a priori* to be related with the (4-dimensional) Planck scale. Actually, the scale involved by such a model is given by

$$E_{QG-D-foam} \sim \frac{M_s}{g_s n^*(z)}, \tag{2.19}$$

where $g_s$ is the string coupling, a free parameter of the model. The result of *Fermi* on GRB 090510 could be explained in the stringy spacetime foam model by invoking inhomogeneous density of D-particles. Anyway, the search for a linear effect should not stop because of the results *Fermi* obtained with only one GRB.

Another common belief is that string theory only predict linear effects. However, it is possible to construct string theory models where the effect is quadratic [67].

The kind of model I discussed in this section was responsible for the first attempts to look for MDR with observations of gamma-ray bursts. For that reason, I spent some time to describe it in some (non-technical) detail. I will now turn to a much shorter discussion of Loop Quantum Gravity.

**Loops**

On the contrary to ST, which aims to a unification of the four interactions, Loop Quantum Gravity (LQG) [150] is a description of quantum spacetime. Its starting point is a Hamiltonian formulation of GR, and its striking outcome is a discretization of volume and area operators: spacetime is discrete. It was argued that this discretization could lead to a departure from Lorentz symmetry at the Planck scale.

LQG is a very complex theory and my understanding of it is very limited beyond what I wrote in the previous paragraph. In the folowing, I will only point to the two publications of interest concerning MDR.

In particular, Gambini & Pullin [69] obtained the following MDR considering a semiclassical regime in which the electromagnetic field is a classical object whereas space is described by LQG:

$$\omega_\pm(k) \simeq ck(1 \mp 2\xi l_P k), \tag{2.20}$$

where $\xi$ is a constant giving the amplitude of the effect and $l_P$ is the Planck length. An important feature of this MDR is that the speed of the photons can depend on their polarization, hence the sign $\pm$ in the equation. This violates parity and leads to birefringence of vacuum. In addition, superluminal propagation is allowed.

In [15], Alfaro and collaborators extended the work of Gambini & Pullin and obtained the following MDR:

$$\omega_\pm(k) \simeq ck \left( 1 + \theta_7 \left( \frac{l_P}{\mathscr{L}} \right)^{2+2\Upsilon} - 2\theta_3(kl_P)^2 \pm 2\theta_8(kl_P) \right), \tag{2.21}$$

where $\theta_7$, $\theta_3$, $\theta_8$ and $\Upsilon$ are parameters of the model and $\mathscr{L}$ is the characteristic size of discrete cells of spacetime. Depending on the value of parameter $\Upsilon$, it can be noticed that a quadratic effect is possible.

### 2.1.3   A common consequence

In the two approaches to QG discussed above, the outcome is the same: the speed of photons in vacuum depends on their energies, which breaks LI. This motivates the introduction of a simple *model-independent* test theory in which the speed of photons can depend on their energy [12]. As we have discussed already, a test theory can be kinematic (like the RMS framework) or dynamic (for example, SME). In the present case, the test theory is purely kinematic. However, it can be anyway related to the SME framework, as we will see later in Section 2.2.1.

Considering the fact that classical dispersion relation $E^2 = p^2 c^2$ is found to be exact at low energies, and the fact that the characteristic energy for LIV effect is probably related in some way to the Planck scale $E_P$, modified dispersion relation (MDR) can be expressed the following way:

$$E^2 \simeq p^2 c^2 \times \left[ 1 \pm \sum_{n=1}^{\infty} k_n \left( \frac{E}{E_P} \right)^n \right], \tag{2.22}$$

where $c$ is the *low energy limit of the speed of light*, and $k_n$ coefficients to be measured, or constrained. The sign $\pm$ in this equation takes into acount the possibility to have subluminal or superluminal effects. Alternatively, it is also possible to write the dispersion relation as

$$p^2 c^2 \simeq E^2 \times \left[ 1 \pm \sum_{n=1}^{\infty} k'_n \left( \frac{E}{E_P} \right)^n \right], \tag{2.23}$$

where $k'_n$ are new coefficients. The form of Eq. 2.22 is more suited to situations where the group velocity of photons needs to be calculated while the form of Eq. 2.23 is prefered when the dispersion relation is interpreted as the result of a non-zero effective mass for the photon, as we shall see later.

A MDR of the form given above was first proposed by G. Amelino-Camelia and collaborators [20] in 1998. In this seminal article, published one year after the first redshift of a GRB was measured, the authors also suggested the use of gamma-ray bursts as a way to probe the quantum nature of spacetime. 1998 can then be considered as the year of birth of LIV searches with gamma-ray sources.

## 2.2   Time of flight studies with high energy gamma-ray sources

### 2.2.1   From modified dispersion relation to time-lag

From Eq. 2.22, it is possible to obtain the group velocity of photons as a function of their energies:

$$v_g(E) = \partial E / \partial p \simeq c \times \left[ 1 - s_\pm \frac{n+1}{2} \left( \frac{E}{E_{\text{QG}}} \right)^n \right]. \tag{2.24}$$

A few remarks can be made at this point:

- Here we consider only the lowest order dominant term [13]. As I will show later, only the first order ($n = 1$) is within our reach with present day experiments, while the second order term ($n = 2$) could be within reach of the next generation of ground-based Cherenkov telescopes.

---

[12]The test theory used here is noted "PKV0" in [17].

[13]Either the term $n = 1$ dominates and the other terms are neglected, either the term $n = 2$ dominates and the others are neglected, etc.

- It is important to note here that the fact that the group velocity is still given by $v_g = \partial E/\partial p$ in the Planck regime was *assumed*. There is no guarantee it is really the case.

- Both subluminal ($s_\pm = +1$) and superluminal ($s_\pm = -1$) LIV effects are allowed. The possibility of a superluminal *group velocity* can be disturbing but it does not bring any problem with the principle of causality [14].

- The parameter to be constrained has been redefined and noted $E_{QG}$, indicating it is expected to be related to some Quantum Gravity energy scale, presumably not too far from the Planck scale $E_P$. As already mentioned in the first item, this scale is not constrained with the same sensitivity for $n = 1$ and $n = 2$. Therefore, different notations are used: $E_{QG,1}$ or $E_{QG}^l$ for the linear effect, and $E_{QG,2}$ or $E_{QG}^q$ for the quadratic effect [15].

From Eq. 2.22, it is now necessary to calculate the time lag, measured at Earth ($z = 0$), between two photons with different energies and *emitted at the same time* at redshift $z > 0$. As the photons have different speeds, they do not take the same time to travel between the source and the Earth. Meanwhile, the Universe is expanding so the two photons do not travel the same proper distance [16] [142]. This difference of proper distances results in the fact the time lag between the two photons when they reach Earth will depend on the redshift of the source and on cosmological parameters, as we shall see now.

The redshift is defined by the relation

$$1 + z = \frac{a_{\text{observation=now}}}{a_{\text{emission}}} = \frac{a_0}{a(t)}, \tag{2.25}$$

where $a$ is the cosmological scale factor. Deriving this expression, we get

$$dz = -\frac{a_0}{a^2(t)}\dot{a}(t)dt = -\underbrace{\frac{a_0}{a(t)}}_{1+z}\underbrace{\frac{\dot{a}(t)}{a(t)}}_{H(t)}\, dt, \tag{2.26}$$

where

$$\dot{a}(t) \equiv \frac{da(t)}{dt}, \tag{2.27}$$

and where

$$H(t) = \frac{\dot{a}(t)}{a(t)} \tag{2.28}$$

is the Hubble parameter, which can be expressed indifferently as a function of time or as a function of redshift, and which depends on the Hubble constant $H_0$ and parameters $\Omega_m$ (matter density), $\Omega_K$ (curvature parameter) and $\Omega_\Lambda$ (dark energy density), all three evaluated at present time:

$$H(z) = H_0 \sqrt{\Omega_m\,(1+z)^3 + \Omega_K\,(1+z)^2 + \Omega_\Lambda}.$$

---

[14]Causality is guaranteed by the fact that a *signal* (a sudden change in amplitude, frequency, etc.) has a speed always lower than $c$. Experiments have shown that it is possible to have *superluminal group velocities* while *signal velocity* is always subluminal. See *e.g.* [37] for a description of such an experiment.

[15]The notation $M$ is also used sometimes ($M_{QG}^l$, $M_{QG}^q$), or ($M_{QG,1}$, $M_{QG,2}$).

[16]*Proper distance* is affected by the expansion, while *comoving distance* is not. Both are equal at present time (for $z = 0$).

The values of cosmological parameters, as measured by the *Planck* satellite [146] are [17]:

$$H_0 = 67.74 \pm 0.46 \text{ km/s/Mpc} = (2.20 \pm 0.02) \times 10^{-18} \text{ s}^{-1}, \tag{2.29}$$

$$\Omega_m = 0.3089 \pm 0.0062, \tag{2.30}$$

$$\Omega_K = 0.0008 \pm 0.004, \tag{2.31}$$

$$\Omega_\Lambda = 0.6911 \pm 0.0062. \tag{2.32}$$

$\Omega_K$ is neglected in all LIV studies and I will do the same in the following. I will simply use the definition

$$H(z) = H_0 \sqrt{\Omega_m (1+z)^3 + \Omega_\Lambda}. \tag{2.33}$$

From Eq. 2.26, we get the time-redshift relation:

$$dt = \frac{dz}{(1+z)H(z)}. \tag{2.34}$$

The time defined here is the *lookback time*: it corresponds to the difference between the age of the Universe when the photon was emitted and when it was received. During this time, a photon with speed $v$ travels a distance

$$dl = v\,dt = \frac{v\,dz}{(1+z)H(z)}. \tag{2.35}$$

The corresponding comoving distance is simply given by

$$d\chi = dl\,(1+z) = \frac{v\,dz}{H(z)}. \tag{2.36}$$

If we now consider two photons with energies $E_h$ and $E_l$, measured at reshift $z = 0$, with $E_h > E_l$, we can express the difference of velocities from Eq. 2.24:

$$\Delta v \simeq c \left[ s_\pm \frac{n+1}{2} \frac{E_h^n - E_l^n}{E_{QG}^n} (1+z)^n \right], \tag{2.37}$$

where we have blue-shifted energies $E_h$ and $E_l$ (factor $(1+z)$) to express them in the rest frame of the source.

As a result, the two photons have proper distances which differs by

$$\Delta\chi_0 = \int_0^z \frac{\Delta v\,dz}{H(z)} \simeq c\,s_\pm \frac{n+1}{2} \frac{E_h^n - E_l^n}{E_{QG}^n} \int_0^z \frac{(1+z')^n}{H(z')} dz', \tag{2.38}$$

and they will be detected with a time difference $\Delta t = \Delta\chi_0/c$. Thus,

$$\boxed{\Delta t_n \simeq s_\pm \frac{n+1}{2} \frac{E_h^n - E_l^n}{E_{QG}^n} \int_0^z \frac{(1+z')^n}{H(z')} dz'.} \tag{2.39}$$

As the time and the energy are both measured, it is usual to put them on the same side of the previous expression, defining a "*time-lag over energy difference*" parameter $\tau_n$ as

$$\boxed{\tau_n \equiv \frac{\Delta t_n}{E_h^n - E_l^n} \simeq s_\pm \frac{n+1}{2\,H_0} \frac{1}{E_{QG}^n} \int_0^z \frac{(1+z')^n}{\sqrt{\Omega_m(1+z')^3 + \Omega_\Lambda}} dz',} \tag{2.40}$$

---

[17]These values are taken from Tables 4 and 5 of [146] with the so called "TT, TE, EE+lowP+lensing+ext" likelihood combination for $\Omega_m$ and $\Omega_\Lambda$ and "TT, TE, EE+lensing+ext" for $\Omega_K$. These likelihoods are used to fit the $\Lambda$CDM model to *Planck* data.
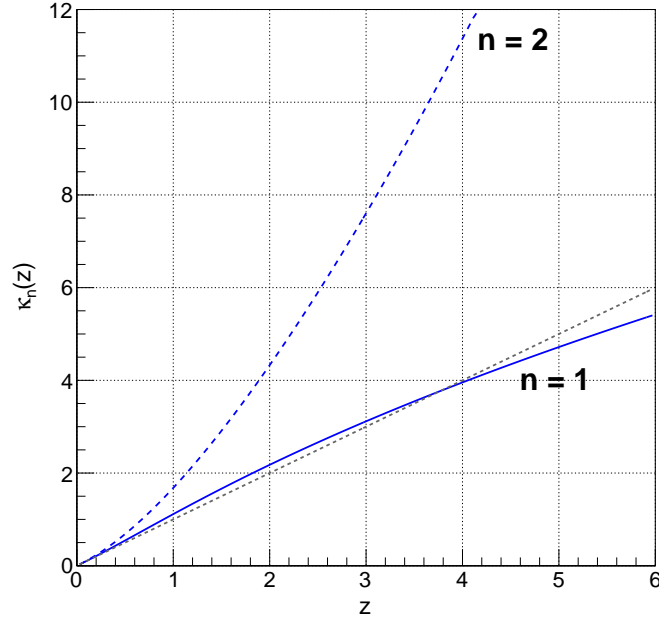
**Figure 2.4:** Function $\kappa_n(z)$ as defined by Eq. 2.41 for $n = 1$ (solid line) and $n = 2$ (dashed line) using *Planck* data. The grey dashed line corresponds to the condition $\kappa_n(z) = z$.

where the Hubble parameter was replaced by its expression (Eq. 2.33). It is also usual to define a *distance parameter* $\kappa_n$:

$$\kappa_n \equiv \int_0^z \frac{(1 + z')^n}{\sqrt{\Omega_m (1 + z')^3 + \Omega_\Lambda}} \, dz'. \tag{2.41}$$

Fig. 2.4 shows the evolution of parameter $\kappa_n$ as a function of redshift using *Planck* data. From this figure, and from Eq. 2.41, we can also point out that for low redshifts, $\kappa_n(z) \sim z$.

It is worth mentioning that the calculation above was not done correctly in all papers published before 2008 dealing with MDR searches with astrophysical sources, leading to a missing factor $(1 + z)$ in the integral. This mistake was pointed out in references [93, 32] and corrected in all subsequent papers. In addition, it was recently pointed out that this calculation may be too simplistic [148]: it implicitly assumes that translations are not affected by Planck-scale effects. Work is still needed though to fully understand the implications of this asumption and eventually get rid of it.

Going back to the time lag expression of Eq. 2.39, it can be noticed that:

- The time lag $\Delta t_n$ is proportional to $\kappa_n$. Distant sources will produce higher time lags, easier to measure. This is in agreement with the idea that if the lag is introduced by quantum nature of space time, the more space there is between the detector and the source, the higher the lag should be. Obviously, in order to be able to measure a time lag, sources also have to show significant variability.

- The time lag is proportional to the energy difference $\Delta E^n \equiv E_h^n - E_l^n$, often referred to as the *energy lever arm*. In principle, this favors multiwavelength observations. We will see however in the next section that such observations can also bring some issues: different emission mechanisms, with different *intrinsic temporal properties* come into play at different wavelengths, which prevent any safe interpretation of data.

- The value of the time lag is deterministic: once the two energies $E_h$ and $E_l$ and the redshift $z$ are set, the value of the lag is set. We will see later (Section 2.4) that quantum spacetime
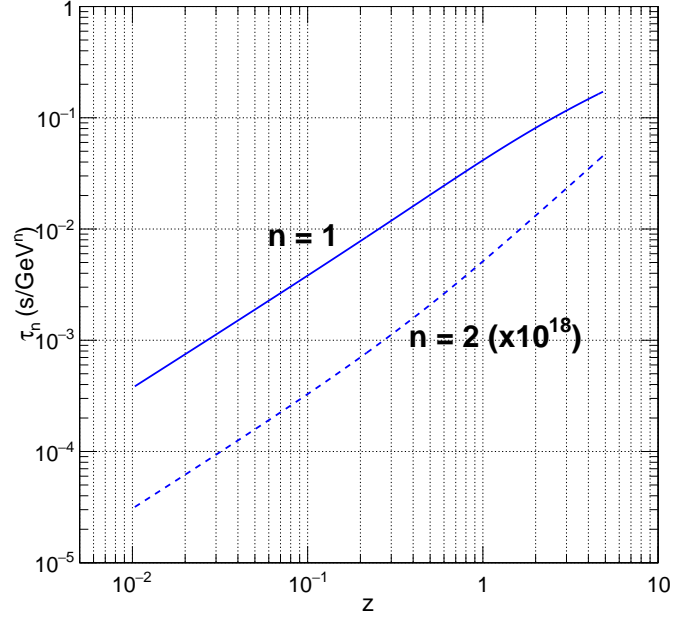
**Figure 2.5:** Parameter $\tau_n$ as a function of redshift for $n = 1$ and $n = 2$, assuming $E_{QG} = E_P$ and for a subluminal propagation. Note that the curve for $n = 2$ was multiplied by $10^{18}$.

could also involve stochastic effects.

Fig. 2.5 shows the evolution of parameter $\tau_n$ as a function of redshift for $n = 1$ and $n = 2$ assuming $E_{QG} = E_P$. It appears from this plot that the gap between linear and quadratic effects is quite large! Any effect with $n > 2$, regardless of its theoretical relevance, will most probably stay forever out of experimental reach. To have a rough idea of the values of the time lags, the reader can consider $\Delta E^n \sim E_h^n$ and take $E_h \approx 100$ GeV for the *Fermi*-LAT, and $E_h \approx 1$ TeV for Imaging Atmospheric Cherenkov Telescopes (IACT). It is important to note that in practice, the measured value of the time lag will depend on several environmental parameters, such as:

- The flux of the source as well as its spectral index. For a given integrated flux, $\Delta E^n$ will be greater for a harder spectrum.

- The distance of the source: especially in the TeV regime, high energy photons can be absorbed due to their interaction with Extragalactic Background Light (EBL, see Section 2.4), decreasing the maximum detectable energy and thus reducing the energy lever arm.

- Observation conditions, especially for IACTs, for which the energy threshold depends on the zenith angle of the source and on atmospheric conditions.

I need now to comment a little further on Eqs. 2.39 and 2.40 in the case the source is nearby, which is the case for pulsars. As of today, all the pulsars detected are located in our galaxy, except one, PSR J0540-6919, which is located in the Large Magellanic Cloud, at 50 kpc. For a source nearby, the redshift is approximated by $z \approx v/c = d/D_H$, where $v$ is the radial velocity of the source, due to the expansion of the universe, $d$ is the *euclidian distance* and $D_H \equiv c/H_0$ is the *Hubble distance* [81]. So, since $\kappa_n(z) \sim z$ when $z \to 0$, we have

$$\tau_n \simeq s_{\pm} \frac{n+1}{2\,H_0} \frac{1}{E_{QG}^n} z,$$

and

$$\tau_n \simeq s_\pm \frac{n+1}{2} \frac{1}{E_{QG}^n} \frac{d}{c}. \tag{2.42}$$

To close this section, I would like to relate parameter $\tau_n$ with the SME parameters I introduced in Section 1.3 (Eq. 1.66). For the anisotropic case, $\tau_n$ is given by:

$$\tau_n \simeq s_\pm \frac{\kappa_n}{H_0} \sum_{jm} {}_0Y_{jm}(\hat{\mathbf{n}}) c_{(I)jm}^{(n+4)}. \tag{2.43}$$

This expression corresponds to Eq. 6 in reference [102]. For the isotropic case, this expression simplifies to

$$\tau_n \simeq s_\pm \frac{\kappa_n}{H_0} \frac{1}{\sqrt{4\pi}} c_{(I)00}^{(n+4)}. \tag{2.44}$$

I need to remind now that Eqs. 2.39 and 2.40 were obtained assuming that photons of different energies are emitted at the same time. It is certainly a questionable assumption, on which I will further comment in the following section.

### 2.2.2 High energy gamma-ray sources for LIV searches and their intrinsic time properties

As compared to particle accelerators, astrophysical sources have two advantages: they come for free and they produce photons with much higher energies than achievable in ground-based facilities. As regard their use in time of flight studies, they have also a major drawback: on the contrary to ground-based accelerators, we cannot be sure of how sources work exactly. Through energy spectra, we can have a good indication of which mechanisms are at play, but the details are hidden to us. In particular, the possible correlations between the energies of photons and the times when they are emitted remain mysterious. As a result, there is no way to guarantee that photons of different energies are emitted at the same time.

There is much evidence, which will be quickly reviewed in the following, of these *intrinsic delays*. Such intrinsic delays add with LIV-induced delay to give the total measured time-lag:

$$\Delta t_{n\,(\text{total})} = \Delta t_{n\,(\text{LIV})} + \Delta t_{(\text{source})}, \tag{2.45}$$

or

$$\tau_{n\,(\text{total})} = \tau_{n\,(\text{LIV})} + \tau_{(\text{source})}. \tag{2.46}$$

In this section, I comment on the different sources used for LIV searches: gamma-ray bursts (GRB), active galactic nuclei (AGN) and pulsars (PSR), focusing on what is known about their intrinsic temporal properties and giving their advantages and drawbacks for LIV studies.

The different possible solutions to minimize the impact of intrinsic delays in LIV searches will be discussed in Section 2.2.4.

**Gamma-Ray Bursts**

GRB are random, short and extremely powerful emissions of gamma-rays [165, 143]. They are actually the brightest explosions observed in the Universe with an energy typically released of $\sim 10^{51-54}$ ergs in few tens of seconds [18], assuming an isotropic emission. This *prompt emission*, observed in the gamma-ray regime up to tens of GeV, is followed by a longer *afterglow* in X-ray, UV, optical, IR, microwave and radio, during which the flux decreases rapidly in time.

---

[18] 1 erg $= 10^{-7}$ J $= 624.15$ MeV.

GRB are located at cosmological distances. The first redshift of a GRB has been measured in 1997 (for GRB 970508, $z = 0.835$, [125]). The possibility to measure the distance of GRB greatly depend on the conditions of the detection, namely the possibility to have a quick and precise localization of the burst allowing the detection of the afterglow by ground based optical telescopes. In some cases, it is possible to *estimate* the redshift (see *e.g.* [140] where this is done from the peak energy and the bolometric luminosity). Between 1997 and 2004, only 398 redshifts were measured or estimated for 1418 bursts detected [19]. The closest burst ever observed is GRB 980425 ($z = 0.0085$) while the furthest is GRB 090429B ($z = 9.4$).

GRB show a high diversity. They are spread in two populations of durations [20] and hardness: short and hard bursts ($T90 < 2$ s) and long and soft bursts ($T90 > 2$ s). Their lightcurves are very different from a burst to another. The fact the bursts are distributed in two populations with different durations suggests they have at least two different types of progenitors. It seems now established that long bursts are due to the collapse of massive stars (*collapsar model*). Several observations of a supernova immediatly following a GRB support this hypothesis. Short bursts are more difficult to explain. It is possible they are due to merger events in compact binary systems involving two neutron stars or a neutron star and a stellar-mass black hole. In both cases, the progenitor results in the creation of a black hole while a collimated relativistic jet is emitted. The ejecta within the jets is not homogeneous: multiple layers with higher densities propagate with different velocities. The gamma-ray emission occurs through Synchrotron Self Compton (SSC) and Inverse Compton (IC) processes when a fast layer catch up and collide with a slower one (*internal shocks*). The observed variability in gamma is explained in this model by the presence of multiple layers in the jet. The afterglow emission is due to the jet interaction with the inter-stellar medium further from the progenitor (*external shocks*). Despite the successes of this model, some observations indicate the details of the origin of gamma-ray emission still remain unclear.

The presence of intrinsic time-lags is well established. For the first time in the late 90s, J. P. Norris and his collaborators pointed out that short bursts give relatively small lags [134, 135]. On the contrary, they found a correlation between the time-lags and luminosities for long GRB [137, 136]. Expressing the luminosity $L$ in units of $10^{53}$ ergs/s, they find the relation

$$L_{53} \approx 1.3 \left( \frac{\tau}{0.01 \text{ s}} \right)^{-1.14},$$

where $\tau$ is the time lag. This result was later confirmed with increased statistics (see [161] and references therein). This effect results in the fact that higher-energy photons arrive before lower-energy ones. Considering in addition the fact that only very bright bursts (small lag) are observed at high redshifts while both high and low luminosity bursts are observed at closer distances, the lag-luminosity relation tends to compensate a LIV propagation effect.

In addition to this effect, a recent key result of *Fermi* is that the onset of GeV emission seems to be systematically delayed as compared to the onset of emission at hundreds of keV. It is shown on Fig. 2.7, where the onset time is compared in the LAT and in the GBM for 18 GRB [143].

A study of the intrinsic lags of five *Fermi* bursts can be found in [39]. The interpretation of these lags is difficult. However, one explanation could be that different spectral components do not evolve in temporal coincidence. Spectral evolution during the burst could also play a role and be misinterpreted as a QG-induced effect. However, this spectral evolution is very fast and affects only a very small fraction of the events.

As a summary of this very quick discussion, allow me to give the main pros (+) and cons (–) of GRB for LIV searches:

---

[19]http://www.mpe.mpg.de/~jcg/grbgen.html

[20]It is usual to define the duration of the burst as the time elapsed between the detection of 5% and 95% of the total number of detected photons. This duration is noted $T90$.
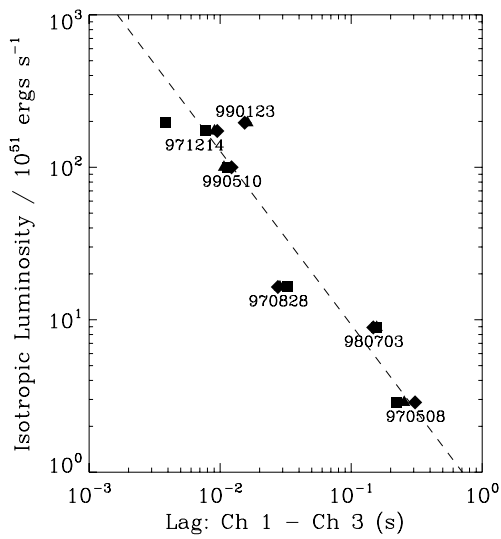
**Figure 2.6:** Luminosity as a function of the time-lag measured between BATSE channel 1 (25–50 keV) and channel 3 (100–300 keV) energy ranges. The lags are measured with a Cross-Correlation procedure (see Section 2.2.5). Figure from [136].
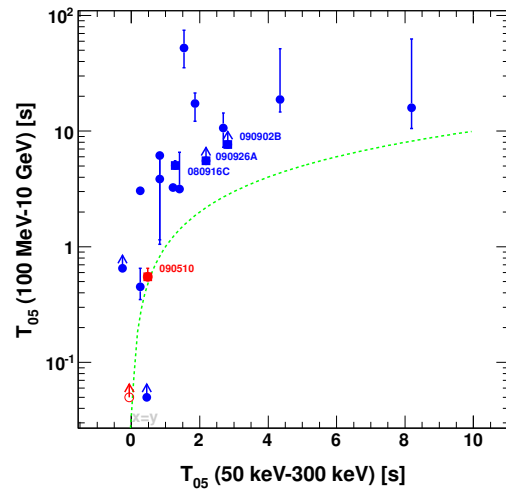


**Figure 2.7:** Onset time ($T05$) in the LAT as a function of the onset time in the GBM for 18 GRB of the first *Fermi*/LAT Catalog. The onset time is measured as the time where 5% of the photons have been detected. Long bursts are displayed in blue, short GRB in red. The dashed green line corresponds to the condition $x = y$. Figure from [143].

+ GRB are located at high redshifts;

+ Some GRB are very short and/or show high variability. This turns into a very good precision of time-lag measurement;

– GRB are random events;

– GRB are detected only with satellites. This implies that the energy lever arm is limited to tens of GeV (with *Fermi*). The Cherenkov Telescope Array [21] (CTA) may change the picture in the future;

– The redshift cannot be measured or estimated for all bursts;

– The details of gamma-ray emission are poorly understood;

– There is evidence of various intrinsic temporal effects. In particular, a lag-luminosity correlation is observed for long bursts but not for short bursts.

Despite these drawbacks, the best limits on the QG energy scale have been obtained with GRB. This is due to the fact that once a GRB is detected and its redshift measured, the high distance and fast variability dominate over all the listed drawbacks.

**Flaring Active Galactic Nuclei**

About 10% of the observed galaxies have a compact and extremely luminous region at their center. These *Active Galactic Nuclei* (AGN) [23, 50], are powered by a supermassive black hole ($10^5$ to $10^{11}$ M$_\odot$), spinning and/or accreting material (mainly gas and dust). Infalling gas onto the black hole powers a relativistic magnetized plasma which is ejected in an outflow, where particles are accelerated following mechanisms which are partly unknown.

---

[21]https://www.cta-observatory.org/

A number of different types of AGN have been observed. The unified model of AGN [162] explains these differences by distinct orientations of the accretion disk symmetry axis with respect to the line-of-sight. About 10% of AGN are strong radio emitters (*radio-loud*) while the other 90% are *radio-quiet*. Radio-quiet AGN include Seyfert galaxies and quasi-stellar objects (QSO, or *Quasars*). Radio-loud AGN include radio galaxies and *blazars*. For blazars, the relativistic jets are oriented close to the line-of-sight with the observer. Blazars can be of two types: BL Lac Objects (named after the first object of this kind ever detected, *BL Lacertae*) and FSRQ (Flat Spectrum Radio Quasars). The main difference between these two subclasses is that BL Lac objects show almost featureless non-thermal spectra while FSRQ show strong emission lines due to the accretion disk and the host galaxy. Therefore, redshift measurement is often difficult or even impossible for BL Lac objects. It is however possible to estimate the distance of an AGN using the high-energy cut-off induced by the EBL (such a method is used *e.g.* in [6]).

Both BL Lac objects and FSRQ are of particular interest for LIV searches since from time to time, they can leave a normal "*quiet state*" and show higher luminosity and variability. Time-lags can be measured only during these high-activity phases, called *flares*.

Up to now, only hints of time-lags between different energy bands have been found for some blazars (see *e.g.* [28] where X-ray emission was found to peak days [22] after the gamma-ray emission for a giant flare of Markarian – Mkn or Mrk – 421). In the TeV range, only one flare of an AGN was detected so far showing a significant lag between high and low energies. This flare of Mkn 501, recorded on July 9 2005 by MAGIC [23], was found to exhibit a lag of $4 \pm 1$ min between energy bands <250 GeV and >1.2 TeV (see Fig. 2.8) [13]. This example of a significant lag points to the fact that intrinsic delays exist in AGN flares, while the fact it is the only one detected suggests that intrinsic effects are certainly different for each AGN. They could also differ from one flare to another.

*Spectral Energy Distributions* (SED) of blazars show a characterisitic "double-bump" shape. Comparing with models, themselves based on a number of different observational inputs, it is possible to state that synchrotron and inverse-Compton are the dominant processes which explain the emission of blazars from the radio to the gamma-ray domains. In simple "*one-zone*" models, accelerated electrons in the jet produce photons through synchrotron and these photons can be further accelerated by the same electrons by inverse Compton diffusion. This process is called Synchrotron Self-Compton (SSC). Despite the success of this simple model, a number of questions remain about how the jets are powered by the black hole, or the causes of the short time-scale variability.

As a summary, here are the main pros (+) and cons (–) of AGN flares for LIV searches:

+ AGN are located at high redshifts;

+ Some flaring AGN have a high flux and a high variability;

+ The energy range available with IACT allows to probe large values of $\Delta E^n$;

– AGN flares are random events;

– Only IACT can be used to study LIV with AGN flares. Due to their limited effective area, satellites cannot access the required short variability;

– High energy gamma-rays produced by distant AGN can be absorbed by low energy photons of the EBL (see Section 2.4). This limits the highest distance for which flares can be observed by IACT;

---

[22]The interpretation of this kind of observations is difficult. Is it really the same flare that is seen? *Simultaneous* multiwavelength observations are not always available to answer that question.
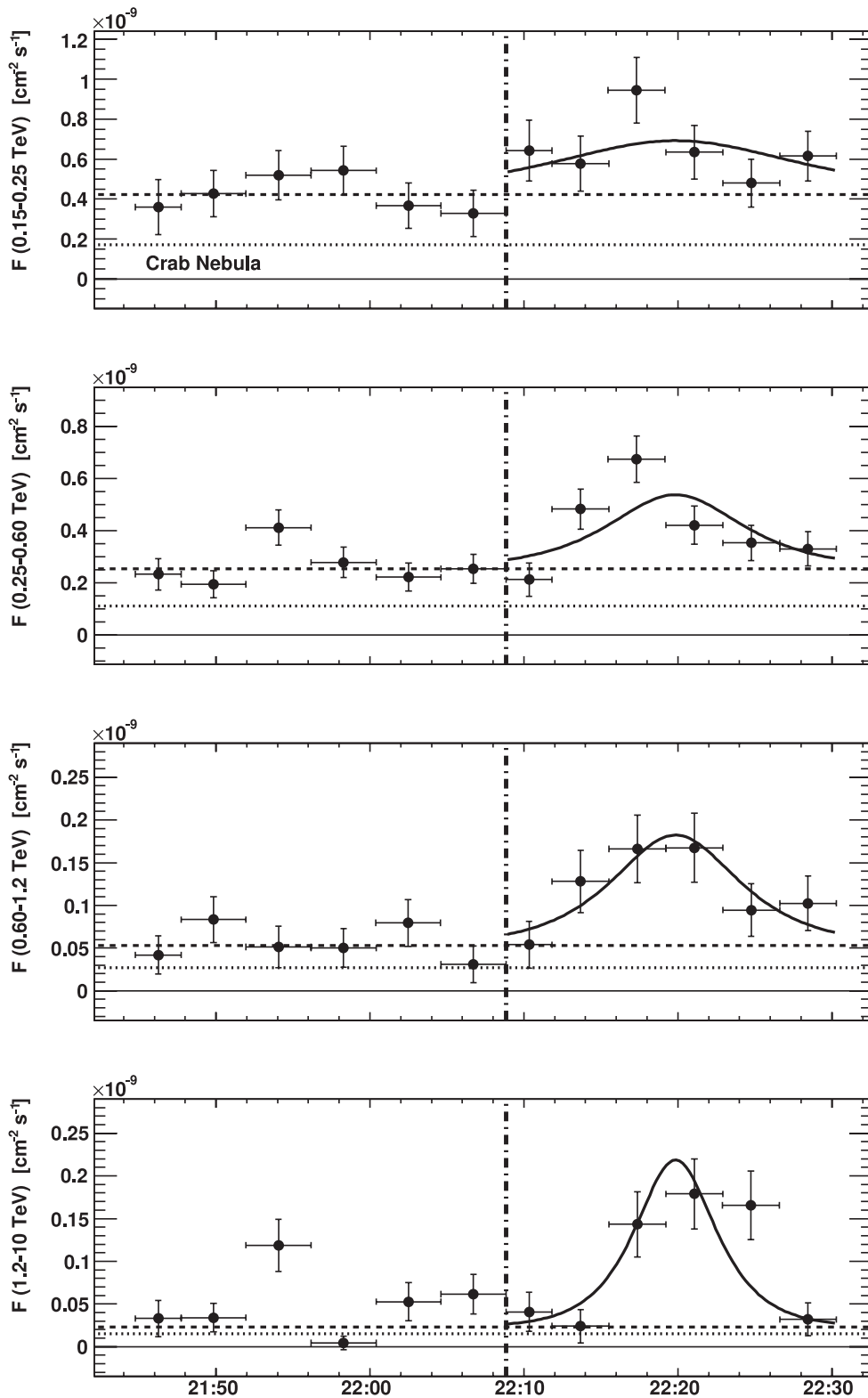
[23]https://magic.mpp.mpg.de/

**Figure 2.8:** Light curves of Mkn 501 for the flare of the night of July 9 2005, in four energy bands, from top to bottom, 0.15–0.25, 0.25–0.6, 0.6–2.1 and 1.2–10 TeV. The horizontal dashed line shows the average of the stable emission, while the dotted line shows the level of the Crab emission. The curves are fitted by a function $F(t) = a + b/(2^{-(t-t_0)/c} + 2^{(t-t_0)/c})$. Figure from [13].

– The redshift cannot be measured or estimated for all AGN;

– Emission mechanisms are poorly understood;

– There is evidence of intrinsic lags, at least for some flares. This suggests that every AGN is different in this regard.

It is important to note here that observation strategies can be optimized to maximize the number of flares detected. In particular, multiwavelength monitoring campaigns and swift reactions to take data when an alert is issued play an important role in flare detections.

**Pulsars**

A pulsar is a highly magnetised rotating neutron star [116, 76]. The neutron star is the result of the death of a massive star (4-8 $M_\odot$) in a supernova. The explosion blows off the outer layers of the star into a Supernova Remnant (SNR). The central region of the star collapses under gravity so that protons and electrons combine to form neutrons. In the process, the angular momentum as well as the magnetic flux are conserved. As a result, the neutron star has a very short rotation period (noted $P$, as low as a few milliseconds), and a very high magnetic flux ($10^8$ to $10^{14}$ G). A part of the rotational energy is lost through electromagnetic radiation or because charged particles escape along magnetic field lines. Then, the period slowly increases in time, with $\dot{P} = dP/dt$ values ranging from $10^{-13}$ to $10^{-20}$ s/s.

The *Fermi* satellite greatly improved the understanding of the mechanisms at play in pulsar high energy gamma-ray emission. It seems now established that polar regions of the neutron star cannot be involved in the GeV emission [41]. However, several other possibilities can still be invoked.

A very interesting feature of pulsar is that their light curves show very sharp peaks (Fig. 2.9). Their emission is periodic, with a slowly increasing period. This is a key point to distinguish between propagation and intrinsic effects. Indeed, any intrinsic lag when expressed *in rotational phase* will not vary in time as the period increases. On the contrary, a propagation effect will show up in the phasogram as slowly increasing with time [138].

As a summary, here are the main pros (+) and cons (–) of pulsars for LIV searches:

+ Pulsars are pulsating all the time;

+ The spikes in the phasogram can have a width of a few milliseconds. This turns into a very good precision on time-lag measurement and a possibility to probe spacetime fuzziness (see Section 2.4);
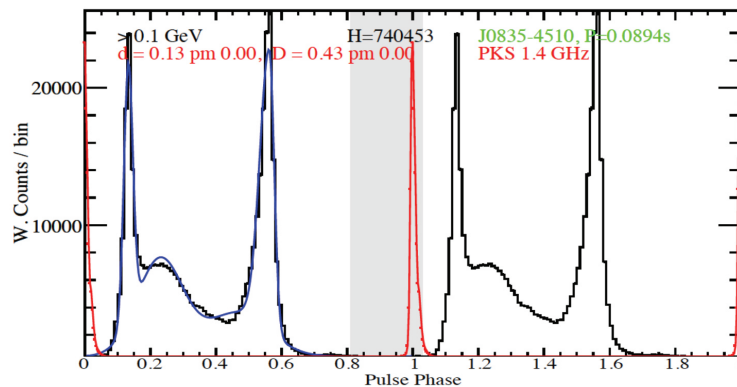


**Figure 2.9:** Comparison of *Fermi* γ-ray (black) and radio (red) light curves of the Vela pulsar for two rotation periods (P= 89 ms). Figure from [4].

+ Emission processes for the pulsed signal at GeV energies are poorly understood, but it is in possible to distinguish between source and propagation effects;

– Pulsars are located at short distances. This can be considered as an advantage only to test the dependance of LIV time-lags with distance: PSR can provide the low redshift points while GRB and AGN give the high redshift points;

– Only two pulsars were detected by IACT at O(100 GeV) energies, the Crab and Vela. These pulsars are probably very peculiar and only a few other known pulsars could have the same properties.

From this list, we can notice that PSR have more advantages than drawbacks. Unfortunately, the two drawbacks totally dominate over the few advantages. The furthest pulsar detected by the *Fermi*-LAT is PSR J0540–6919, located in the Large Magellanic Cloud (LMC) at 51 kpc. Despite its brightness (~20×Crab), more than 5 years of data taking were necessary to detect this object [7]. It could be detected with CTA if a significant amount of time is allocated for the observation of the LMC.

### 2.2.3   Complementarity of GRB, AGN and PSR

Since we have listed all the advantages and drawbacks of each kind of source, it is interesting now to summarize what we have seen, emphasizing on how the complementary of AGN, GRB and PSR could be used to obtain the best constraints on MDR.

In my view, four comments can be made:

- For GRB, a large amount of data is available from satellites. No GRB has been seen at TeV energies by ground-based experiments so far. Satellites can detect photons up to a few hundred GeVs. At these energies, very distant GRB can be detected, since the photons are only weakly absorbed by the EBL;

- For AGN observed by ground-based experiments, not only a detection is necessary, but also a significant variability is needed. This condition, added to the fact that a redshift measurement is also needed, has led to the fact that only four AGN were analyzed so far to search for LIV. AGN are seen by space-based experiments, but with low statistics due to their limited effective area. Ground-based Cherenkov telescopes have an energy range going from a few hundred GeVs to a few TeVs. At these energies, only nearby sources can be detected because of the EBL absorption;

- PSR are observed at GeV energies by satellites and a few are seen at TeV energies by IACT. The precision of time-lag measurement is extreme as compared to other sources. They are located at short distances, so they are essential to test the dependance of LIV time-lags with distance;

- GRB, PSR and AGN have different origins and therefore do not have the same intrinsic effects. For the moment, there is no fully accepted model, either for GRB or for AGN. The situation is a little better for pulsars, where it is possible to distinguish between intrinsic and extrinsic lags.

For these reasons, it is necessary to study GRB, AGN and PSR to look for LIV, not only separately but also in joined analyses. This is an important task for the close future, in particular when CTA will start to operate.

### 2.2.4 How to deal with source effects ?

Observations of GRB, AGN and PSR show that these ojects have intrinsic temporal properties that could compensate or amplify LIV effects. The question is now how to deal with these intrinsic effects in LIV searches ? Several strategies can be followed.

**Full modeling –** The best solution to manage intrinsic effects would be to precisely model the emission mechanisms. In an ideal world, the value of $\tau_{(source)}$ could be computed for each particular source under study and this value could be subtracted to the measured lag to deduce the lag due to LIV. Unfortunatly, we are far from this ideal picture. As we have seen, PSR are probably the sources for which the emission mechanisms are understood the best. This is probably due to the fact a rotating neutron star is a much simpler system to study than a black hole accreting gas and dust.

**Conservative modeling –** In [164], Vasileiou *et al.* introduce a conservative modeling of source effects for the first time. First, a Confidence Interval (CI) is obtained on $\tau_{n\,(total)}$ (see Eq. 2.46) assuming there is no intrinsic effect. Then, considering that the CI of $\tau_{(source)}$ is not likely larger than the width of the CI on $\tau_{n\,(total)}$, it is assumed that the CI on $\tau_{(source)}$ has the same width as the CI on $\tau_{n\,(total)}$ and that $\tau_{(source)}$ is zero on average. In principle, there are infinite choices for a particular value of $\tau_{(source)}$ given the constraints for its width and (zero) mean value. Then, Vasileiou *et al.* choose the one that produces the least stringent (the most conservative) overall constraints on $\tau_{n\,(LIV)}$, by modeling $\tau_{(source)}$ so that it reproduces the allowed range of possibilities of $\tau_{n\,(total)}$. See [164] for further details.

**Neglect intrinsic effects –** Since it is not possible to model the sources with enough details yet, a possibility is to neglect source effects altogether. There are several reasons why it is usually reasonable to do that:

- Up to know, the measured lags have always been found to be compatible with zero [24]. This suggest that either there is no LIV and no intrinsic effect, either the intrinsic effects compensate LIV effects exactly. The latter conspiracy scenario is highly improbable, of course;

- It is reasonable to state that source effects are maximized when several mechanisms are involved in photon emission. This can have an impact on LIV analyses when the data is spread over a wide energy range. By reducing the energy range, it is possible to ensure that the photons are emitted by one process in particular. Using more stringent energy selections, it is then possible to minimize source effects, at the expense of statistics. This criteria forbid the use of multi-wavelength observations to measure a time-lag;

- To measure time-lags, we have seen it is necessary that the light curves show variability. If the flux is high enough, it is common that light curves show multiple substructures (spikes). It is reasonable to assume that a given spike is the result of a single event at the source. Therefore, for a given spike, one could expect that intrinsic effects are the same for all photons. Selecting photons in a narrow time interval around a spike would minimize the intrinsic lag, at the expense of statistics. Note however that for AGN and GRB, intrinsic lags could be different for different spikes and that a particular spike could be made of several un-resolved sub-spikes with different intrinsic properties.

---

[24]We have seen however a notable exception with the flare of Mkn 501 detected by MAGIC in 2005. This is the only exception I know of.

**Use population studies –**    With a high number of PSR, GRB or flaring AGN detected, population studies would be possible.  The goal of these studies would be to extract average common properties for each of the three kinds of sources. Here again, several cases have to be considered:

- Source effects are universal. In that case, all sources of a given kind would have about the same intrinsic delays. At least, the dispersion of intrinsic lags $\sigma_{\tau_{(source)}}$ would be minimized to experimental uncertainties. With a high number of sources detected, it could be possible in principle to derive the averages intrinsic delay $\bar{\tau}_{(source)}$ to deduce an averaged LIV induced time-lag;

- Each source has its own intrinsic properties. In that case, which is certainly more likely than the previous one, we can only hope that values of $\sigma_{\tau_{(source)}}$ would be bounded to some limit, imposed by the inner engine of the sources.

In any case, as only the LIV delay is supposed to vary with distance, study of time-lags as a function of the distance of the sources will be essential. It is worth mentionning that population studies would anyway be of great interest to improve our understanding of sources and their modelization.

In the future, as there will be more and more sources observed, modelization and population studies will certainly progress drastically. As there will be more sources observed, the probability to observe a significant lag will also increase, which will forbid the possibility to neglect intrinsic lags.

### 2.2.5   How to measure the time-lags ?

A number of different methods can be used to measure the lags, from the simplest to the most elaborated. Some of these methods use the distributions of detection times (DDT) or the lightcurves [25] as basic ingredients. Some others do not.

The simplest method which does not use DDT was used by the *Fermi* collaboration to derive limits with GRB 080916C and GRB 090510 [2, 3]. In these papers, the authors simply compare the detection time of the highest energy photon detected by the LAT with the trigger time given by the GBM. Assuming that the highest energy photon cannot be emitted before the photons which triggered the GBM, they are able to derive very stringent limits. However, these limits, obtained with only one photon, cannot be considered as robust.

Another method which doe not use lightcurves is called PairView (PV), used by Vasileiou *et al.* [164]. The PV method calculates the spectral lags between all pairs of photons in a data set and uses the distribution of their values to estimate the LIV parameter.

For all the other analyses which were done until now, the first step starting from the raw data is always the same: split the data sample in two sub-sets to build lightcurves in two different energy bands. The energy selection used to split the initial sample in two energy ranges is chosen on a compromise: maximizing the energy lever arm ($\Delta E$) while keeping statistics as high as possible in the two ranges. The methods differ in the next steps.

The simplest one is certainly a direct comparison of spike positions in the two energy bands. Boggs *et al.* fit the two light curves and compute the difference between the fitted maxima positions in the two energy ranges [30]. Kaaret *et al.* [96] directly use the average of the main peak in the phasogram of the Crab pulsar in six energy bands. They also fit it with a Lorentzian.

Another very simple method is to use the Cross Correlation Function (CCF), a standard signal processing method which is used to measure the time shift between two signals. In the

---

[25]Strictly speaking, a DDT is not the same as a lightcurve: lightcurves give the flux as a function of time, while DDT give only a number of photons (actually gamma-like events) as a function of time.

first paper published by the H.E.S.S. collaboration [26] on the giant flare of PKS 2155-304 of 2006 [11], the authors use a standard cross correlation function modified (hence the acronym MCCF, for Modified CCF) to be applied to oversampled light curves [110]. The lag is obtained by fitting the position of the maximum of the MCCF, usually with a Gaussian function.

The Sharpness-Maximization Method (SMM) used by Vasileiou *et al.* [164] is based on the fact that the application of any form of spectral dispersion to the data (*e.g.*, by LIV) will smear the lightcurve decreasing its sharpness. Based on this, SMM tries to identify the degree of dispersion that when removed from the data maximizes its sharpness. This approach is similar to the Dispersion Cancellation (DisCan) technique [152] and the Energy Cost Function (ECF) method [14]. The most important difference between these approaches is the way the sharpness of the light curve is measured.

The next method I need to discuss is based on the use of wavelet transforms (WT) [117]. As CCF, this method is a well-known signal processing technique. However, WT does not provide the value of the time lag. It is used instead in two steps: to denoise the lightcurve and to localize the extrema. The result of this procedure is a list of extrema. Extrema, one in the low energy band and the other in the high energy band, need to be associated in pairs. Once this is done, the time lag can be computed for each pair of extrema, and averaged over all pairs.

Finally, the method which is commonly used in the most recent papers is a maximum-likelihood technique. Proposed by Martínez & Errando [122], this technique allows to study the correlations between the arrival time and the energy of the photons. A template lightcurve needs to be constructed first. This is done by parameterizing the (binned) lightcurve at low energies, which is less influenced by LIV dispersion. The high energy photons are then shifted in time depending on their energy and following a given model (either linear or quadratic) and "compared" to the template. The resulting probability density function is then used to compute the likelihood, which peaks at the preferred value of the time-lag.

To end this section, let me emphasize that each method has its advantages and drawbacks. As an example, CCF and PV are undoubtedly very simple to implement, while WT requires complex algorithms and a good understanding of the underlying mathematics. Different methods could be more or less sensitive to probe different aspects of the lightcurves. The choice of a method in particular should result from a detailed comparison involving the analyses of the same *simulated* data sets (as done in [164]). Such a comparison is anyway needed to evaluate the systematic uncertainties introduced by the time-lag measurement method.

## 2.3 Recent results

In this section, I will review the latest results obtained on MDR with astrophysical sources. Table 2.2 gives a summary of these results. I will first give some general comments and then I will focus in particular on my own work.

### 2.3.1 Overview

Looking at Table 2.2, we notice immediately that the best limit obtained so far is above the Planck scale. This limit, obtained with GRB 090510 by *Fermi*, is $E_{QG,1} > 7.6 \, E_P$, for a subluminal propagation. The same GRB is also the record holder for quadratic effects with $E_{QG,2} > 1.3 \times 10^{11}$ GeV. Even taking into acount possible source intrinsic effects with a conservative modeling (as discussed in Section 2.2.4), the linear limit is still above the Planck scale: $E_{QG,1} \gtrsim 2E_P$.

---

[26]https://www.mpi-hd.mpg.de/hfm/HESS/

**Table 2.2:** A selection of limits obtained with various instruments and methods for GRBs AGNs, and the Crab and Vela pulsars. Limits obtained for linear ($E_{QG,1}$) and quadratic ($E_{QG,2}$) corrections and for a subluminal effect, at 95% CL. The results are split in four categories: "Individual GRB", "Several GRB", "Individual flaring AGN" and "Individual PSR". By "individual", I mean that only one source was analyzed to derive the limit. On the contrary, for the second category, "Several GRB", a global fit was done to look for a dependance of the time-lags with redshift.

| Category | Source(s) | Experiment | Method | Results[a] | | Reference | Note |
|---|---|---|---|---|---|---|---|
| Individual GRB | GRB 021206 | RHESSI | Fit + mean arrival time in a spike | $E_{QG,1} > 1.8 \times 10^{17}$ GeV | | [30] | b,c |
| | GRB 080916C | Fermi GBM + LAT | associating a 13 GeV photon with the trigger time | $E_{QG,1} > 1.3 \times 10^{18}$ GeV | $E_{QG,2} > 0.8 \times 10^{10}$ GeV | [3] | |
| | GRB 090510 | Fermi GBM + LAT | associating a 31 GeV photon with the start of any observed emission, DisCan | $E_{QG,1} > 1.5 \times 10^{19}$ GeV | $E_{QG,2} > 3.0 \times 10^{10}$ GeV | [2] | d |
| | | Fermi LAT | PairView, SMM, likelihood | $E_{QG,1} > 9.3 \times 10^{19}$ GeV | $E_{QG,2} > 1.3 \times 10^{11}$ GeV | [164] | j,★ |
| Several GRB | 35 GRBs | BATSE + HETE-2 + Swift | wavelets | $E_{QG,1} > 1.4 \times 10^{16}$ GeV | | [61, 62] | g,h |
| | 17 GRBs | INTEGRAL | likelihood | $E_{QG,1} > 3.2 \times 10^{11}$ GeV | | [106] | f |
| | 15 GRBs | HETE-2 | wavelets | $E_{QG,1} > 0.4 \times 10^{16}$ GeV | $E_{QG,2} > 2.9 \times 10^{6}$ GeV | [32] | e,★ |
| | 9 GRBs | BATSE + OSSE | wavelets | $E_{QG,1} > 0.7 \times 10^{16}$ GeV | | [63] | b |
| | 9 GRBs | BATSE + OSSE | Fit | $E_{QG,1} > 10^{15}$ GeV | | [58] | b |
| Individual flaring AGN | Mrk 421 | Whipple | likelihood | $E_{QG,1} > 0.4 \times 10^{17}$ GeV | | [25] | b,i |
| | Mrk 501 | MAGIC | ECF, likelihood | $E_{QG,1} > 0.2 \times 10^{18}$ GeV | $E_{QG,2} > 2.6 \times 10^{10}$ GeV | [14] | |
| | | | likelihood | $E_{QG,1} > 0.3 \times 10^{18}$ GeV | $E_{QG,2} > 5.7 \times 10^{10}$ GeV | [122] | |
| | PKS 2155-304 | H.E.S.S. | MCCF | $E_{QG,1} > 7.2 \times 10^{17}$ GeV | $E_{QG,2} > 0.1 \times 10^{10}$ GeV | [11] | |
| | | | wavelets | $E_{QG,1} > 5.2 \times 10^{17}$ GeV | | | |
| | | | likelihood | $E_{QG,1} > 2.1 \times 10^{18}$ GeV | $E_{QG,2} > 6.4 \times 10^{10}$ GeV | [5] | ★ |
| | PG 1553+113 | H.E.S.S. | likelihood | $E_{QG,1} > 4.1 \times 10^{17}$ GeV | $E_{QG,2} > 2.1 \times 10^{10}$ GeV | [6] | k,★ |
| Individual PSR | Crab pulsar | EGRET | average time of the main pulse in different energy bands, fit of main pulse | $E_{QG,1} > 0.2 \times 10^{16}$ GeV | | [96] | |
| | | VERITAS | DisCan | $E_{QG,1} > 1.9 \times 10^{17}$ GeV | | [171] | |
| | | MAGIC | likelihood | $E_{QG,1} > 7 \times 10^{17}$ GeV | $E_{QG,2} > 4.6 \times 10^{10}$ GeV | [157] | |
| | Vela pulsar | H.E.S.S. | likelihood | $E_{QG,1} > 3.5 \times 10^{15}$ GeV | $E_{QG,2} > 6.4 \times 10^{8}$ GeV | [43] | ★ |

a Results can be expressed in the SME framework using Eqs. 2.43 and 2.44.
b Limit obtained not taking into account the factor $(1 + z)$ in the integral of Eq. 2.40.
c The pseudo-redshift estimator [140] was used. This estimator can be wrong by a factor of 2.
d Only the most conservative limit is given here.
e Photon tagged data was used.
f The pseudo-redshift estimator [140] was used for 6 GRB out of 11.
g For HETE-2, fixed energy bands were used.
h The limits of [61] were corrected in [62] taking into account the factor $(1 + z)$ in the integral of Eq. 2.40. Only the limit obtained for a linear correction is given.
i A likelihood procedure was used, but not on an event-by-event basis.
j In this study, four bursts were analyzed. Only the best limits are given here, obtained for GRB 090510 with the PairView ($n = 1$) and SMM ($n = 2$) methods.
k The redshift of this source was not measured but only estimated.
★ Analyses in which I've been involved.

It is necessary to note that this burst is very bright and very short, with a very simple lightcurve showing only one spike of width < 1 s. Its redshift is moderate: $z = 0.903 \pm 0.15$. The characteristics resulting in this very stringent limit are its short duration, and the fact the highest energy photon is detected at ~30 GeV, resulting in the highest energy lever arm ever obtained with a GRB. This result can certainly be considered exciting. However, it is necessary to stress that no conclusion on LIV at the Planck scale should be drawn on only one source. In addition, as we have seen earlier when discussing a model of stringy spacetime foam, the relevant energy scale could be different from the Planck scale.

In Table 2.2, two results have been obtained using a population of GRB detected by different experiments. In [63], data from *BATSE* and *OSSE* are used, while in [61, 62] the data of three experiments are combined. Because each experiment introduces different systematics, this kind of combination must be done with caution. In my opinion, this problem was overlooked in these papers.

The next result I need to comment is the one obtained with a flare of Mkn 501 observed by MAGIC. This flare is particularly interesting since, as we have seen already, Mkn 501 is the only AGN showing time-lag between high and low energies for a linear LIV. Using ECF, Albert *et al.* [14] find delay parameters of $\tau_1 = (0.030 \pm 0.012)$ s/GeV and $\tau_1 = (3.71 \pm 2.57)$ s/GeV². These values were cross-checked with a likelihood technique and compatible values were found.

The corresponding values of $E_{QG,1}$ and $E_{QG,2}$ can still be found in the first version of the paper available on the arXiv: $E_{QG,1} = (0.47^{+0.31}_{-0.13}) \times 10^{18}$ GeV and $E_{QG,2} = (0.61^{+0.49}_{-0.14}) \times 10^{11}$ GeV. These results did not make it to the final version of the paper where only the limits quoted in table Table 2.2 are given. Of course, the authors carefully discussed the possible interpretation of these results. They exclude in particular the possibility that the measured delay is due to a conventional QED plasma refraction effect [108] as photons propagate through the source (see Section 2.5.2). However, they cannot exclude an intrinsic lag.

Finally, it is interesting I think to comment on the results currently obtained from observations of the Crab and Vela pulsars at TeV energies. These pulsars are the only two detected by ground based experiments. The Crab pulsar is located at a distance of 2.2 kpc and its period is P = 33 ms. The Vela pulsar's distance is 294 pc and its period is P = 89 ms. The other main difference between these two sources is the time spent to observe them. MAGIC and VERITAS [27] have published their limits for the Crab with 300 hours and 107 hours of data, respectively. The H.E.S.S. result for the Vela pulsar was obtained with 24 hours of data taking. All these differences explain the fact that the limits on LIV with the Vela pulsar are two orders of magnitude below the ones obtained with the Crab pulsar.

It is worth pointing out the limit obtained on the quadratic LIV effect with the Crab pulsar by MAGIC. This limit at $4.6 \times 10^{10}$ GeV is more stringent than some results obtained with flaring AGN. It is a clear indication that pulsars, as soon as a significant observation time is allocated for them are valuable candidates for LIV searches, despite their small distance. This is another argument to support an increased effort to detect more pulsars at TeV energies.

I turn now to a discussion about my own contributions.

### 2.3.2 Comments on my contributions

I have been working on MDR tests with photons for about 13 years. I had the opportunity to work with GRB, AGN and PSR and to use different methods for time-lag measurement. In this section, I will comment on my different publications.

In chronological order, I have been involved in the analyses of:

---

[27] http://veritas.sao.arizona.edu/

- 15 GRB detected by the satellite *HETE-2* [32]. A global fit was done to look for a dependance of the time-lag with the redshift;

- The giant flare of PKS 2155-304, recorded by H.E.S.S. in 2006 [5];

- 4 GRB detected by the *Fermi*-LAT [164]. A limit was obtained for each individual GRB;

- A flare of PG 1553+113, recorded by H.E.S.S. in 2012 [6];

- The Vela pulsar, observed during 24 hours by the fifth telescope of H.E.S.S. in 2013 [43, 44]. The analysis was done by my first PhD student, M. Chretien.

In addition, I also wrote (together with A. Jacholkowska) a review article [31], which gives a broad picture, as of 2011, of LIV searches with astrophysical sources. I will discuss all the papers and the PhD listed above in the following paragraphs. I will not give the limits, which are already listed in Table 2.2.

**Gamma-Ray Bursts: comments on Bolmont *et al.* (2008) and Vasileiou *et al.* (2013)**

**Bolmont *et al.* (2008) –**   My first paper concerning MDR was about the analysis of 15 GRB detected by the satellite *HETE-2* between 2001 and 2006, with redshifts ranging from 0.16 to 3.37. Source intrinsic effects were assumed to be the same for all bursts, and I looked for a dependance of the average $\Delta t_1$ as a function of $z$:

$$\langle \Delta t_1 \rangle = a\,\kappa_1(z) + b\,(1+z),$$

where a and b parameters represent extrinsic (QG) and intrinsic effects, respectively.

The analysis of the 15 GRB was done with Wavelet Transforms and involved the following steps:

- De-noising of the light curves by a Discrete Wavelet Transform (DWT);

- Search for spikes in the light curves using a Continuous Wavelet Transform (CWT). The result of this step is a list of maxima candidates, along with a coefficient characterizing their regularity (Lipschitz coefficient);

- Association in pairs of the maxima, one maximum of the low-energy light curve and one at high energies. A criterium on the Lipschitz coefficients was used to ensure that the two maxima really belong to the same pair.

The result of this (complex) procedure is a set of associated pairs of extrema, one per GRB, from which the averaged time-lag $\langle \Delta t_1 \rangle$ is calculated. The next step consists in studying the variation of $\langle \Delta t_1 \rangle$ as a function of the redshift. This was done using a likelihood fit (different from the procedure described above).

The limit obtained in this study is of course quite low as compared to the results obtained later with *Fermi* or with H.E.S.S. This is due to the limited energy range available with *HETE*, which translates into a mean energy lever arm of $\Delta E \sim 130$ keV. This is about five orders of magnitude below the one obtained by *Fermi* and seven orders of magnitude below the lever arm typically reached with IACT. Nonetheless, this analysis is still valuable considering it is a prototype of the population studies which will have to be performed in the future.

As an aside, let me mention that a full toy Monte Carlo calibration of the WT method has never been done and should have been included in this paper.

**Vasileiou *et al.* (2013) –** Before the work on this paper began, the Large Area Telescope (LAT) on board the *Fermi* satellite had already provided the most constraining limits on $E_{QG}$ using GRB 080916C [3] and GRB 090510 [2]. These past results were derived studying the highest energy photon detected in coincidence with the bursts or using the DisCan method in the case of GRB 090510.

In this new paper, four GRB were analyzed. All have a bright GeV prompt emission and a measured redshift. These GRB are 080916C, 090510, 090902B and 090926A, located respectively at $z = 4.35 \pm 0.15$, $0.903 \pm 0.003$, $1.822$ and $2.107$. Three different statistical methods were used to measure the time-lags: SMM, PV and a likelihood procedure. All these methods are discussed earlier in this monograph.

All measured lags were found to be compatible with zero and the three methods are in good agreement with each other. No evidence was seen for a variation of $\tau$ with $\kappa_n$ as would be expected for a LIV effect. An in-depth study of systematics showed that the intrinsic effects are the main source of systematics. Other systematics, due to the instrument response, the errors on redshift and cosmological parameters, were found to be negligible.

I have already commented on the obtained limits. A major breakthrough, in addition to the limits themselves, is the statistical treatment of source intrinsic effects (that I discussed too). It is certainly the reasonable thing to do in the lack of a full modelization of emission mechanisms.

## Active Galactic Nuclei: comments on Abramowski *et al.* (2011) and Abramowski *et al.* (2015)

**Abramowski *et al.* (2011) –** On July 28, 2006, H.E.S.S. observed an extreme flare of the BL Lac object PKS 2155-304 ($z = 0.116$) [12]. More than 8000 photons were detected above ~120 GeV in ~85 minutes of data taking and negligible background. This high statistics allowed the observation of variability at the minute time scale. This data was first analyzed using CCF and wavelets [11] and I was involved in a second analysis based on the likelihood procedure introduced in [122].

In my opinion, an important added value of [5], in addition to the good limits on $E_{QG,n}$, is the amount of work done to check the accuracy of the likelihood fit and to evaluate the effect of different factors on the results. This was done with toy Monte Carlo simulations. These checks had not been fully reported in [122]. The main systematics were found to be related to the parameterization of the low energy lightcurve. This can be easily explained since the lightcurve shows five different spikes with a significant overlap.

The limits obtained in this study are still the most constraining ever obtained with an AGN. They are almost ten times better than those obtained with the flare of Mrk 501 recorded by MAGIC. They are also a factor of ~3 higher than the previous H.E.S.S. result [11].

The increase in sensitivity as compared to the MAGIC result is mainly due to excellent parameters of the data taken on July 28, 2006: low zenith angle (~ 10°) which leads to a low energy threshold, high statistics, high variability and negligible background. On the other hand, the softness of the PKS 2155-304 energy spectrum (the spectral index is ~3) was the main penalizing factor in this study.

**Abramowski *et al.* (2015) –** During the nights of 2012 April 26 and 27, H.E.S.S. detected a flare of the high-frequency peaked BL Lac object PG 1553+113 [6]. The spectrum is softer as the one of PKS 2155-304 with an index of ~5. This is in part due to the fact that PG 1553+113 is much further than PKS 2155-304: although the redshift is not known precisely, it was estimated to be $z = 0.49 \pm 0.04$ [6]. Another big difference with the flare of PKS 2155-304 is the much lower statistics: ~300 signal events were recorded and the signal-to-background ratio was ~2.

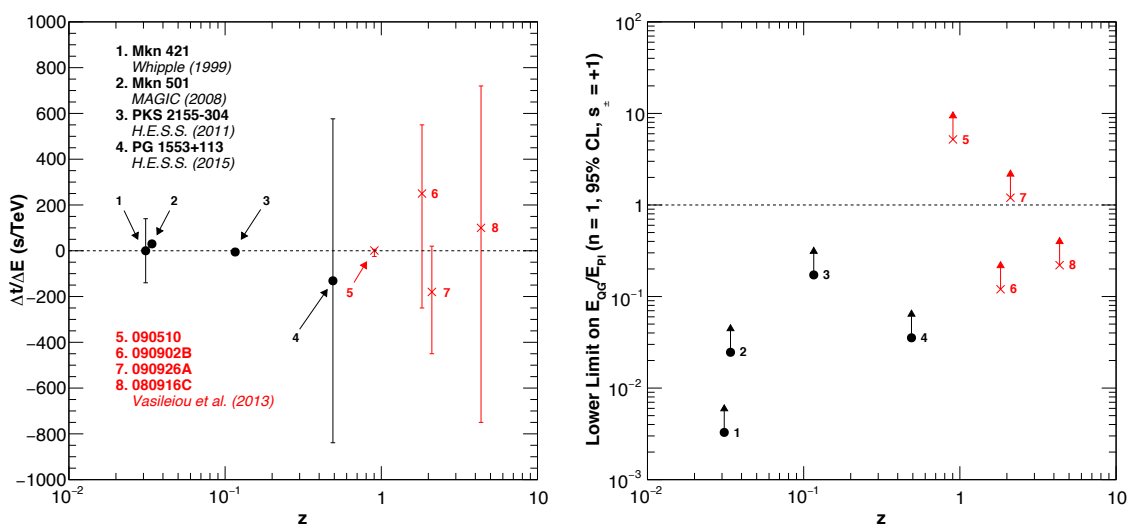**Figure 2.10:** Spectral lags (left) and corresponding lower limits on $E_{QG,1}$ obtained in [164] (red crosses) and in previous works (black dots) using AGN high energy gamma-ray observations: 1. *Whipple* observation of Mkn 421 [25]; 2. MAGIC observation of Mkn 501 [122]; 3. H.E.S.S. observation of PKS 2155-304 [5]. See the text for comments.

These low statistics required a modification of the likelihood procedure used for the analysis of PKS 2155-304 in order to properly take into account the effect of background events.

Due to the poor statistics, the limit on the linear LIV cannot compete with the one obtained with PKS 2155-304. However, the quadratic LIV effect is constrained at about the same level, due to the larger distance of PG 1553+113. This lead to two important lessons for future studies: (*i*) it is possible to get constraining limits even in case of background contamination, and (*ii*) distance can compensate low statistics to constrain quadratic effects.

Fig. 2.10 allows to compare the results obtained with GRB and AGN in the GeV-TeV domain. All these results were obtained using a likelihood method and all correspond to a subluminal propagation. The furthest AGN in this plot is PG 1553+113, with $z = 0.49$ while the most distant GRB is 080916C ($z = 4.35$). On the left plot, the error bars are smaller for AGN than for GRB. It is a direct consequence of the fact the energy lever arm (related to the energy coverage of the instruments) is much larger in ground-based observations. On the plot on the left, one can see that the limits obtained with AGN are on average less constraining than those obtained with GRB. However, a giant flare as the one of PKS 2155-304 in 2006 gives a constraint which is at the level of some GRB with higher redshifts. Finally, we have to point out again that GRB 090510 can be considered as peculiar in a sense that it is very short, very bright and very energetic.

### Pulsars: comments on M. Chretien's PhD (2015)

From March 2013 to April 2014, the 28-meter H.E.S.S. telescope collected 24 hours of good quality data from the Vela pulsar. About 9000 pulsed events were recorded between ~20 GeV and 100 GeV at low zenith angles. The detection was confirmed using two independent analysis pipelines. The signal-to-noise ratio was estimated to be ~0.025.

The likelihood procedure described earlier and used in [6] (including a proper treatment of the background) has been slightly modified to be more suited to the case of periodic sources. In particular, a *phase-lag* $\Delta\phi$ is used instead of the time-lag $\Delta t$. $\Delta\phi$ is given by $\Delta\phi = \Delta t \times f_0$, where $f_0$ is the pulsar rotational frequency.

As in [5, 6, 164], a toy Monte Carlo procedure was used to control the accuracy of the method and to evaluate the different systematics. The obtained limits were already discussed earlier.
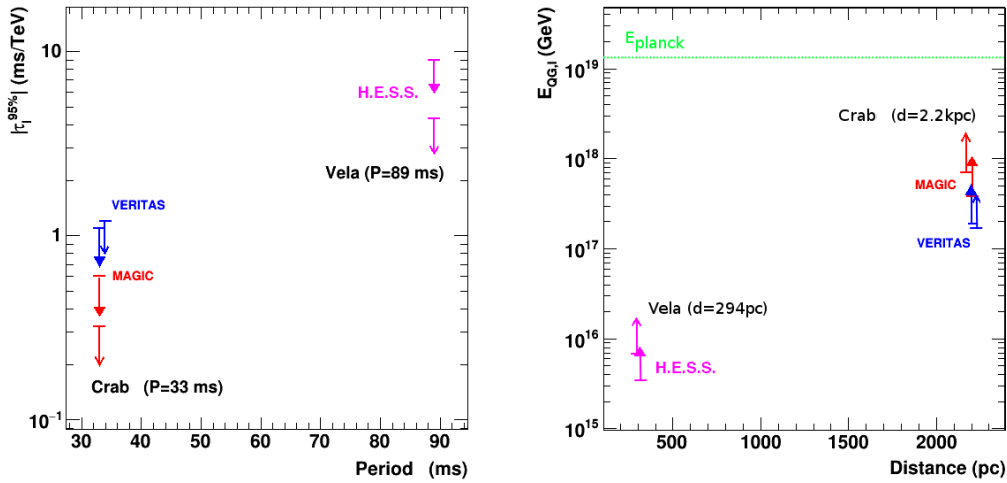
**Figure 2.11:** Upper limits obtained on the time-lag parameter $\tau_1$ as a function of the period (left) and lower limits obtained on the QG energy scale (linear effect) as a function of the distance for the two pulsars ever observed at TeV energies. Full arrows correspond to a subluminal LIV effect while open arrows correspond to a superluminal propagation. The plots are taken from [43]. Data points are taken from [43, 157, 171].

Of course, the work of M. Chretien during the three years of his PhD was not limited to this particular analysis.

Fig. 2.11 summarize the results presently available with pulsars observed at TeV energies. The differences between these results were already commented in Section 2.3.1: Vela is penalized by its smaller distance and by the fact the limits were obtained with only 24 hours of data taking.

## 2.4 Other possible QG-induced effects on gamma-rays

Until now, I focused on MDR searches because they are my main topic of interest. However, a modification of dispersion relations is not the only possible effect that could be the result of the quantum nature of spacetime.

In the last section of this chapter, I would like to quickly go back to three other possibilities, that I have already mentioned earlier: (*i*) spacetime fuzziness (mentioned in Section 2.1.2 as a possible result of a stringy spacetime foam), (*ii*) vacuum birefringence (mentioned in the same section as a possible result of LQG-inspired models) and (*iii*) LIV-induced modification of photon-photon interaction cross section (mentioned in Section 1.2.4 as a result of MDR if the photon is considered to have an effective mass).

### 2.4.1 Fuzziness and foaminess

When discussing the stringy spacetime foam model in Section 2.1.2, we have seen that D-particles popping in and out of our universe can introduce a stochastic spread of the velocities of the photons of the same energy. This phenomenon would result in an energy-dependent broadening of the sharp emission spikes of variable or transient astrophysical sources. Quantum fluctuations of spacetime could also have an effect on macroscopic distances. These distances could fluctuate randomly so that light waves emitted coherently at the source would lose their coherence while they propagate. I will now discuss briefly these two kind of effects, which are usually referred to respectively as *fuzziness* and *foaminess* (of spacetime).

When searching for a broadening of emission spikes, the speed of the photons is expressed

as [163]:

$$v(E) = c + \delta v(E), \tag{2.47}$$

where $\delta v(E)$ is a normally distributed and zero average random variable, with a standard deviation

$$\sigma_n(E) = \frac{1+n}{2} \left( \frac{E}{E_{QG,n}} \right)^n c. \tag{2.48}$$

In this last equation, $n$ gives the leading-order energy dependence of the effect and $E_{QG,n}$ is the energy scale of stochastic LIV. Using the very short burst GRB 090510, which has a lightcurve showing substructures as short as ~10 ms, Vasileiou *et al.* were able to obtain constraints above the Planck scale, at 2.8 $E_P$ (95% CL). Due to their very short spikes, distant pulsars could be very interesting to probe this kind of fuzziness.

When looking for a loss of coherence of light waves, the path-length fluctuations are usually expressed as

$$\delta l \simeq l^{1-\alpha} l_P^{\alpha} \tag{2.49}$$

where $l_P$ is the Planck length, $l$ is the line-of-sight comoving distance of the source and where $\alpha$ allows to consider different types of quantum foams [132]. The corresponding phase fluctuation is then simply

$$\delta \phi \simeq l^{1-\alpha} l_P^{\alpha} \frac{2\pi}{\lambda}, \tag{2.50}$$

where $\lambda$ is the observed wavelength. Since the phase shift is different for different wavelengths, all the light waves emitted by a distant sources would ultimately cancel out. As a result, an observer would not be able to observe a distant source at arbitrary high energies. In [141], this approach is used to constrain parameter $\alpha$ with distant quasars observed by *Chandra* [28] and AGN observed by *Fermi* and IACT. Observations at TeV energies of objects as far as $z = 0.9$ allow to obtain the best limit on $\alpha$ to date: $\alpha > 0.72$. See also [154, 46, 45] for more details.

### 2.4.2   Vacuum birefringence

We have seen earlier that the MDR obtained from a LQG perspective introduces vacuum birefringence. Following [73], the dispersion relation is approximated as

$$\omega_{\pm}(k) \simeq |k| \left( 1 \pm \frac{\xi k}{M_P} \right), \tag{2.51}$$

where $\xi$ is a constant giving the amplitude of the effect and $M_P$ is the Planck mass. If photons are initially linearly polarized, this MDR leads to a rotation of the polarization during propagation. The polarization plane rotates by an angle

$$\Delta\theta(p) = \frac{\omega_+(k) - \omega_-(k)}{2} d \simeq \xi \frac{k^2 d}{2 M_P}, \tag{2.52}$$

where $d$ is the distance of the source. From this equation, we see that the angle increase with the distance of the source. If this distance is large enough, polarization will ultimately vanish.

Using *INTEGRAL*-IBIS data for GRB 140206A ($z = 2.739$) in the range 200-400 keV, Götz *et al.* [73] found a polarization angle of 80±25 at the 90% CL. They derived the best constraint available today: $\xi < 1 \times 10^{-16}$. This kind of constraint disfavor the LQG-inspired model I discussed earlier while stringy spacetime foam model forbids birefringence.
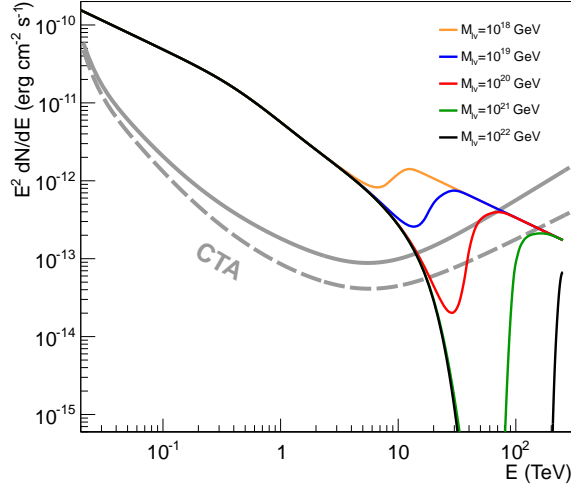
---

[28]http://chandra.si.edu

**Figure 2.12:** Expected spectrum of the blazar Mkn 501 for different valeus of the QG energy scale. Two sensitivity curves are plotted. The continuous grey line correpsonds to a nominal 5-$\sigma$ detection for 50 hours of observations with 0.2 in $\log(E)$ bins and a minimum of 10 signal events required in each bin. The dashed line correspond to a relaxed criterium without the requirement for 10 signal events per bin, and wider bins of 0.6 in $\log(E)$. Figure from [65].

### 2.4.3 Energy threshold of gamma-gamma interaction

If the photon is allowed to have a non-zero mass $m_\gamma$, it will naturally obey a dispersion relation of the form

$$p^2 c^2 = E^2 - m_\gamma^2 c^4. \tag{2.53}$$

By comparing Eqs. 2.23 and Eq. 2.53, considering only the lowest order dominant term in the expansion and a subluminal effect, we obtain the effective mass

$$m_\gamma^2 \simeq \frac{k_n'}{c^4} \frac{E^{n+2}}{E_P^n}. \tag{2.54}$$

As a result, kinematic constraints from energy-momentum conservation will be different from the usual Lorentz invariant case: reactions involving photons which are normally forbidden will take place, and thresholds for other reactions will be modified. For example, photon decay ($\gamma \to e^+ e^-$) and vacuum Tcherenkov radiation ($e^- \to \gamma e^-$) will be allowed and the threshold for photon-photon interaction ($\gamma\gamma \to e^+ e^-$) will be modified. I focus in the following on this last interaction.

Because high energy gamma-rays can interact during their propagation with photons of the Extragalactic Background Light (EBL), a modification of photon-photon interaction dynamics should lead to modifications in the measured spectra of very high energy gamma-ray sources. In particular, the threshold of pair-creation would become (following notations of [26]):

$$\epsilon_{thr} = \frac{m_e^2 c^4}{E} \times \left[ 1 + \left( \frac{E}{E_{\gamma, LIV}} \right)^{n+2} \right], \tag{2.55}$$

where

$$E_{\gamma, LIV} = 29.6 \text{ TeV} \times \left( \frac{E_{QG,1}}{E_P} \right)^{1/3} \tag{2.56}$$

for $n = 1$.

These relations result in the fact the optical depth of the EBL would be reduced above 10 TeV. This would in turn change the shape of the spectra of distant sources. Analyzing a sample of 86 AGN spectra, Biteau & Williams [26] were able to set a limit at $E_{QG,1} > 0.6\, E_P$. Note however that a few AGN certainly dominate in this result, because of their higher brighness (in particular PKS 2155-304 and Mkn 501). In addition, the results strongly depend on the considered EBL model.

More recently, using the data recorded in 1997 by HEGRA [29] during a flare of Mn 501, Tavecchio & Bonnoli [156] set a limit at $E_{QG,1} \gtrsim 2.5\, E_P$.

As discussed in [65, 156], CTA will be a great tool to look for this effect. Fig. 2.12 shows the result of a simulation of the spectrum of Mkn 501 for different values of the QG energy scale. The reduction of the optical path appears as a dip in the spectra around 10 TeV.

## 2.5 Some possible non-QG-induced photon delays

To close this chapter, I would like to mention some (hypothetic or real) phenomena, not related to QG phenomenology, which could induce delays in photon propagation. The delays described here are energy-dependent, but we will see that their magnitude is either so small or so big than they do not compete at all with the delays expected in QG appoaches with MDR. This list is not exhaustive !

### 2.5.1 Non-zero mass of the photon

Several methods can be used to constrain the mass of the photon. According to the review article [71], the best "safe" limit on the photon mass was obtained by studying the solar wind plasma as far as Pluto's orbit. The solar wind plasma would indeed have very different density, velocity and pressure in the case the photon would have a mass. Using *Voyager-1* [30] data, the limit $m_\gamma \lesssim 10^{-18}$ eV is derived in [151].

If we now consider Eq. 2.54, assuming $n = 1$, $k'_1 = 1$ (this sets the QG energy scale at the Planck scale), and $E = 100$ TeV (a rough estimate of the highest energy CTA will be able to detect), we get $m_\gamma \sim 3 \times 10^{-5}$ eV. We then can conclude that the expected QG-induced LIV effects are much higher in magnitude than those resulting from a possible non-zero mass of the photon.

### 2.5.2 Plasma effects

Right after their emission, the photons produced by an astrophysical source can cross a rather complex medium, namely a QED plasma, where the refraction index is non-trivial [108]. This non-trivial refractive index leads to a delay between high and low energy photons. This delay is of the form (expressed in natural units $c = \hbar = 1$):

$$\Delta t = D\, \frac{\alpha^2 T^2}{6q^2} \ln^2\left(\frac{qT}{m_e^2}\right), \tag{2.57}$$

where $\alpha$ is the fine structure constant, $q$ the photon momentum, $T$ the plasma temperature, $m_e$ the mass of the electron and $D$ the size of the plasma.

Considering photons of $q = 1$ TeV and possible values of $T \sim 10^{-2}$ MeV and $D = 10^9$ km (values taken from [14]), we obtain a delay $\Delta t \sim 1$ ps, which is much smaller than the temporal resolution reached by present day experiments.

---

[29] https://en.wikipedia.org/wiki/HEGRA
[30] http://voyager.jpl.nasa.gov

### 2.5.3 Interaction of photons with dark matter particles

About 27% of the mass and energy of the observable universe is composed of dark matter (DM). This matter is dark because it does not emit or interact with electromagnetic radiation. However, it has observable effects, *e.g.* on the motion of visible matter (rotation of galaxies) or on the path of light rays through the universe (gravitational lensing).

Since DM is present everywhere in the universe, photons emitted by distant sources do not truly propagate in vacuum. In [70, 107], the authors claim that photons could actually scatter on DM particles which would result in an energy-dependent refractive index. The effect is very weak, however. For a DM candidate of mass ~100 GeV, the DM effect on photon propagation would compete with quadratic LIV effects only at energies above $10^{29}$ GeV. No DM effect is found that could mimic a linear LIV.

# Chapter 3

# Conclusions and outlook

> *We shall have the basic framework of the quantum theory of gravity by 2010, 2015 at the outside.*

– L. Smolin, *Three Roads to Quantum Gravity* (2001)

> *I propose as a hypothesis, [...] that single gravitons may be unobservable by any conceivable apparatus. If this hypothesis were true, it would imply that theories of quantum gravity are untestable and scientifically meaningless.The classical universe and the quantum universe could then live together in peaceful coexistence. No incompatibility between the two pictures could ever be demonstrated. Both pictures of the universe could be true, and the search for a unified theory could turn out to be an illusion.*

– F. Dyson, "The Edge annual question" (2012), www.edge.org

## Summary

In this monograph, I started by introducing in some detail what is Lorentz Invariance and Lorentz Invariance Violation (LIV). This allowed me to discuss the tests of Lorentz Invariance which are not primarily related to Quantum Gravity (QG) phenomenology. Then I came to my main topic of interest: the search for modified dispersion relations (MDR) for photons in vacuum. These MDR imply a violation of Lorentz Invariance and are predicted in some models of QG. I explained how these MDR can be tested with astrophysical gamma-ray sources: Active Galactic Nuclei, Gamma-Ray Bursts and pulsars. I discussed each of these sources and explained that their emission mechanisms are not fully understood at present. Then, I answered the question of the

title: yes, as of today, the speed of light in vacuum is really constant! Finally, I reviewed in detail the limits available in the litterature on the QG energy scale as well as my own contributions.

I would like to conclude this memoir by some additional comments.

## Uncertainties on a theory

None of the proposed approaches to QG (ST, LQG, Causal sets, Non-commutative geometry, etc.) is fully understood at present. The fact that the number of different possible ways to QG has increased a lot these last years is at the same time a good and a bad thing. It is a good thing since it proves the dynamism of the community in that field, and it is a bad thing since we are ultimately looking for a unique theory. At this point, we can only hope that one day, a common picture will emerge in the different appraoches, and that this picture will help to unveil the underlying truly fundamental theory of QG. This point of view, advocated by L. Smolin (see the optimistic quotation above) and many others, is not shared by all (see e.g. the pessimistic claim by F. Dyson).

In any case, a lot remains to be done on our way to a full theory of Quantum Gravity.

## We need to explore all possible ways to Quantum Gravity

Experimentalists have a very important role to play on that way looking for deviations in standard physics. Any such deviation could be a good hint for theorists so that they can tune their models, or even reject some ideas. In the few cases where approaches to QG are able to predict some effects, all these effects must be tested. As experimentatlists, *we need to explore all possible ways to Quantum Gravity*.

As explained in this monograph, I have followed one way in particular: the possibility that the speed of photons would depend on their energy in vacuum, because of the fundamental quantum nature of spacetime. QG phenomenology is not restricted to this effect in particular and other particles than photons can be affected by various QG-related effects. Since I mainly focused on MDR, I did not mention all these tests. Review articles exist where they are discussed in detail (see in particular [17]).

Furthermore, we need to keep in mind that some other experimental directions could have a profound impact on our understanding of QG. These other ways include the search for microscopic black-holes at the LHC, the search for B-modes in the polarization of the CMB, the search for Supergravity, etc.

For the following points, I focus again on tests of MDR with high energy gamma-ray sources.

## Progress is needed on emission models

CTA, the Cherenkov Telescope Array [8], with a larger energy range (10 GeV – 100 TeV), a higher sensitivity (×10 with respect to the present generation of IACT) and observation strategies to optimize the number of transient or variable objects detections, is expected to allow significant progress. PSR observations will also be favored by the energy threshold of ~10 GeV.

With better and better instrumental performance and with the increasing number of observations of PSR, GRB, AGN flares, it can be expected that more and more significant lags will be measured. One of the main drawback I mentioned in the previous chapter about astrophysical sources is that in general we do not know exactly how they work. It will be necessary to interpret these lags, either as propagation delays, or as effects intrinsic to the sources, or as a superposition of the two effects.

Therefore *it is crucial that some progress is made on emission models*. With that goal in mind, I decided in 2015 to appoint a PhD student (C. Pérennes) who is currently working both on MDR searches with the AGN flares observed by H.E.S.S., and on AGN modelization. I direct this PhD together with a specialist of AGN, H. Sol of the *Laboratoire Univers Théorie* in Meudon. The goal of this PhD is twofold: gain knowledge about intrinsic effects on the modelization side, and use this knowledge to get more robust constraints on MDR.

## Population studies

Another important step forward expected with CTA is the possibility to achieve *population studies*. These population studies will help on the modelization side. They will be also of great importance for LIV studies. In particular, it will be necessary in the future to study the possile variation of time-lags as a function of the distance of sources. As discussed in Chapter 2, this has already been done, but only with ten to twenty GRB, and only with soft gamma-rays. If a high number of sources is used, maybe it will be possible to dicriminate between source intrinsic effects and propagation effects.

Pulsars will be also very important targets for CTA. As permanent variable sources, they have a decisive advantage over AGN or GRB. Due to their very short spikes, they could be used to test spacetime fuzziness.

Before CTA starts to operate [1], to evaluate how the data of different sources could be combined, a collaboration started in late 2016 between a few members of the three major IACT experiments: VERITAS, MAGIC and H.E.S.S. The goal of this group, in which I participate together with A. Jacholkowska, M. Martinez, N. Otte and some others, is to re-analyze all data (flaring AGN, pulsars, GRB if one is detected soon) available in the three experiments and to perform a global fit including the redshift dependance. A dedicated likelihood method will have to be designed in order to achieve that goal with the best possible sensitivity. It is expected that the obtained results will be more performant and robust than the limits available presently.

## The story is not over

Before 2009, all published limits on MDR were below the Planck scale. The picture drastically changed when the paper by *Fermi* [2] was published with the first limit ever obtained above $E_P$. Due to the fact only one photon was used in the analysis, this result was judged as quite weak. But then it was confirmed later using other methods [164].

At that point, some people claimed that all models predicting LIV at the Planck scale should be discarded. Some others claimed it was pointless to keep looking for modifications in dispersion relations.

Of course, I cannot agree with any of these claims. Focusing on GeV energies at which the energy lever arm is larger, only four GRB, four flaring AGN and two pulsars were analyzed. Certainly it is far from being enough to draw any firm conclusion. Population studies are needed. Progress on emission models for AGN and GRB is needed. Limits on the quadratic effect can be improved. I will pursue these goals in the coming years.

A lot remains to be done.

Paris, 2016/10/26

---

[1] Probably around 2018, but only with a part of the array.

# References

[1] B. P. Abbott *et al. Observation of gravitational waves from a binary black hole merger*. Phys. Rev. Lett., **116**, 061102, 2016. (Cited on page 45.)

[2] A. A. Abdo, M. Ackermann, M. Ajello, *et al. A limit on the variation of the speed of light arising from quantum gravity effects*. Nature, **462**, 331–334, 2009. (Cited on pages 64, 66, 69, and 79.)

[3] A. A. Abdo, M. Ackermann, M. Arimoto, *et al. Fermi Observations of High-Energy Gamma-Ray Emission from GRB 080916C*. Science, **323**, 1688, 2009. (Cited on pages 64, 66, and 69.)

[4] A. A. Abdo, M. Ajello, A. Allafort, *et al. The Second Fermi Large Area Telescope Catalog of Gamma-Ray Pulsars*. ApJS, **208**, 17, 2013. arXiv:1305.4385. (Cited on page 61.)

[5] A. Abramowski, F. Acero, F. Aharonian, *et al. Search for Lorentz Invariance breaking with a likelihood fit of the PKS 2155-304 flare data taken on MJD 53944*. Astroparticle Physics, **34**(9), 738–747, 2011. arXiv:1101.3650. (Cited on pages 66, 68, 69, and 70.)

[6] A. Abramowski, F. Aharonian, F. A. Benkhali, *et al. The 2012 flare of PG 1553+113 seen with H.E.S.S. and Fermi-LAT*. The Astrophysical Journal, **802**(1), 65, 2015. arXiv:1501.05087. (Cited on pages 59, 66, 68, 69, and 70.)

[7] M. Ackermann, A. Albert, L. Baldini, *et al. An extremely bright gamma-ray pulsar in the large magellanic cloud*. Science, **350**(6262), 801–805, 2015. (Cited on page 62.)

[8] M. Actis, G. Agnetta, F. Aharonian, *et al. Design concepts for the Cherenkov Telescope Array CTA: an advanced facility for ground-based high-energy gamma-ray astronomy*. Experimental Astronomy, **32**, 193–316, 2011. arXiv:1008.3703. (Cited on page 78.)

[9] R. J. Adler. *Six easy roads to the Planck scale*. American Journal of Physics, **78**, 925–932, 2010. arXiv:1001.1205. (Cited on pages 43 and 44.)

[10] G Agamben. *What is a paradigm?*, 2002. http://www.maxvanmanen.com/files/2014/03/Agamben-What-is-a-paradigm1.pdf. (Cited on page 8.)

[11] F. Aharonian, A. G. Akhperjanian, U. Barres de Almeida, & the H.E.S.S. Collaboration. *Limits on an Energy Dependence of the Speed of Light from a Flare of the Active Galaxy PKS 2155-304*. Physical Review Letters, **101**, 170402, 2008. arXiv:0810.3475. (Cited on pages 65, 66, and 69.)

[12] F. Aharonian, A. G. Akhperjanian, A. R. Bazer-Bachi, *et al. An Exceptional Very High Energy Gamma-Ray Flare of PKS 2155-304*. The Astrophysical Journal Letters, **664**, L71–L74, 2007. arXiv:0706.0797. (Cited on page 69.)

[13] J. Albert, E. Aliu, H. Anderhub, *et al. Variable Very High Energy Gamma-Ray Emission from Markarian 501*. The Astrophysical Journal, **669**, 862–883, 2007. astro-ph/0702008. (Cited on pages 59 and 60.)

[14] J. Albert, E. Aliu, H. Anderhub, *et al. Probing quantum gravity using photons from a flare of the active galactic nucleus Markarian 501 observed by the MAGIC telescope*. Physics Letters B, **668**, 253–257, October 2008. arXiv:0708.2889. (Cited on pages 65, 66, 67, and 74.)

[15] J. Alfaro, H. A. Morales-Técotl, & L. F. Urrutia. *Loop quantum gravity and light propagation*. Physical Review D, **65**, 103509, 2002. hep-th/0108061. (Cited on page 50.)

[16] G. Amelino-Camelia. *Doubly-Special Relativity: Facts, Myths and Some Key Open Issues*. Symmetry, **2**, 230–271, 2010. arXiv:1003.3942. (Cited on page 26.)

[17] G. Amelino-Camelia. *Quantum-spacetime phenomenology*. Living Reviews in Relativity, **16**(5), 2013. Cited on 12/02/2015, http://www.livingreviews.org/lrr-2013-5. (Cited on pages 51 and 78.)

[18] G. Amelino-Camelia & D. V. Ahluwalia. *Relativity in Spacetimes with Short-Distance Structure Governed by an Observer-Independent (Planckian) Length Scale*. International Journal of Modern Physics D, **11**, 35–59, 2002. gr-qc/0012051. (Cited on page 26.)

[19] G. Amelino-Camelia, J. Ellis, N. E. Mavromatos, & D. V. Nanopoulos. *Distance Measurement and Wave Dispersion in a Liouville-String Approach to Quantum Gravity*. International Journal of Modern Physics A, **12**, 607–623, 1997. hep-th/9605211. (Cited on page 49.)

[20] G. Amelino-Camelia, J. Ellis, N.E. Mavromatos, D. V. Nanopoulos, & S. Sarkar. *Tests of quantum gravity from observations of gamma-ray bursts*. Nature, **393**, 763–765, 1998. (Cited on page 51.)

[21] G. Amelino-Camelia & S. Majid. *Waves on Noncommutative Spacetime and Gamma-Ray Bursts*. Int. J. Mod. Phys. A, **15**, 4301–4324, 2000. hep-th/9907110. (Cited on page 47.)

[22] A. Barrau & J. Grain. *Relativité générale*. Dunod, 2011. (Cited on page 45.)

[23] V. Beckmann & C. R. Shrader. *Active Galactic Nuclei*. Wiley-VCH, 2012. (Cited on page 58.)

[24] G. Bertone, D. Hooper, & J. Silk. *Particle dark matter: evidence, candidates and constraints*. Physics Reports, **405**, 279–390, 2005. hep-ph/0404175. (Cited on page 46.)

[25] S. D. Biller, A. C. Breslin, J. Buckley, M. Catanese, *et al. Limits to Quantum Gravity Effects on Energy Dependence of the Speed of Light from Observations of TeV Flares in Active Galaxies*. Physical Review Letters, **83**, 2108–2111, 1999. gr-qc/9810044. (Cited on pages 66 and 70.)

[26] J. Biteau & D. A. Williams. *The extragalactic background light, the Hubble constant, and anomalies: conclusions from 20 years of TeV gamma-ray observations*. The Astrophysical Journal, **812**, 60, 2015. arXiv:1502.04166. (Cited on pages 73 and 74.)

[27] E. D. Black. *An introduction to Pound-Drever-Hall laser frequency stabilization*. American Journal of Physics, **69**, 79, 2001. (Cited on page 35.)

[28] M. Błażejowski, G. Blaylock, I. H. Bond, *et al. A Multiwavelength View of the TeV Blazar Markarian 421: Correlated Variability, Flaring, and Spectral Evolution*. The Astrophysical Journal, **630**, 130, 2005. astro-ph/0505325. (Cited on page 59.)

[29] R. Bluhm, V. A. Kostelecký, C. D. Lane, & N. Russell. *Clock-Comparison Tests of Lorentz and CPT Symmetry in Space*. Physical Review Letters, **88**, 090801, 2002. hep-ph/0111141. (Cited on page 32.)

[30] S.E. Boggs, C.B. Wunderer, K. Hurley, *et al.* *Testing Lorentz Invariance with GRB 021206*. The Astrophysical Journal, **611**, L77–L80, 2004. astro-ph/0310307. (Cited on pages 64 and 66.)

[31] J. Bolmont & A. Jacholkowska. *Lorentz Symmetry breaking studies with photons from astrophysical observations*. Advances in Space Research, **47**, 380–391, 2011. arXiv:1007.4954. (Cited on page 68.)

[32] J. Bolmont, A. Jacholkowska, J.-L. Atteia, F. Piron, & G. Pizzichini. *Study of Time Lags in HETE-2 Gamma-ray Bursts with redshift : Search for Astrophysical Effects and a Quantum Gravity Signature*. ApJ, **676**, 532–544, 2008. astro-ph/0603725. (Cited on pages 54, 66, and 68.)

[33] B. Botermann *et al.* *Test of Time Dilation Using Stored Li+ Ions as Clocks at Relativistic Speed*. Physical Review Letters, **113**, 120405, 2014. arXiv:1409.7951. (Cited on page 34.)

[34] C. Braxmaier, H. Müller, O. Pradl, J. Mlynek, A. Peters, & S. Schiller. *Tests of relativity using a cryogenic optical resonator*. Physical review letters, **88**, 010401, 2002. (Cited on pages 37, 38, and 39.)

[35] A. Brillet & J. L. Hall. *Improved Laser Test of the Isotropy of Space*. Phys. Rev. Lett., **42**, 549–552, 1979. (Cited on page 36.)

[36] M. P. Bronstein. *Quantentheorie schwacher Gravitationsfelder*. Physikalische Zeitscrift der Sowjetunion, **9**, 140–157, 1936. (Cited on page 43.)

[37] N. Brunner, V. Scarani, M. Wegmüller, M. Legré, & N. Gisin. *Direct Measurement of Superluminal Group Velocity and Signal Velocity in an Optical Fiber*. Physical Review Letters, **93**(20), 203902, 2004. quant-ph/0407155. (Cited on page 52.)

[38] X. Calmet, B. Carr, & E. Winstanley. *Quantum Black Holes*. Springer, 2014. (Cited on page 47.)

[39] G. Castignani, D. Guetta, E. Pian, L. Amati, S. Puccetti, & S. Dichiara. *Time delays between Fermi-LAT and GBM light curves of gamma-ray bursts*. Astronomy & Astrophysics, **565**, A60, 2014. arXiv:1403.1199. (Cited on page 57.)

[40] J. P. Cederholm & C. H. Townes. *A New Experimental Test of Special Relativity*. Nature, **184**, 1350–1351, 1959. (Cited on page 36.)

[41] B. Cerutti, A. A. Philippov, & A. Spitkovsky. *Modeling high-energy pulsar lightcurves from first principles*, 2015. Accepted for publication in MNRAS. arXiv:1511.01785. (Cited on page 61.)

[42] A. Cho. *Higgs boson makes its debut after decades-long search*. Science, **337**(6091), 141–143, 2012. (Cited on page 42.)

[43] M. Chretien. *Détection du pulsar de Vela et recherche de violation d'invariance de Lorentz avec le cinquième télescope de H.E.S.S.* PhD thesis, Université Pierre et Marie Curie, 2015. (Cited on pages 66, 68, and 71.)

[44] M. Chretien, J. Bolmont, Jacholkowska A., & the H.E.S.S. Collaboration. *Constraining the photon dispersion relations from observation of the Vela pulsar with H.E.S.S.* In *Proceedings of ICRC2015*, 2015. arXiv:1509.03545. (Cited on page 68.)

[45] W. A. Christiansen, Y. J. Ng, D. J. E. Floyd, & E. S. Perlman. *Limits on spacetime foam*. Phys. Rev. D, **83**, 084003, 2011. arXiv:0912.0535. (Cited on page 72.)

[46] W. A. Christiansen, Y. J. Ng, & H. van Dam. *Probing spacetime foam with extragalactic sources*. Physical Review Letters, **96**(5), 051301, 2006. gr-qc/0508121. (Cited on page 72.)

[47] D. Clowe, M. Bradač, A. H. Gonzalez, M. Markevitch, S. W. Randall, C. Jones, & D. Zaritsky. *A Direct Empirical Proof of the Existence of Dark Matter*. The Astrophysical Journal, **648**(2), L109–L113, sep 2006. astro-ph/0608407. (Cited on page 46.)

[48] D. Colladay & V. A. Kostelecký. *CPT Violation and the Standard Model*. Physical Review D, **55**, 6760, 1997. hep-ph/9703464. (Cited on page 29.)

[49] D. Colladay & V. A. Kostelecký. *Lorentz Violating extension of the standard model*. Physical Review D, **58**, 116002, 1998. hep-ph/9809521. (Cited on page 29.)

[50] C. Dennison Dermer & B. Giebels. *Active galactic nuclei at gamma-ray energies*, 2016. arXiv:1602.06592. (Cited on page 58.)

[51] R. W. P. Drever *et al.* *Laser phase and frequency stabilization using an optical resonator*. Appl. Phys. B: Photophys. Laser Chem., **31**, 97–105, 1983. (Cited on page 35.)

[52] A. S. Eddington & Physical Society of London. *Report on the Relativity Theory of Gravitation*. Fleetway Press, Limited, 1920. Available online: https://archive.org/details/reportontherelat028829mbp. (Cited on page 42.)

[53] A. Einstein. *Zur Elektrodynamik bewegter Körper*. Annalen der Physik, **322**, 891–921, 1905. A translation is available on Wikisource: http://en.wikisource.org/wiki/Translation:On_the_Electrodynamics_of_Moving_Bodies. (Cited on page 15.)

[54] A. Einstein. *Feldgleichungen der Gravitation*. Sitzungsberichte der Preussische Akademie der Wissenschaften, **1915**, 844–847, 1915. This paper is the fourth published by Einstein about General Relativity, but it is considered as the true defining paper of GR. (Cited on page 42.)

[55] A. Einstein. *Näherungsweise Integration der Feldgleichungen der Gravitation*. Preussische Akademie der Wissenschaften, Sitzungsberichte, **1916**, 688–696, 1916. (Cited on page 42.)

[56] A. Einstein. *Gravitationswellen*. Preussische Akademie der Wissenschaften, Sitzungsberichte, **1918**, 154–167, 1918. (Cited on page 42.)

[57] G. F. R. Ellis & J.-P. Uzan. *'C' Is the Speed of Light, isn't It?* American Journal of Physics, **73**, 240, 2005. gr-qc/0305099. (Cited on page 19.)

[58] J. Ellis, K. Farakos, N. E. Mavromatos, *et al.* *A Search in Gamma-Ray Burst Data for Nonconstancy of the Velocity of Light*. The Astrophysical Journal, **535**, 139–151, 2000. astro-ph/9907340. (Cited on page 66.)

[59] J. Ellis, N. E. Mavromatos, & D. V. Nanopoulos. *Probing Models of Quantum Space-Time Foam*. In *Beyond the Desert 99, Ringberg*, 1999. gr-qc/9909085. (Cited on page 49.)

[60] J. Ellis, N. E. Mavromatos, & D. V. Nanopoulos. *Quantum-Gravitational Diffusion and Stochastic Fluctuations in the Velocity of Light*. Gen. Rel. Grav., **32**, 127–144, 2000. gr-qc/9904068. (Cited on page 49.)

[61] J. Ellis, N. E. Mavromatos, D. V. Nanopoulos, *et al. Robust limits on Lorentz violation from gamma-ray bursts*. Astroparticle Physics, **25**, 402–411, 2006. astro-ph/0510172. (Cited on pages 66 and 67.)

[62] J. Ellis, N. E. Mavromatos, D. V. Nanopoulos, *et al. Corrigendum to "Robust limits on Lorentz violation from gamma-ray bursts [Astropart. Phys. 25 (2006) 402]"*. Astroparticle Physics, **29**, 158–159, 2008. (Cited on pages 66 and 67.)

[63] J. Ellis, N. E. Mavromatos, D. V. Nanopoulos, & A. S. Sakharov. *Quantum-gravity analysis of gamma-ray bursts using wavelets*. Astronomy and Astrophysics, **402**, 409–424, 2003. astro-ph/0210124. (Cited on pages 66 and 67.)

[64] L. Essen. *A new Aether-Drift Experiment*. Nature, **175**, 793–802, 1955. (Cited on page 36.)

[65] M. Fairbairn, A. Nilsson, J. Ellis, J. Hinton, & R. White. *The CTA sensitivity to Lorentz-violating effects on the gamma-ray horizon*. JCAP, **6**, 005, 2014. arXiv:1401.8178. (Cited on pages 73 and 74.)

[66] B. Famaey & S. S. McGaugh. *Modified newtonian dynamics (mond): Observational phenomenology and relativistic extensions*. Living Reviews in Relativity, **15**(10), 2012. Cited 01/12/2016, http://www.livingreviews.org/lrr-2012-10. (Cited on page 46.)

[67] K Farakos, N.E Mavromatos, & P Pasipoularides. *Bulk photons in asymmetrically warped spacetimes and non-trivial vacuum refractive index*. Journal of High Energy Physics, **0901**, 057–057, 2009. arXiv:0807.0870. (Cited on page 50.)

[68] G. Fras. Fitz Gerald. *The Ether and the Earth's Atmosphere*. Science, **13**, 390, 1889. (Cited on page 35.)

[69] R. Gambini & J. Pullin. *Nonstandard optics from quantum spacetime*. Physical Review D, **59**, 124021, 1999. gr-qc/9809038. (Cited on page 50.)

[70] S. Gardner & D. C. Latimer. *Dark matter constraints from a cosmic index of refraction*. Phys. Rev. D, **82**(6), 063506, 2010. arXiv:0904.1612. (Cited on page 75.)

[71] A. S. Goldhaber & M. M. Nieto. *Photon and graviton mass limits*. Reviews of Modern Physics, **82**, 939–979, 2010. arXiv:0809.1003. (Cited on page 74.)

[72] G. E. Gorelik & V. Y. Frenkel. *Matvei Petrovich Bronstein and Soviet Theoretical Physics in the Thirties*. Birkhäuser Verlag, 1994. (Cited on page 43.)

[73] D. Götz, P. Laurent, S. Antier, *et al. GRB 140206A: the most distant polarized gamma-ray burst*. MNRAS, **444**, 2776–2782, 2014. arXiv:1408.4121. (Cited on page 72.)

[74] E. Gourgoulhon. *Special Relativity in General Frames, From Particles to Astrophysics*. Springer-Verlag, Berlin, Heidelgerg, 2013. Translation from *Relativité Restreinte: Des Particules à l'Astrophysique*, EDP Sciences, CNRS Editions, 2010. (Cited on pages 15, 17, 21, and 23.)

[75] H. Greaves & T. Thomas. *On the CPT theorem*. Studies in History and Philosophy of Modern Physics, **45**, 46–65, 2014. (Cited on page 27.)

[76] I. A. Grenier & A. K. Harding. *Gamma-ray pulsars: A gold mine*. Comptes Rendus Physique, **16**, 641–660, 2015. arXiv:1509.08823. (Cited on page 61.)

[77] S. W. Hawking. *Particle Creation by Black Holes*. Commun. math. Phys., **43**, 199–220, 1975. (Cited on page 46.)

[78] S. Herrmann, A. Senger, E. Kovalchuk, H. Müller, & A. Peters. *Test of Lorentz Invariance Using a Continuously Rotating Optical Resonator*. Lect. Notes Phys., **702**, 385–400, 2006. (Cited on page 36.)

[79] S. Herrmann, A. Senger, K. Möhle, M. Nagel, E. V. Kovalchuk, & A. Peters. *Rotating optical cavity experiment testing Lorentz invariance at the $10^{-17}$ level*. Phys. Rev. D, **80**, 105011, 2009. arXiv:1002.1284. (Cited on page 36.)

[80] D. Hils & J. L. Hall. *Improved Kennedy-Thorndike experiment to test special relativity*. Physical Review Letters, **64**, 1697–1700, 1990. (Cited on pages 37 and 39.)

[81] D. W. Hogg. *Distance measures in cosmology*, 1999. astro-ph/9905116. (Cited on page 55.)

[82] D. J. Hopper. *Investigation of Laser Frequency Stabilisation Using Modulation Transfer Spectroscopy*. PhD thesis, Queensland University of Technology, 2008. Available online: http://eprints.qut.edu.au/16667/1/David_John_Hopper_Thesis.pdf. (Cited on page 38.)

[83] S. Hossenfelder. *Minimal length scale scenarios for quantum gravity*. Living Reviews in Relativity, **16**(2), 2013. Cited 11/25/2015, http://www.livingreviews.org/lrr-2013-2. (Cited on page 44.)

[84] C. D. Hoyle, D. J. Kapner, B. R. Heckel, *et al.* *Submillimeter tests of the gravitational inverse-square law*. Physical Review D, **70**, 042004, 2004. hep-ph/0405262. (Cited on page 44.)

[85] W. Ignatowsky. *Einige allgemeine Bemerkungen über das Relativitätsprinzip*. Physikalische Zeitschrift, **11**, 972–976, 1910. (Cited on page 15.)

[86] W. Ignatowsky. *Das Relativitätsprinzip*. Archiv der Mathematik und Physik, **17**, 1–24, 1911. (Cited on page 15.)

[87] W. Ignatowsky. *Das Relativitätsprinzip*. Archiv der Mathematik und Physik, **18**, 17–40, 1911. (Cited on page 15.)

[88] W. Ignatowsky. *Eine Bemerkung zu meiner Arbeit: "Einige allgemeine Bemerkungen zum Relativitätsprinzip"*. Physikalische Zeitschrift, **12**, 779, 1911. (Cited on page 15.)

[89] K. K. Illingworth. *A Repetition of the Michelson-Morley Experiment Using Kennedy's Refinement*. Phys. Rev., **30**, 692–696, 1927. (Cited on page 36.)

[90] C.J. Isham. *Prima facie questions in quantum gravity*. In J. Ehlers & H. Friedrich, editors, *Canonical Gravity: From Classical to Quantum*, volume 434 of *Lecture Notes in Physics*, pages 1–21. Springer Berlin Heidelberg, 1994. gr-qc/9310031. (Cited on page 47.)

[91] H. E. Ives & G. R. Stilwell. *An experimental study of the rate of a moving atomic clock*. J. Opt. Soc. Am., **28**, 215, 1938. (Cited on page 34.)

[92] H. E. Ives & G. R. Stilwell. *An Experimental Study of the Rate of a Moving Atomic Clock. II*. J. Opt. Soc. Am., **31**, 369–374, 1941. (Cited on page 34.)

[93] U. Jacob & T. Piran. *Lorentz-violation-induced arrival delays of cosmological particles*. JCAP, **1**, 031, 2008. arXiv:0712.2170. (Cited on page 54.)

[94] T. S. Jaseja, A. Javan, J. Murray, & C. H. Townes. *Test of Special Relativity or of the Isotropy of Space by Use of Infrared Masers*. Phys. Rev., **133**, A1221–A1225, 1964. (Cited on page 36.)

[95] G. Joos. *Die Jenaer Wiederholung des Michelsonversuchs*. Annalen der Physik, **399**, 385–407, 1930. (Cited on page 36.)

[96] P. Kaaret. *Pulsar radiation and quantum gravity*. Astronomy and Astrophysics, **345**, L32–L34, 1999. astro-ph/9903464. (Cited on pages 64 and 66.)

[97] D. B. Kaplan. *Five lectures on effective field theory*, 2005. nucl-th/0510023. (Cited on page 30.)

[98] R. J. Kennedy. *A Refinement of the Michelson-Morley Experiment*. Proceedings of the National Academy of Science, **12**, 621–629, November 1926. (Cited on page 36.)

[99] R. J. Kennedy & E. M. Thorndike. *Experimental establishment of the relativity of time*. Physical Review, **42**, 400–418, 1932. (Cited on pages 33, 36, 37, 38, and 39.)

[100] V. A. Kostelecký. *Sensitivity of CPT Tests with Neutral Mesons*. Physical Review Letters, **80**, 1818–1821, March 1998. hep-ph/9809572. (Cited on page 27.)

[101] V. A. Kostelecký. *Gravity, Lorentz violation, and the standard model*. Physical Review D, **69**, 105009, 2004. hep-th/0312310. (Cited on page 29.)

[102] V. A. Kostelecký & M. Mewes. *Astrophysical Tests of Lorentz and CPT Violation with Photons*. The Astrophysical Journal, **689**, L1–L4, 2008. arXiv:0809.2846. (Cited on pages 30 and 56.)

[103] V. A. Kostelecký & M. Mewes. *Electrodynamics with Lorentz-violating operators of arbitrary dimension*. Physical Review D, **80**, 015020, 2009. arXiv:0905.0031. (Cited on pages 30 and 32.)

[104] V. A. Kostelecký & N. Russell. *Data tables for Lorentz and CPT violation*. Reviews of Modern Physics, **83**, 11–31, 2011. An up-to-date version of the tables can be found here: arXiv:0801.0287. (Cited on pages 32 and 39.)

[105] T. S. Kuhn. *The structure of scientific revolutions*. University of Chicago Press, 1962. Available online: http://projektintegracija.pravo.hr/_download/repository/Kuhn_Structure_of_Scientific_Revolutions.pdf. (Cited on page 8.)

[106] R. Lamon, N. Produit, & F. Steiner. *Study of Lorentz violation in INTEGRAL gamma-ray bursts*. General Relativity and Gravitation, **40**, 1731–1743, 2008. arXiv:0706.4039. (Cited on page 66.)

[107] D. C. Latimer. *Dispersive light propagation at cosmological distances: Matter effects*. Phys. Rev. D, **88**, 063517, 2013. arXiv:1308.1112. (Cited on page 75.)

[108] J. I. Latorre, P. Pascual, & R. Tarrach. *Speed of Light in Non-Trivial Vacua*. Nuclear Physics B, **437**, 60–82, 1995. hep-th/9408016. (Cited on pages 67 and 74.)

[109] J.-M. Lévy-Leblond. *One more derivation of the Lorentz transformation*. American Journal of Physics, **44**, 271, 1976. (Cited on page 15.)

[110] T.-P. Li, J.-L. Qu, H. Feng, *et al.* *Timescale Analysis of Spectral Lags*. Chinese Journal of Astronomy & Astrophysics, **4**, 583–598, 2004. astro-ph/0407458. (Cited on page 65.)

[111] S. Liberati. *Tests of Lorentz invariance: a 2013 update*. Classical and Quantum Gravity, **30**, 133001, 2013. arXiv:1304.5795. (Cited on pages 15 and 26.)

[112] A. P. Lightman & D. L. Lee. *Restricted proof that the Weak Equivalence Principle implies the Einstein Equivalence Principle*. Phys. Rev. D, **8**, 364–376, 1973. (Cited on page 28.)

[113] H. A. Lorentz. *The Relative Motion of the Earth and the Aether*. Zittingsverlag Akad. V. Wet., **1**, 74–79, 1892. (Cited on page 35.)

[114] H. A. Lorentz. *Electromagnetic phenomena in a system moving with any velocity smaller than that of light*. Koninklijke Akademie van Wetenschappen te Amsterdam, **6**, 809–831, 1904. Available on Wikisource: http://en.wikisource.org/wiki/Electromagnetic_phenomena. (Cited on page 35.)

[115] M. Ludvigsen. *La relativité générale, une approche géométrique*. Dunod, 1999. (Cited on page 45.)

[116] A. Lyne & F. Graham-Smith. *Pulsar Astronomy*. Cambridge University Press, 2012. (Cited on page 61.)

[117] S. Mallat. *A Wavelet Tour of Signal Processing, Third Edition: The Sparse Way*. Academic Press, 2008. (Cited on page 65.)

[118] R. Mansouri & R. U. Sexl. *A test theory of special relativity: I. Simultaneity and clock synchronization*. General Relativity and Gravitation, **8**, 497–513, 1977. (Cited on page 28.)

[119] R. Mansouri & R. U. Sexl. *A test theory of special relativity: II. First order tests*. General Relativity and Gravitation, **8**, 515–524, 1977. (Cited on page 28.)

[120] R. Mansouri & R. U. Sexl. *A test theory of special relativity: III. Second-order tests*. General Relativity and Gravitation, **8**, 809–814, 1977. (Cited on page 28.)

[121] J. Martin. *Everything you always wanted to know about the cosmological constant problem (but were afraid to ask)*. Comptes Rendus Physique, **13**, 566–665, 2012. arXiv:1205.3365. (Cited on page 46.)

[122] M. Martínez & M. Errando. *A new approach to study energy-dependent arrival delays on photons from astrophysical sources*. Astroparticle Physics, **31**, 226–232, 2009. arXiv:0803.2120. (Cited on pages 65, 66, 69, and 70.)

[123] D. Mattingly. *Modern Tests of Lorentz Invariance*. Living Reviews in Relativity, **8**, 2005. Cited 10/23/2015, http://www.livingreviews.org/lrr-2005-5. (Cited on pages 34 and 39.)

[124] N. E. Mavromatos. *String Quantum Gravity, Lorentz-Invariance Violation and Gamma Ray Astronomy*. International Journal of Modern Physics A, **25**, 5409–5485, dec 2010. arXiv:1010.5354. (Cited on page 49.)

[125] M. R. Metzger, S. G. Djorgovski, S. R. Kulkarni, *et al.* *Spectral constraints on the redshift of the optical counterpart to the γ-ray burst of 8 May 1997*. Nature, **387**, 878–880, 1997. (Cited on page 57.)

[126] A. A. Michelson. *The relative motion of the Earth and of the luminiferous ether*. American Journal of Science, **22**, 120–129, 1881. Available online: http://www.ajsonline.org/content/s3-22/128/120. (Cited on pages 33 and 36.)

[127] A. A. Michelson & E. W. Morley. *On the Relative Motion of the Earth and the Luminiferous Ether*. The American Journal Of Science, **34**, 333–345, 1887. Available on Wikisource: http://en.wikisource.org/wiki/On_the_Relative_Motion_of_the_Earth_and_the_Luminiferous_Ether. (Cited on pages 33, 34, and 36.)

[128] H. Minkowski. *Die Grundgleichungen für die elektromagnetischen Vorgänge in bewegten Körpern*. Mathematische Annalen, **68**, 472, 1910. Reprint of the original article of 1908. (Cited on page 15.)

[129] C. W. Misner, K. S. Thorne, & J. A. Wheeler. *Gravitation*. W. H. Freeman and Company, New York, 1973. (Cited on page 45.)

[130] E. W. Morley & Miller D. C. *Extract from a Letter dated Cleveland, Ohio, August 5th, 1904, to Lord Kelvin from Profs. Edward W. Morley and Dayton C. Miller*. Philosophical Magazine, **8**, 753–754, 1904. (Cited on page 36.)

[131] H. Müller, S. Herrmann, C. Braxmaier, S. Schiller, & A. Peters. *Modern Michelson-Morley Experiment using Cryogenic Optical Resonators*. Phys. Rev. Lett., **91**, 020401, 2003. physics/0305117. (Cited on pages 34, 35, and 36.)

[132] Y. J. Ng. *Slected topics in Planck-scale physics*. Mod. Phys. Lett. A, **18**, 1073–1097, 2003. gr-qc/0305019. (Cited on page 72.)

[133] H. Nguyen. *CPT Results from KTeV*. In V. A. Kostelecký, editor, *CPT and Lorentz Symmetry*, pages 122–131, February 2002. hep-ex/0112046. (Cited on page 27.)

[134] J. P. Norris. *Gamma-Ray Bursts: The Time Domain*. Astrophysics and Space Science, **231**, 95–102, 1995. (Cited on page 57.)

[135] J. P. Norris & J. T. Bonnell. *Short Gamma-Ray Bursts with Extended Emission*. The Astrophysical Journal, **643**, 266–275, 2006. astro-ph/0601190. (Cited on page 57.)

[136] J. P. Norris, G.F. Mirani, & J. T. Bonnell. *Connection between Energy-dependent Lags and Peak luminosity in Gamma-Ray Bursts*. The Astrophysical Journal, **534**, 248, 2000. astro-ph/9903233. (Cited on pages 57 and 58.)

[137] J. P. Norris, R. J. Nemiroff, J. T. Bonnell, *et al. Attributes of Pulses in Long Bright Gamma-Ray Bursts*. The Astrophysical Journal, **459**, 393, 1996. (Cited on page 57.)

[138] N. Otte. *Prospects of performing Lorentz invariance tests with VHE emission from pulsars*. In *Proceedings of the 32nd ICRC*, volume 7, pages 256–259, 2011. arXiv:1208.2033. (Cited on page 61.)

[139] T. G. Pavlopoulos. *Breakdown of Lorentz Invariance*. Physical Review, **159**(5), 1106–1110, 1967. (Cited on page 26.)

[140] A. Pélangeon, J.-L. Atteia, D. Q. Lamb, & the HETE-2 Science Team. *An improved redshift indicator for Gamma-Ray Bursts, based on the prompt emission*. In S. S. Holt, N. Gehrels, & J. A. Nousek, editors, *Gamma-Ray Bursts in the Swift Era*, volume 836 of *American Institute of Physics Conference Series*, pages 149–152, May 2006. astro-ph/0601150. (Cited on pages 57 and 66.)

[141] E. S. Perlman, S. A. Rappaport, W. A. Christiansen, *et al.* *New Constraints on Quantum Gravity from X-Ray and Gamma-Ray Observations*. ApJ, **805**, 10, 2015. arXiv:1411.7262. (Cited on page 72.)

[142] P. Peter & J.-P. Uzan. *Cosmologie primordiale*. Belin, 2005. (Cited on pages 45 and 52.)

[143] F. Piron. *Gamma-Ray Bursts at high and very high energies*, 2015. To be published in C. R. Physique. arXiv:1512.04241. (Cited on pages 56, 57, and 58.)

[144] M. Planck. *Über irreversible Strahlungsvorgänge*. Sitzungsberichte der Preussische Akademie der Wissenschaften, **1899**, 440–480, 1899. (Cited on page 42.)

[145] Planck Collaboration. *Planck 2013 results. XXVII. Doppler boosting of the CMB: Eppur si muove*. A&A, **571**, A27, 2014. arXiv:1303.5087. (Cited on pages 24 and 25.)

[146] Planck Collaboration. *Planck 2015 results. XIII. Cosmological parameters*, 2015. arXiv:1502.01589. (Cited on page 53.)

[147] H. P. Robertson. *Postulate versus Observation in the Special Theory of Relativity*. Rev. Mod. Phys., **21**, 378–382, 1949. (Cited on page 28.)

[148] G. Rosati, G. Amelino-Camelia, A. Marcianò, & M. Matassa. *Planck-scale-modified dispersion relations in FRW spacetime*. Physical Review D, **92**(12), 124042, 2015. 1507.02056. (Cited on page 54.)

[149] C. Rovelli. *Notes for a brief history of quantum gravity*, June 2000. gr-qc/0006061. (Cited on page 43.)

[150] C. Rovelli. *Loop quantum gravity*. Living Reviews in Relativity, **11**(5), 2008. Cited on 01/13/2016, http://www.livingreviews.org/lrr-2008-5. (Cited on page 50.)

[151] D. D. Ryutov. *Using plasma physics to weigh the photon*. Plasma Physics and Controlled Fusion, **49**, B429–B438, 2007. (Cited on page 74.)

[152] J. D. Scargle, J. P. Norris, & J. T. Bonnell. *An Algorithm for Detecting Quantum Gravity Photon Dispersion in Gamma-Ray Bursts: DisCan*. The Astrophysical Journal, **673**, 972–980, 2008. astro-ph/0610571. (Cited on page 65.)

[153] J. Stachel. *The early history of quantum gravity (1916–1940)*. In B. R. Iyer & B. Bhawal, editors, *Black Holes, Gravitational Radiation and the Universe*, volume 100 of *Fundamental Theories of Physics*, pages 525–534. Springer Netherlands, 1999. (Cited on page 43.)

[154] F. Tamburini, C. Cuofano, M. Della Valle, & R. Gilmozzi. *No quantum gravity signature from the farthest quasars*. A&A, **533**, A71, 2011. arXiv:1108.6005. (Cited on page 72.)

[155] J. D. Tasson. *What do we know about Lorentz invariance?* Reports on progress in physics. Physical Society (Great Britain), **77**, 062901, 2014. arXiv:1403.7785. (Cited on page 27.)

[156] F. Tavecchio & G. Bonnoli. *On the detectability of Lorentz invariance violation through anomalies in the multi-TeV γ-ray spectra of blazars*. Astronomy & Astrophysics, **585**, A25, 2016. arXiv:1510.00980. (Cited on page 74.)

[157] D. G. Terrats. *Limits to violation of Lorentz invariance using the emission of the crab pulsar at TeV energies, discovered with archival data from the Magic telescopes*. PhD thesis, Universitat Autónoma de Barcelona, 2015. (Cited on pages 66 and 71.)

[158] M. E. Tobar, P. Wolf, S. Bize, G. Santarelli, & V. Flambaum. *Testing local Lorentz and position invariance and variation of fundamental constants by searching the derivative of the comparison frequency between a cryogenic sapphire oscillator and hydrogen maser*. Physical Review D, **81**, 022003, 2010. arXiv:0912.2803. (Cited on pages 38 and 39.)

[159] R. Tomaschek. *Über Aberration und Absolutbewegung*. Annalen der Physik, **329**, 136–145, 1924. (Cited on page 36.)

[160] P. Tourrenc. *Relativité et Gravitation*. Armand Colin, 1992. (Cited on page 45.)

[161] T. N. Ukwatta, M. Stamatikos, K. S. Dhuga, *et al. Spectral Lags and the Lag-Luminosity Relation: An Investigation with Swift BAT Gamma-ray Bursts*. The Astrophysical Journal, **711**, 1073–1086, 2010. arXiv:0908.2370. (Cited on page 57.)

[162] C. M. Urry & P. Padovani. *Unified Schemes for Radio-Loud Active Galactic Nuclei*. Publications of the Astronomical Society of the Pacific, **107**, 803, 1995. astro-ph/9506063. (Cited on page 59.)

[163] V. Vasileiou, J. Granot, T. Piran, & G. Amelino-Camelia. *A Planck-scale limit on spacetime fuzziness and stochastic Lorentz invariance violation*. Nature Physics, **11**, 344–346, 2015. (Cited on page 72.)

[164] V. Vasileiou, A. Jacholkowska, F. Piron, J. Bolmont, *et al. Constraints on Lorentz invariance violation from Fermi-Large Area Telescope observations of gamma-ray bursts*. Physical Review D, **87**(12), 122001, 2013. arXiv:1305.3463. (Cited on pages 63, 64, 65, 66, 68, 70, and 79.)

[165] G. Vedrenne & J.-L. Atteia. *Gamma-Ray Bursts: the brightest explosions in the Universe*. Springer, 2009. (Cited on page 56.)

[166] R. M. Wald. *General Relativity*. The University of Chicago Press, 1984. (Cited on page 45.)

[167] J. A. Wheeler. *Geons*. Physical Review, **97**, 511–536, 1955. (Cited on page 43.)

[168] E. T. Whittaker. *A History of the Theories of Aether and Electricity*. Hodges, Figgis, & Co., Dublin, 1910. (Cited on page 13.)

[169] C. M. Will. *The Confrontation between General Relativity and Experiment*. Living Reviews in Relativity, **4**, 2001. Cited on 10/23/2015, http://www.livingreviews.org/lrr-2001-4. (Cited on pages 27, 28, and 42.)

[170] P. Wolf, S. Bize, A. Clairon, A. N. Luiten, G. Santarelli, & M. E. Tobar. *Tests of Lorentz Invariance using a Microwave Resonator*. Phys. Rev. Lett., **90**, 060402, 2003. gr-qc/0210049. (Cited on pages 36, 37, and 39.)

[171] B. Zitzer & the VERITAS Collaboration. *Lorentz Invariance Violation Limits from the Crab Pulsar using VERITAS*. In *Proceedings of ICRC2013*, 2013. arXiv:1307.8382. (Cited on pages 66 and 71.)

## Is the speed of light in vacuum really constant?

A challenge of modern physics is to develop a theory of Quatum Gravity. Some models elaborated with this purpose predict measurable effects on photon propagation in vacuum. In particular, the quantum nature of spacetime at the Planck scale could result in a modified dispersion relation: the velocity of photons could depend on their energies. This would break Lorentz invariance. This effect can be tested, and the models can be constrained with energetic, variable and distant astrophysical sources.

I start this monograph by explaining in detail what Lorentz Invariance is: the fundamental symmetry of all relativistic theories. I quickly review the results of the optical experiments designed to test Lorentz invariance out of Quantum Gravity phenomenology.

The second part deals in particular with my contributions on the tests of modified dispersion relation of photons in vacuum. I begin by describing two models of Quantum Gravity which predict a violation of Lorentz invariance. I then comment on the use of astrophysical sources to test this prediction. These sources (gamma-ray bursts, pulsars, active galactic nuclei) all have advantages and drawbacks for this kind of studies. Finally, I review the results available in the litterature, commenting in particular on my personal contributions.

To conclude, I give the possible ways which, in my opinion, will have to be followed to improve the current constraints.

## La vitesse de la lumière dans le vide est-elle vraiment constante ?

L'élaboration d'une théorie quantique de la gravitation est un des enjeux majeurs de la physique moderne. Certains modèles proposés pour aboutir à une telle théorie prédisent des effets mesurables sur la propagation des photons dans le vide. En particulier, la nature quantique de l'espace-temps à l'échelle de Planck pourrait entraîner une modification de la relation de dispersion des photons : la vitesse des photons dans le vide pourrait dépendre de leur énergie. Cela violerait l'invariance de Lorentz. Cet effet peut être testé et les modèles contraints avec les sources astrophysiques, très énergétiques, variables et lointaines.

Je commence ce mémoire par expliquer en détail ce qu'est l'invariance de Lorentz, la symétrie fondamentale de toutes les théories relativistes. Je passe rapidement en revue les résultats des expériences optiques conçues dans le but de tester cette symétrie hors du cadre de la gravitation quantique.

La deuxième partie aborde plus particulièrement mes contributions sur les tests de la relation de dispersion modifée pour les photons dans le vide. Je commence par décrire deux modèles de gravitation quantique qui prédisent la violation de l'invariance de Lorentz. Je commente ensuite sur l'utilisation des sources astrophysiques pour tester cette prédiction. Ces sources (sursauts gamma, pulsars et noyaux actifs de galaxies) ont tous des avantages et des inconvénients pour ce type d'études. Enfin, je passe en revue les différents résultats disponibles dans la littérature, en commenttant en particulier mes contributions personnelles.

Pour conclure, je donne les différentes pistes qui, selon moi, devront être suivies pour améliorer les contraintes actuelles.

LPNHE
PARIS